RSC Advances

REVIEW

View Article Online
View Journal | View Issue

Cite this: *RSC Adv.*, 2022, **12**, 26319

Electrochemical detection of selected heavy metals in water: a case study of African experiences

Enyioma C. Okpara,[a] Omolola E. Fayemi,[bc] Olanrewaju B. Wojuola,[a] Damian C. Onwudiwe[bc] and Eno E. Ebenso *[d]

The safety of water resources throughout the globe has been compromised by various human activities and climate change over the last decades. Consequently, the world is currently confronted with a severe shortage of water supply and a water safety crisis, amidst a growing population. With poor environmental regulations, indiscriminate budding of urban slums, poverty, and a lack of basic knowledge of hygiene and sanitation, the African water supply has been critically threatened by different organic and inorganic contaminants, which results in several health issues. Inorganic pollutants such as heavy metals are particularly of interest because they are mostly stable and non-biodegradable. Therefore, they are not easily removed from water. In different parts of the continent, the concentration of heavy metals in drinking water far exceeds the permissible level recommended by the World Health Organization (WHO). Worse still, this problem is expected to increase with growing population, industrialization, urbanization, and, of course, corruption of government and local officials. Most of the African population is ignorant of the standards of safe water. In addition, the populace lack access to affordable and reliable technologies and tools that could be used in the quantification of these pollutants. This problem is not only applicable to domestic, but also to commercial, communal, and industrial water sources. Hence, a global campaign has been launched to ensure constant assessment of the presence of these metals in the environment and to promote awareness of dangers associated with unsafe exposure to them. Various conventional spectroscopic heavy metal detection techniques have been used with great success across the world. However, such techniques suffer from some obvious setbacks, such as the cost of procurement and professionalism required to operate them, which have limited their applications. This paper, therefore, reviews the condition of African water sources, health implications of exposure to heavy metals, and the approaches explored by various indigenous electrochemists, to provide a fast, affordable, sensitive, selective, and stable electrochemical sensors for the quantification of the most significant heavy metals in our water bodies.

Received 29th April 2022
Accepted 30th August 2022

DOI: 10.1039/d2ra02733j

rsc.li/rsc-advances

1. Introduction

Water is an essential element that is fundamental to the existence of life on earth, thus making living impossible without it.[1] It has also been estimated to play the most significant role in the development of any society,[2] due to its property as a universal solvent, factory coolant, *etc.*[3] About 70.9% of the Earth's space is covered with water, providing habitation for many of the organisms in the ecosystem.[4] Yet the scarcity of clean water is a major concern in today's growing global population because the water capacity of the cosmos is fixed, while the existing freshwater sources are constantly threatened by various human activities. The capacity of the hemisphere is projected to be approximately 388×10^{15} m^3, which is made up of 96.5% oceanic saltwater, 0.93% saline groundwater, 0.07% saline lakes and 2.5% freshwater (Fig. 1). Meanwhile, this small capacity of freshwater is made up of 68.6% glacier and ice-caps, 30.1% groundwater, and only 1.3% is from surface and freshwater. Out of the 1.3% of the surface and freshwater, 73.1% is made up of ice and snow, 20.1% of lakes, 0.22% of atmospheric water, 0.22% of biological water, 0.46% of rivers, 2.53% of swamps and marshes, and 3.52% soil moisture. This data puts the volume of accessible and useable earth water at just 1%, with an overwhelming 99% of Earth's water capacity termed unusable.[5] About 99% of the usable water is sourced from

[a]*Department of Physics, School of Physical and Chemical Sciences, Faculty of Natural and Agricultural Sciences, North-West University (Mafikeng Campus), Private Bag X2046, Mmabatho 2735, South Africa*

[b]*Department of Chemistry, School of Physical and Chemical Sciences, Faculty of Natural and Agricultural Sciences, North-West University (Mafikeng Campus), Private Bag X2046, Mmabatho 2735, South Africa*

[c]*Material Science Innovation and Modelling (MaSIM) Research Focus Area, Faculty of Natural and Agricultural Sciences, North-West University (Mafikeng Campus), Private Bag X2046, Mmabatho 2735, South Africa*

[d]*College of Science, Engineering and Technology, University of South Africa, Johannesburg 1710, South Africa. E-mail: ebensee@unisa.ac.za*

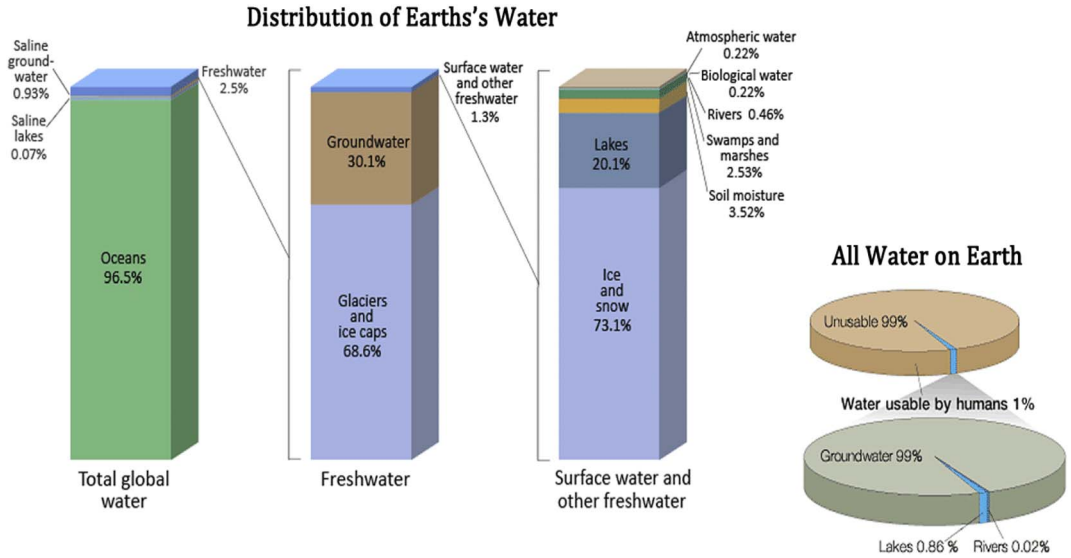

Fig. 1 Earth's water reservoirs. Bar chart distribution of Earth's water resources including total global water, freshwater, surface water, and other freshwater and pie chart water usable by humans and sources of usable water. Source: United States Geographical Survey Igor Skiklomanov's chapter "World freshwater resources". This figure has been reproduced from ref. 9 with permission from Oxford University Press, copyright 1993.

groundwater, while 0.86% comes from lakes, and then 0.02% from river water.[6]

The quality of water must be safe physically, chemically, and biologically to be regarded as useful for drinking and other domestic purposes.[2] Currently, the World Water Council reported that close to 1.2 billion people globally lack access to quality water, and a projected number of 2.5 billion people lack access to improved sanitation. Additionally, the availability and distribution of water are on the decline with a projected severe impact around 2020 and 2050.[1] More than 6 billion people all over the globe could lack access to clean water by 2050.[7] This is driven by increasing world population, irrigation, industrialization, and consequently overexploitation, which has stressed the water situation globally.[5] More so, constant exposure of the naturally occurring water resources to different sources of contamination has lowered their fitness for consumption. Hence, exploiting best water management practices for its conservation, and safety about quality cannot be underrated. Coincidentally too, over the past few decades, global awareness of making potable water available to people has comparably been improved.[8]

According to Joan Clos, Executive Director of UN-HABITAT, "Africa is the fastest urbanizing continent on the planet, and the demand for water and sanitation is outstripping the supply in cities".[10] Sub-Saharan Africa (SSA) and Northern Africa are indeed on the same continent, but their degrees of progress towards attainment of the Millennium Development Goal (MDG) on the water varies significantly. Northern Africa, was given a 94% target before 2015, out of which they have achieved 92% coverage.[11,12] Contrarily, only 57% of more than 783 million Southern African population have access to potable water supply, throughout the whole region. As a result, out of the 75% MDG target stipulated for the SSA region, only 61% coverage was achieved. Additionally, the available data from 35 countries in the SSA, covering 84% of the population in the region, shows high discrimination between the poorest and wealthiest in both urban and rural places. More than 90% of their wealthy populace live in urban places and have access to a better water supply. On the other hand, over 50% of the population living in rural areas do not have access to any form of an improved water source.

Concerns about poor sanitation have also heightened the existential threats to the supply of safe water for the majority of the population. As of 2015, Africa was ranked as one of the two continents lagging in the fulfilment of MDG on sanitation. A growing population that does not have basic sanitary orientation could only indulge in environmentally hazardous sanitation practices such as indiscriminate disposal of solid wastes into water bodies and open defecation.[13–15]

Additionally, population growth in the continent has accelerated the demand for more water, while depleting the supply source as shown in Fig. 2 (see also Table 1). SSA has the highest emergence of urban slums when compared with other developing regions, and this is expected to double to approximately 0.4 billion by the year 2020.[14,15]

Consequently, constant assessment of the safety of aquatic systems in many African countries has emerged as a top priority among many researchers.[17,18] Such regular monitoring of the environmental water in circulation requires a constant, effective, low cost, and outdoor sensing strategy and tools, for both economic development and biological survival.[18,19]

Exposure to some classes of heavy metals (HMs), even in trace concentrations could pose a serious threat to humans, while exerting harmful consequences on the ecosystem, and other biological receptors.[20,21] Therefore, reliable identification and efficient extraction of these metals from water, especially for domestic, communal, and industrial uses, has become very significant and drawn a lot of attention on diverse

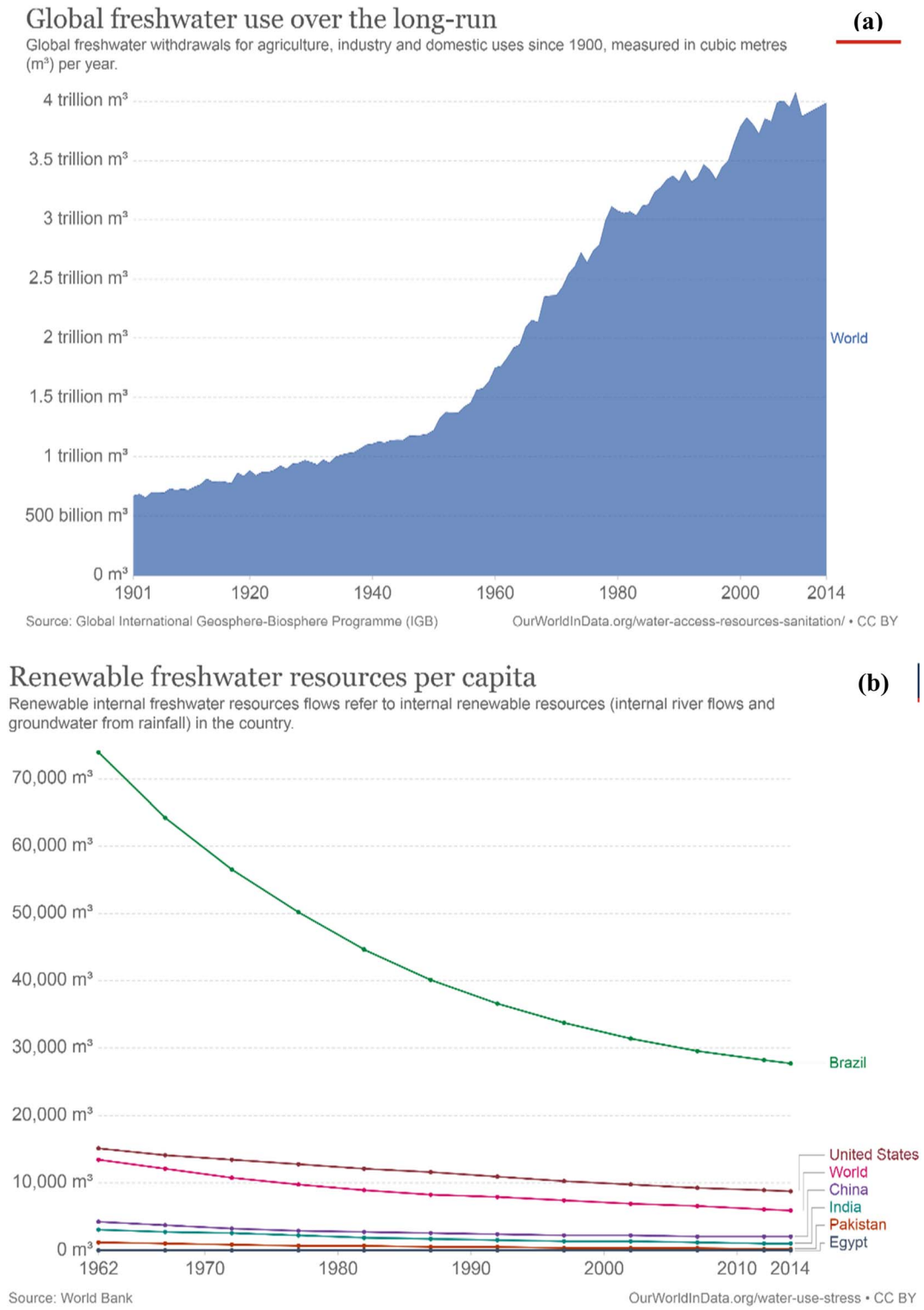

Fig. 2 Global freshwater demand and supply from 1962 to 2014. Long term freshwater use (a) and renewable freshwater resource per capita (b). This figure has been reproduced from ref. 16 with permission from World in Data, copyright 2017.

research fronts. Traditional strategies used to detect HM ions such as the inductively coupled plasma optical emission spectrometry (ICP-OES),[22,23] UV-vis spectrometry,[24–26] atomic absorption/emission spectroscopy,[27–29] and laser-induced breakdown spectroscopy (LIBS)[30,31] would be notoriously insufficient for *in situ*, fast, easy and low-cost operations hereby needed. This increasing mandate for real-time, on-site tracking of water quality, for human health and the

Table 1 Global fresh water use per annum. This table has been adapted from ref. 17 with permission from International Water Association Publications, copyright 2013[a]

Country	Start (billions m^3)	End (billions m^3)	Absolute change (billions m^3)	Relative change
BRICS	301.17 in 1901	1690 in 2010	+1390	+462%
OECD	117.35 in 1901	892.29 in 2010	+774.94	+660%
ROW	252.78 in 1901	1290 in 2010	+1040	+409%
World	671.31 in 1901	3990 in 2014	+3310	+494%

[a] Key: OECD nations: Organization for Economic Cooperation and Development. BRICS countries: Brazil, Russia, India, China, and South Africa. ROW: rest of the world.

environment, when compared to the growing threats to water safety in most African countries, requires competitively sensitive, affordable, and reliable technique, which exerts less pressure on the environment. Emerging electrochemical techniques for environmental monitoring offer significant potentials for portable, low-cost alternatives with high selectivity and low detection limits.[23]

Instrument-based electrochemical analysis techniques exploit the electrochemical properties of analytes in an electrolyte solution. This method began with C. Wickelman in the 19th century. A chemical battery provides part of its solution, while the concentration of the heavy metal ions is determined by varying diverse electrical parameters of the battery, such as its power, resistivity, conductivity, potential, current–voltage curve, which are dependent on the amount of the analytes. Although, ionic analysis that employs electrochemistry suffers from poor selectivity, it has other numerous potentials such as a broad range of measurement, extraordinary sensitivity, high accuracy, and simple instrumentation, based on measurable electrical parameters. Electrochemical analysis can be grouped into voltammetry, polarography, amperometry, potentiometry, and conductivity study,[32] which functions on three-electrode schemes: a counter electrode (CE), the working electrode (WE), and a reference electrode (RE), that is used to suggest a basis for evaluation and comparison of the electrical properties of the electrochemical setup.

The performance of the WE can be optimized by the modification. Voltametric analysis is commonly employed in the assessment of HMI, due to its high sensitivity, quick response, affordability, easy coupling with a chip, and simplicity in operation when compared with other detection techniques. Recently, different electrochemical voltametric techniques which include cyclic voltammetry (CV), square wave voltammetry (SWV), linear sweep voltammetry (LSV), staircase voltammetry (SV), anodic stripping voltammetry (ASV), cathodic sweeping voltammetry (CSV), adsorptive stripping voltammetry (AdSV), have been greatly exploited by numerous researchers and used in HMI detection in aqueous samples.[33,34]

This paper, hence, examines the sources and conditions of African waters, likely origins of HMs contamination of the water bodies, potential health hazards posed, and ultimately, the contribution of indigenous African electrochemists in the compelling demand to provide low-cost, on-site sensing and sensitive electrochemical strategies, for the assessment of heavy metal contamination of the available water sources.

1.1 Heavy metals and health hazards

Heavy metals are elements with atomic weights that range between 63.5 and 200.6, and bear a specific gravity above 5.0.[35] There are over 50 elements in this classification as HMs, and they are comprised of some metalloids, transition metals, actinides, and lanthanides. Among them, 17 elements are classified as being both extremely toxic and relatively accessible.[36] The impact of the increasing accessibility and/or discharge of some of these extremely toxic, environmentally harmful, and humanly carcinogenic metals, has been of grave research,[37,38] environmental,[39,40] and health[41–43] concern. There are millions of people with protracted poisoning from heavy metals. About 1.6 million children die annually from disease, which is often caused by contaminated water.[8]

In ideal cases of organic wastes deposited in an environment, microbial activities over some time result in microbial degradation that restores eco-balance and sometimes enriches the ecosystem. Contrarily, a number of the HMs connected with these biodegradable inorganic and organic contaminants, are non-biodegradable themselves, and therefore cannot be extracted or deactivated through any biological processes. Consequently, owing to their non-biodegradability, these metals stay long in the ecosystem, after any form of exposure.[36]

Even though some of these metals are required in trace concentrations for biological survival, their capability to displace other essential metals or modification of the veritable arrangement of biological molecules, resulting in the blockage of important functional groups in the biological system, affects the biological processes adversely.[41,43–47] However, some minimum amounts of some species of the HMs, such as manganese (Mn), iron (Fe), zinc (Zn), copper (Cu), and nickel (Ni), are vital elements in the human body and organisms. Above the permissible level referred to as the maximum concentration limit (MCL), they constitute a great danger to the environs as well as human health[48] (Table 2). For example, when the concentration of Ni is higher than the MCL, it could result in serious lung and kidney problems, as well as distress in the gastro-intestine, skin dermatitis, and pulmonary fibrosis.[49–52] Trace concentration of Zn is also essential in the human body. It plays a vital role in the physiological performance of living tissues, and regulations of various other biochemical processes.

Table 2 Selected HMs, their anthropogenic sources, provisional maximum tolerable daily intake (PMTDI) according to WHO, symptoms and resultant diseases when consumed beyond the PMTDI dose. This table has been adapted from ref. 68 with permission from MDPI, copyright 2019

HMs	Anthropogenic sources	PMTDI (mg L^{-1})	Symptoms and diseases	Ref.
As	Discarded wastes from industries, mining activities, insecticides, ceramics, pesticides herbicides, components of electronics, arsenic-based additives, electrical generation, biosolids, tanning, fertilizers, pyrite oxidation (FeS), arsenopyrite (FeAsS), feed additives, textile, and veterinary medicine, and metallurgy	10	Skin, bladder, kidneys, and lungs cancer, impact the peripheral nervous system (PNS), central nervous system (CNS), and results in heart and pulmonic diseases, and arsenicosis Diseases of the gastrointestinal tract, haemopoietin, genitourinary, skin, fetus and teratogen, brown skin-coloring and hyper-pigmentation, edema that is localized, and anorexia	69–71
Cd	Electroplating industries, batteries made up of nickel and cadmium, combustion of coals, plastic stabilizers, alloying industry, synthetic rubber, photographic and engraving process, petroleum refining photoconductors, paints, pigments, photovoltaic cells, electroplated parts, and plastics	3	Pulmonary fibrosis, hypertension, malformation of the skeleton, lymphocytosis, diabetes mellitus, toxicity in the renal system, loss of weight and strength, microcytic hypochromic anemia, and emphysema Osteomalacia, peripheral neuropathy, cancer of the lungs, osteoporosis, atherosclerosis, and hyperuricemia	72 and 73
Cr	Chemicals, coasting operations, data storage, textiles, leather tanning, pigments, wood treatment, metallurgy, achrome, and electroplating industries	50	Skin rash and ulcers, irritations and bleedings in the nose, debilitated immune system, mutation of genetic material, liver and kidney impairment, teratogenicity, toxicity in reproduction, embryotoxicity, causes mutation and cancer, dermatitis, septum perforation, and adverse reactions	71 and 74–77
Co	Aerospace, Li-ion batteries, porcelain, preparation of semiconductors, grinding wheels, hydrometers, nuclear medicine, electroplating, materials, enamel, and painting on glass	2	Diarrhea, irritations in the lung, defects of the bones, low blood pressure, genetic mutations in cells, and paralysis	78
Cu	Mining processes, kitchenware, pharmaceutical and chemical apparatus, manufacturing of papers	1500	Alzheimer's, convulsions, Parkinson's diseases, Wilson, liver and eye problems, cramps, vomiting, and Menkes	79
Fe	Mining, corrosion of metals, steel, and iron industries	N/A	Cancer, hemochromatosis, heart diseases, and eyes disorder	80
Pb	Sanitation PVC pipes, lead rich batteries, fuels, even lunch boxes, PVC lead paints recycling, electronics parts	10	Damage in the reproductive systems, damage of the CNS, kidney and liver diseases, barriers to protective blood	81–84

Table 2 (*Contd.*)

HMs	Anthropogenic sources	PMTDI (mg L^{-1})	Symptoms and diseases	Ref.
	manufacturing, processing of metals, pigments of painting, electroplating, mining activities, leather tanning, agriculture, jewelry, and lead batteries		in the brain which signifies a cause of Alzheimer's disease alongside doddering dementia, lowering of IQ and reduces the growth of the bones, attitudinal dysfunctions, hyperirritability, stupor, and ataxia	
Hg	Fungicides, facilities for plating metals, tanneries, pharmaceuticals, solders, vapor from mercury lamps, chemical compounds, emissions from volcanoes, filling of the teeth, catalysts, rectifiers, coal, solid and municipal waste burning, and, mining activities	1	Damage in the reproductive systems, impairment of the CNS, liver syndromes, distorted development of the neurons, impacts on the digestive and immune systems, kidneys, lungs, eyes, and skin, Minamata, acrodynia, surges in salivation, hypertension, and hypotonia	85
Mn	Manganese steels production, alloys of ferromanganese, and iron pipe corrosion	500	Psychological disorders, trembling, respiratory diseases, and lethargy	86
Ni	Surgical implants, nickel-based steel, super-alloys, electroplating, magnets from alnico, coinage, non-ferrous alloys, catalysts, microphone pods, rechargeable batteries, plumbing fittings plating, and dental prostheses	20	Anaemia, encephalopathy, hepatitis, lung, diarrhea, kidney impairment, gastrointestinal pain, pulmonic fibrosis, renal edema, dermatitis of the skin, dysfunction of the CNS	87 and 88
Zn	Zn alloys, anti-corrosion coating, rubber industry, cans, chemical industry producing pigments, paints, batteries, and soldering	3000	Respiratory breakdown, loss of appetite, diarrhea, headaches, lethargy, fever from metal fume, leukocytes of bronchiolitis, neuronal illness, risks of prostate cancer, macular deterioration, depression, and impotence	89–92
Ag	Copper refineries, zinc–nickel, gold, electroplating, and jewelry industries	100	Gastroenteritis, neuronal ailments, knotting, argyria, cytopathological influences in fibroblast, keratinocytes, rheumatism, mast cells, cartilage, and mental tiredness	93 and 94
Cu	Tanning, fertilizers, and photovoltaic cells	1300	Kidney dysfunctions, anemia, allergies, arthritis, diabetes, hemorrhaging, alopecia, adreno-cortical hyperactivity, autism, and cystic fibrosis	95

Nonetheless, above the permissible level, it could result in critical health threats, spiraling from vomiting, stomach cramps, nausea, anemia, to skin irritation.[53,54] Copper is vital for metabolism in animals. However, when the exposure becomes disproportionate, it could result in serious toxicological threats such as vomiting cramps, convulsions, and in some severe cases lead to death.[55]

Contrarily, some others (Pb, Cd, Hg, As, Sb, Cr, *etc.*) are highly toxic even in trace concentrations, could adversely affect the biological degradation process of organic matters, and are

Fig. 3 The sources of heavy metal pollution in African water bodies.

also harmful to humans.[36] With significant exposure in humans (through contact with some parts of the body, especially the mouth, skin, and airways) and subsequent adsorption and attachment to the erythrocytes, Pb could lead to pathological changes in the endocrine system and kidney which could cause failure in reproduction. Worst still is that apart from the extremely slow passage through urine, there are no other biological channels for removing the metal from the human body.[56] Mercury contamination in water is reported to be a neurotoxin that could result in the damage to the central nervous system.[57] A higher amount of mercury results in pulmonary and kidney function impairment, dyspnoea, and chest pain.[58,59] Minamata Bay is one of the classic instances of mercury poisoning.[60]

Exposure to Cd has been responsible for permanent tubular damage in the kidney,[61] increased chances of gene mutations,[60] reduction of semen quality,[62,63] impairment of visual motor, and loss of concentration.[64] Therefore, metals such as cadmium, lead, arsenic, chromium, and mercury are termed "environmental health hazards" and ranked among the first ten on the list of hazardous elements from "Agency for Toxic Substances and Disease Registry Priority List of Hazardous Substances", relative to substance toxicity and possible exposure to infested soil, air and water.[65–67]

Primary sources of the HMs contamination include anthropogenic-based release, and other natural sources like rainwater, weathering, and erosion from soil and rocks, domestic effluents, wastewater, industrial activities, *etc.*[8] (Fig. 3). In Table 2, different HMs, their origins in the ecosystem, and various threats to human exposure are represented.

1.2 Freshwater sources in Africa

Africa is the largest and the most populated continent on the globe after Asia.[45] The oldest sources of water in the then primitive African countries were streams, rivers, and natural rainfall.[96] With growing technology, groundwater supply *via* wells and boreholes began to slowly replace dependence on the streams, rivers and natural rainfall.[96] In some urban places, these same sources of water have become necessary substitutes to the unsteady supply of pipe-borne water, which would have been a more dependable source of potable water for African sprouting population.[96] Likewise, the greater percentage of the world population of about 7 billion people (UNFPA, 2011) depend on groundwater supplies and close to 16% of them lack access to safe water and have to resort to the available but unsafe surface and groundwater[96] (Fig. 4).

1.3 Sources of heavy metal pollution in African water bodies

Population growth, leading to expanding settlement, urbanization, and accompanying industrialization has increasingly exposed African water bodies to heavy metal contamination.[97–100] Poorly treated or incompletely treated industrial and domestic effluents are steadily discharged into the ecosystem. These sources accidentally account for the greatest origin of HM contamination of the aquatic system across the globe.[99,101]

The classification of HM contamination in terms of the source is either anthropogenic or natural sources.[99] Most HM contamination in rural sources originates from natural activities, while that of the urban regions is generated from anthropogenic (human) activities.[99,100] However, indiscriminate mining activities in some rural areas could also lead to significant contamination of

Fig. 4 Some freshwater sources in African countries. Copied from different Google Sources (2020).

freshwaters in such vicinity.[102] Natural origins of HM pollution in numerous African rural settlements include bush burning, weathering of mineral deposits, wind-borne dust, leachate, dry and wet fallouts of atmospheric particulate matters, and volcanic eruptions.[99,102] Anthropogenic origins include indiscriminate discharge of industrial effluents, production of steel and refining of petroleum, fossil fuel and coal combustion, mining and metal processing, production of ceramics and cement, solid waste disposal, fertilizers, manufacturing of paint and batteries,.[102] Other sources also include ore transportation, mineral explosion, refining and smelting, tailings and disposals of mine wastes and heaped waste materials in mining sites and rocks' weathering, *etc.*[103,104]

In a report by Reza and co-workers[105] mines and abandoned runoffs, and associated industrial discharges make up the main origins of HM pollution, total dissolved solids (TDS), and high acidity for streams near mining sites.[106–109] The rivers in urban areas suffer largely from pollution. This is due to the tradition of disposing small scale industrial and domestic wastes into the water bodies, consequently resulting in a rise in the degree of concentration of metals in river water.[110–114]

The majority of the existing scientific reports about the various sources of water in Africa and their condition relative to their safety are very concerning. A closer examination of them leaves environmentalists worried about the fate of the populace that depends on such water for livelihood, given the concomitant health risks. A broad spectrum of such scientific studies was considered in specific detail to bring home the picture and create a tangible background to this review. A summary of reports indicating the ratio of the HMI concentration found in some of the African water samples studied to their corresponding maximum concentration limit (MCL), permissible by some environmental agencies (Table 3) and World Health Organization (WHO) (Table 4) were calculated and represented in Table 5. Such levels of contamination present serious environmental threat.

Table 3 Guidelines for metals in seawater and sediment. This table has been adapted from ref. 115 with permission from African Journal Online (AJOL), copyright 2001[a]

	Seawater (ppb)		Sediment (mg g^{-1})	
HM	EEC	ANZECC	CEPA	PSAG
Cd	2.5	2	2	10
Cu	5	5	8	500
Fe	—	—	—	—
Pb	15	5	22	500
Mn	—	—	—	—
Zn	40	50	40	750

[a] EEC: European Economic Community; ANZECC: Australian and New Zealand Environmental Conservation Council; CEPA: Canadian Environmental Protection Agency; PSAG: Proposed South African Guidelines.

1.4 Point-of-care monitoring

Considering the status quo, sensors fabricated primarily for the detection of HMIs and techniques for the removal of HM are indispensable in the environmental,[120,121] food,[122] drinking water and biological fluids,[123] and health[124] analysis. In addition to the broad sensing spectrum, quick response, and high sensitivity that is generally expected in sensing parameters,[125] other factors including reduced cost and ease of operation are consequently and increasingly becoming very pivotal.[126] Top ranking conventional techniques such as inductively coupled plasma optical emission spectrometry (ICP-OES), atomic absorption/emission spectroscopy, UV-vis spectrometry, laser-induced breakdown spectroscopy (LIBS)[123] were used in all the

Table 4 Standards and guidelines for HMs concentration (mg L^{-1}) in drinking water as recommended by the WHO, US-EPA, ECE, FTP-CDW, PCRWR, ADWG, and NOM-127. This table has been adapted from ref. 116 with permission from Nigerian Journal of Technological Development, copyright 2016[a]

Metal	WHO	EPA	ECE	FTPCDW	PCRWR	ADWG	NOM-127
Nickel	0.07	0.04	0.020	—	0.020	0.020	—
Copper	2	1.3	0.200	0.100	0.200	0.200	0.200
Zinc	3	5	—	5.000	5.000	3.000	5.000
Cadmium	0.003	0.005	0.005	0.005	0.010	0.002	0.005
Mercury	0.001	0.002	0.001	0.001	0.001	0.001	0.001
Lead	0.01	0.015	—	—	—	—	—
Arsenic	0.010	0.010	0.010	0.010	0.050	0.010	0.025
Antimony	0.020	0.006	0.005	0.006	0.005	0.003	—
Iron	—	0.300	0.200	0.300	—	0.300	0.300
Uranium	0.030	0.030	—	0.020	—	0.017	—
Manganese	0.10	0.500	0.500	0.500	0.500	0.500	0.150
Thallium	—	0.002	—	—	—	—	—
Silver	—	0.100	—	—	—	0.100	—
Chromium	0.050	0.100	0.050	0.050	0.050	0.050	0.050

[a] WHO (2011): World Health Organization; USEPA (2011): The United States Environmental Protection Agency; ECE (1998): European Commission Environment; FTP-CDW (2010): Federal-Provincial-Territorial Committee on Drinking Water Health Canada; PCRWR (2008) Pakistan Council of Research in Water Australian Drinking Water Guidelines, DDWG (2011); Australian Drinking Water Guidelines; NOM (127-SSA1-1994): Norma Official Mexicana.

Table 5 Heavy metal pollution level in some selected African water bodies. This table has been reproduced from ref. 117 with permission from IntechOpen, copyright 2021[a]

HM/water source	$\frac{[Pb]}{[Pb]_{WHO}}$	$\frac{[Cd]}{[Cd]_{WHO}}$	$\frac{[Hg]}{[Hg]_{WHO}}$	$\frac{[Cr]}{[Cr]_{WHO}}$	$\frac{[Cu]}{[Cu]_{WHO}}$	$\frac{[Zn]}{[Zn]_{WHO}}$	$\frac{[Fe]}{[Fe]_{WHO}}$	$\frac{[Mn]}{[Mn]_{WHO}}$	$\frac{[As]}{[As]_{WHO}}$	Ref.
LVEA-MGP	2.2	2.3	0	1.4	—	0.006	—	—	—	118
LVEA-WGP	82.3	0	0	3.56	—	0.017	—	—	—	118
BHMPRSAJ	>8	—	—	>0.2	>0.01	>0.03	—	>1		104
Dzindi river	3	—	—	—	0.025	0.033	4.4 33	1.5		102
AAP	—	1.7	2	—	—	0.043	2.233	8.54	0.3	119
OAP	—	1.7	3	—	—	0.00167	3.11	7.92	0.3	119
US	—	1.7	2	—	—	0.00167	4	7.23	0.3	119
MS	—	5666.7	9	—	—	0.0097	4.74	5.77	0.2	119
DS	—	1.7	154	—	—	0.0547	22.2	8.72	0.2	119
AB	—	2.7	2	—	—	0.0013	5.9	1.13	0.4	119
LWW	102	183.3	—	22	0.255	1	—	—		61
PBW	279	476.7	—	100	1.51	4	45.4	175		96
BH	455	463.3	—	326.8	0.58	4.923	77.5	991.4		96
STREAM	29	746.7	—	402.2	1.755	2.063	20	113.2		96
RIVER	669	1546.7	—	101.2	1.075	1.547	105.8	61.2		96
HDW	401	320	—	2275.6	23.175	49.1	47.1	936.5		96

[a] LVEA-WGP: Lake Victoria East Africa-Winam Gulf Point; LVEA-MGP: Lake Victoria East Africa-Mwanza Gulf Point. BHMPRSAJ: Borehole at Mpumalanga South Africa, ELH: East London Harbour, PEH: Port Elizabeth Harbour; Accra Abandoned Pit (AAP), OAP: Obuasi Abandoned Pit, AB: Accra Borehole, US: upstream, MS: main stream, DS: down stream; WW: Lagoon wastewater; BH: borehole, HDW: hand-dug well; PBW: pipe borne water.

studies summarized in Table 5. Nonetheless, some abhorrent limitations such as wearisome sample preparation and pre-concentration, high professionalism required in personnel operation, and huge investment and maintenance costs impede the use of such techniques, notwithstanding their high sensitivity, and selectivity.[125,127] Consequently, these methods are not congruent with the fast, cheap, and on the site measurement required in the compelling and continuous assessment of HMI in most African countries.[121] The expanding demand for *in situ*, on-site tracking of the quality of water especially for environmental safety and human health, demands a comparatively highly sensitive and dependable technique that is cost-friendly and exerts less pressure on the ecosystem.[121,128]

Therefore, electrochemical sensors (ECS) could be easily put into a compact system that is affordable, easy to operate, and possible for the required outdoor application. Additionally, because HMs ions have pronounced redox potentials, the selectivity towards particular metal ions can be obtained by ordinary electrodes that do not necessarily involve a probe for molecular recognition. This technique depends on the electrocatalytic oxidation of pre-concentrated deposited analyte on the prepared electrode surface. They have been employed in a broad scope of applications such as food quality control, detection of chemical threats, environmental safety monitoring, and medical diagnostics. Several electrochemical strategies often recently employed include amperometry, voltammetry, impedemetry, conductometry, and potentiometry.[32,129]

1.5 Electrochemical sensor (ECS) materials

The choice of electrode material is one of the most important aspects of electrochemical sensing strategies.[130] Different authors have reviewed, in some very impressive detail, the various electrode materials deployed in different electrochemical techniques.[121,130–132] Mercury-based electrodes have been the traditional choice for HMI detection.[129] However, mercury-based electrodes are highly toxic and not easy to handle. Hence, the quest for environmentally benign electrodes necessitated the complete replacement of such electrodes despite having high sensitivity, and a broad range of cathodic potential reproducibility. To respond to this quest, a bismuth-modified electrode became a good alternative to the toxic electrode. Although, concerns over the environmental friendliness of mercury electrodes were being sufficiently addressed by the use of bismuth (Bi) modified electrodes, a narrow range of cathodic potential and quick natural oxidation in the air became a huge setback on the use of the latter. To address this setback once again, researchers have shown that the incorporation of certain carbon-based materials such as graphene oxides and carbon nanotubes could enhance the senility and performance in the electrochemical sensing of HMIs.

Summarily and similarly, other solid electrodes including boron (B), platinum (Pt), glassy carbon electrodes (GCE), graphite, and gold doped diamond electrodes have also been employed in the quantification of HMIs using the ASV techniques.[133] But the general sensing parameters of these electrodes without modification in mercury sensing rudimentary analysis has been poor. The films deposited and contact surfaces interact in multiple orders, leading to a multiplicity of stripping peaks. Likewise, the use of bulk electrodes (BE) in HMI detections is limited by low sensitivity, significant overpotential for analyte deposition, high stripping potential, and ionic interferences originating from both the attached metals and supporting electrolyte. These drawbacks render the BE invalid for the detection of HMI. To address this setback again,

the modification of the bulk electrode surface with NPs for enhanced performance was introduced.[134,135]

With the introduction of screen printing technology, screen-printed electrodes (SPEs) mass production has been largely achieved.[136] Screen-printed electrodes share similar electrochemical properties with traditional BE and possess the superiority of easy operation, the ability for outdoor and real-time sensing applicability over the bulk counterpart. These portable tools are made up of planar plastic or ceramic matrix, which carry the reference, counter and WEs configured on them. Hence, SPEs are applicable test strips that could be disposed off after use, for electroanalytical measurements. Additionally, the necessity of micro capacity of analyte and lesser power, shorter time of response, and extraordinary sensitivity put the SPEs as the most appropriate ECS for *in situ* analysis.

More so, the ease of modification of the surface of the SPEs using materials like, organic compounds or mediators and nanoparticles has immensely enhanced their sensing parameters, *vis-à-vis* sensitivity, and selectivity.[137] This has made them viable tools as transducers in a broad range of biosensors: enzymatic, chemical, immuno- and geno, and apta sensors among others. The use of these electrodes in electrochemical analysis, following modifications, has demonstrated spectacular improvement in selectivity and sensitivity and amplified the possibility of multiple detections of HMIs. Other benefits of this single-use disposable sensor consist of riddance of the difficulties inherent with the residue of biofouling or impurity and lowering the concern of damaging sensors that could be reused.

In the final analysis, to offset these limitations, most literature reports concluded that superior electrode/sensor materials are hybrid materials, incorporating various materials with diverse complementary and supplementary properties.[138,139] Such a blend of materials would include those with: (1) higher conductivity to foster electron transfer, (2) greater porosity for higher surface area with more active sites for either bonding of metal ion or loading of the active component, and (3) surface functional groups for improved bonding of metal and/or selectivity towards a particular target metal ion.[121]

1.6 Electrochemical detection of HMs: indigenous African contributions

1.6.1. Single detection

1.6.1.1. Arsenic detection. To investigate the presence of arsenic (As) in water samples, using electrochemical strategies, Jimana and co-workers[140] carried out a voltametric analysis of As^{3+} in a river in Pretoria, South Africa, using Co NPs/rGO modified exfoliated graphite electrode (eGE) (Fig. 5). Using the SWASV technique, HCl supporting electrolyte, a deposition potential (DP) of −1.0, deposition time (DT) of the 90 s, and a concentration range of 1–50 ppb of As(III), they obtained a linear variation of the peak currents with As^{3+} concentration with a regression coefficient (R^2) of 0.9984. The limit of detection (LOD) and limit of quantification (LOQ) calculated were 0.31 ppb and 1.01 ppb respectively, which is far lower than the limits set by WHO (Table 3). They also considered the performance of the modified electrodes relative to other sensing parameters such as reproducibility, repeatability, and selectivity. The modified electrodes were found to be reproducible and selective with only Cu^{2+} ion serving as the interference in the presence of other anions like Na^+, Ca^{2+}, Mg^{2+}, Cr^{6+}, and Pb^{2+}. Subsequently, real sample analysis was reported using river water samples from Pretoria, South Africa, and compared the result with the ICP-OES analysis. The As^{3+} concentration found in the water samples using the proposed sensor and ICP-OES were 9.35 ± 0.25 ppb and 9.44 ± 0.18 ppb respectively. The closeness of these values further validated their conclusion that the modified electrode could be adapted for monitoring As^{3+} in real environmental samples.

Mafa and co-workers[141] also employed the SWASV to inspect the presence of As(III) in industrial influent and effluent water samples in South Africa, using the same eGE modified with gold nanoparticles (Au NPs) (Fig. 6).

Given an optimal pH of 3, DT of 180 s, the potential of −0.8 V, 0.05 V pulse amplitude, and 5 Hz frequency, a LOD and LOQ of 0.58 μg L^{-1} and 1.95 μg L^{-1} respectively with $R^2 = 0.9993$ were calculated on EG-AuNPs electrode. Over a detection range of 1–50 ppb, they obtained a corresponding linear equation represented by:

$$I_p\,(A) = 4.6321 \times 10^{-6} C\,(ppb) + 4.2878 \times 10^{-7}$$

where C = concentration in ppb (Fig. 7).

The fabricated electrode was tested for reproducibility, repeatability, and selectivity. The result showed that the electrode was of analytical significance. However, Cu^{2+} at a higher concentration (>20 ppb) proved to be an interference, which was mitigated with the introduction of ethylenediaminetetraacetic acid (EDTA). Nonetheless, they reported that Cu^{2+} did not interfere with As^{3+} in real sample analysis. The real sample analysis of the industrial water was compared with the results from the ICP-OES data and found to be reasonably close. The concentration of the influent water as measured by this technique and ICP-OES were 5.8 2 ± 0.42 ppb and 5.60 ± 0.44 respectively, while the concentration of As(III) in the effluent water measured by this technique and ICP-OES were 11.9 ± 10.19 and 10.70 ± 0.07 respectively. This was considered an improvement on earlier work using Bi-NPs to modify eGE to detect As(III), which resulted in an LOD of 5 ppb[142] under optimum conditions itemized in Table 6.

Idris and co-workers,[143] advanced the study and reported a LOD of 0.28 ppb of As(III) under the optimum condition of pH 1, DP of −0.6 V, 60 s pre-concentration time, and 0.1 M H_2SO_4 supporting electrolyte using SWASV on Au-NPs/GCE. Over a broader As(III) concentration ranging from 0.01–50 mg L^{-1}, a linear regression of $I_p = 5.4923 \times 10^{-4} C + 8.58 \times 10^{-3}$ with a correlation coefficient of 0.98843 was generated. The stability and selectivity analysis posit that the modified AuNPs/GCE could be used repeatedly without compromising its sensitivity and selectivity in interference of Ca^{2+}, Na^+, K^+, and Mg^{2+} respectively. However, it was prone to interferences from Cd^{2+}, Cu^{2+}, and Hg^{2+}. In some sense, this work improved on previous works by the group, *viz.* LOD, sensitivity, and stability.

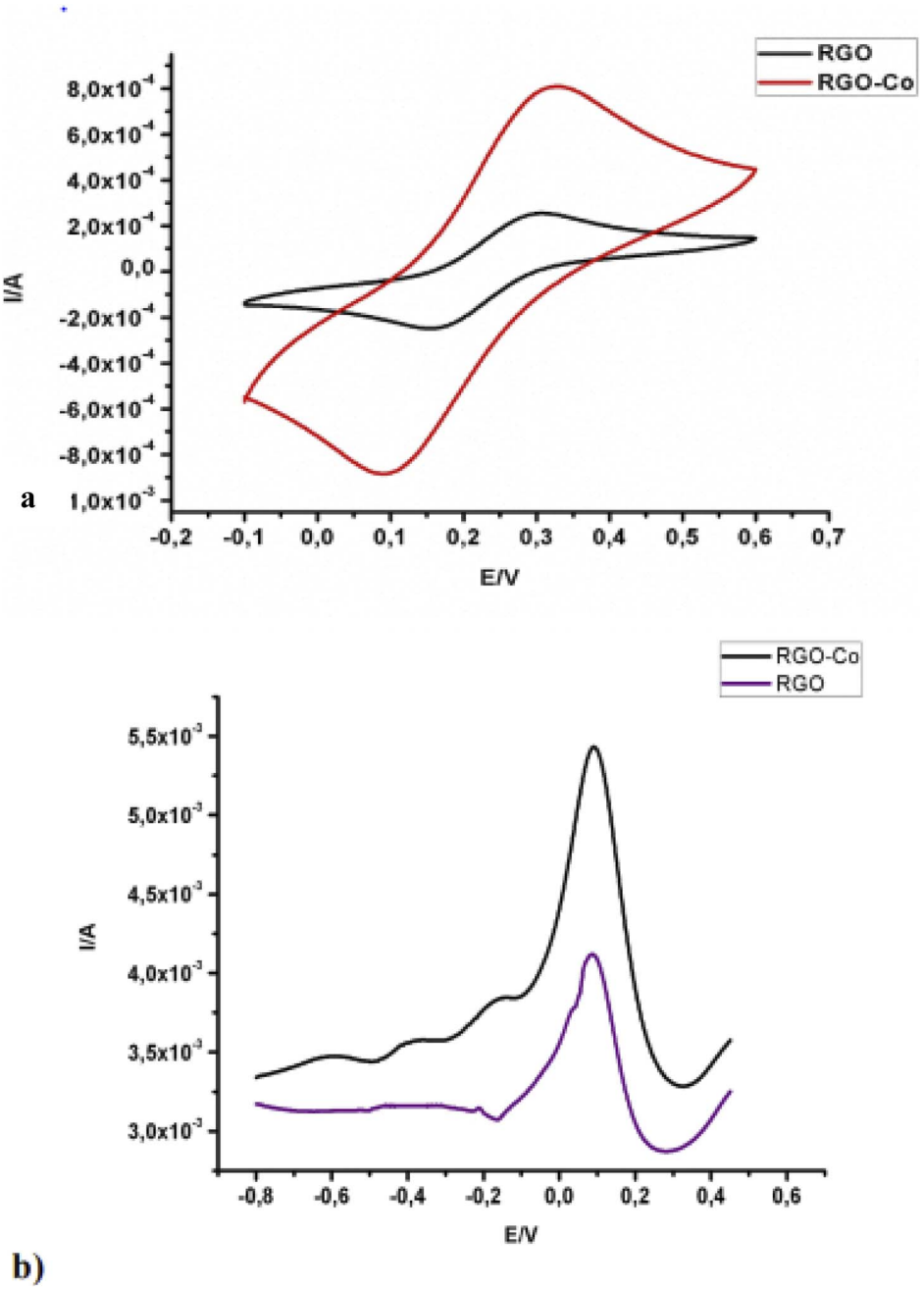

Fig. 5 CV of (a) rGO, and rGO-Co electrodes in 5 mM $[Fe(CN)_6]^{3-/4-}$, (b) SWV at rGO and rGO-Co in As^{3+} solution. This figure has been reproduced from ref. 140 with permission from Elsevier, copyright 2014.

The real-life sample validated the potential of the applicability of the fabricated electrode in environmental monitoring. The GCE-AuNPs and ICP-OES analysis at $n = 3$ resulted in As(III) concentrations of 10.4 (±0.26) ppb and 10.7 (±0.22) respectively.

Bimetallic nanostructured materials (Fig. 8), either as alloys or core–shell NPs have been exploited as sensing elements for the electrochemical analysis of HMIs.[144–146]

The advantage of this group of materials is due to their optical, catalytic, and magnetic characteristics that present pronounced additional benefits over those of their constituent individual counterparts.[145,147] By deploying the suitable functional monomers, cross-linking, and template ions, the technique can be employed to assemble a very selective, sensitive, and cheap probe that is hinged on printed techniques for the detection of HM in water and biological samples, because of its rich properties featuring high surface area and a 3D framework made of highly open spaces that are interconnected to each other. Arotiba and co-workers[148] used aptamer-carbon-gold binanoparticle modified GCE (Apt/CNPs/AuNPs-GCE) on ASV strategy to trace As^{3+} in water samples. Good reproducible, sensitive, stable, and selective (Fig. 9) results were generated, at

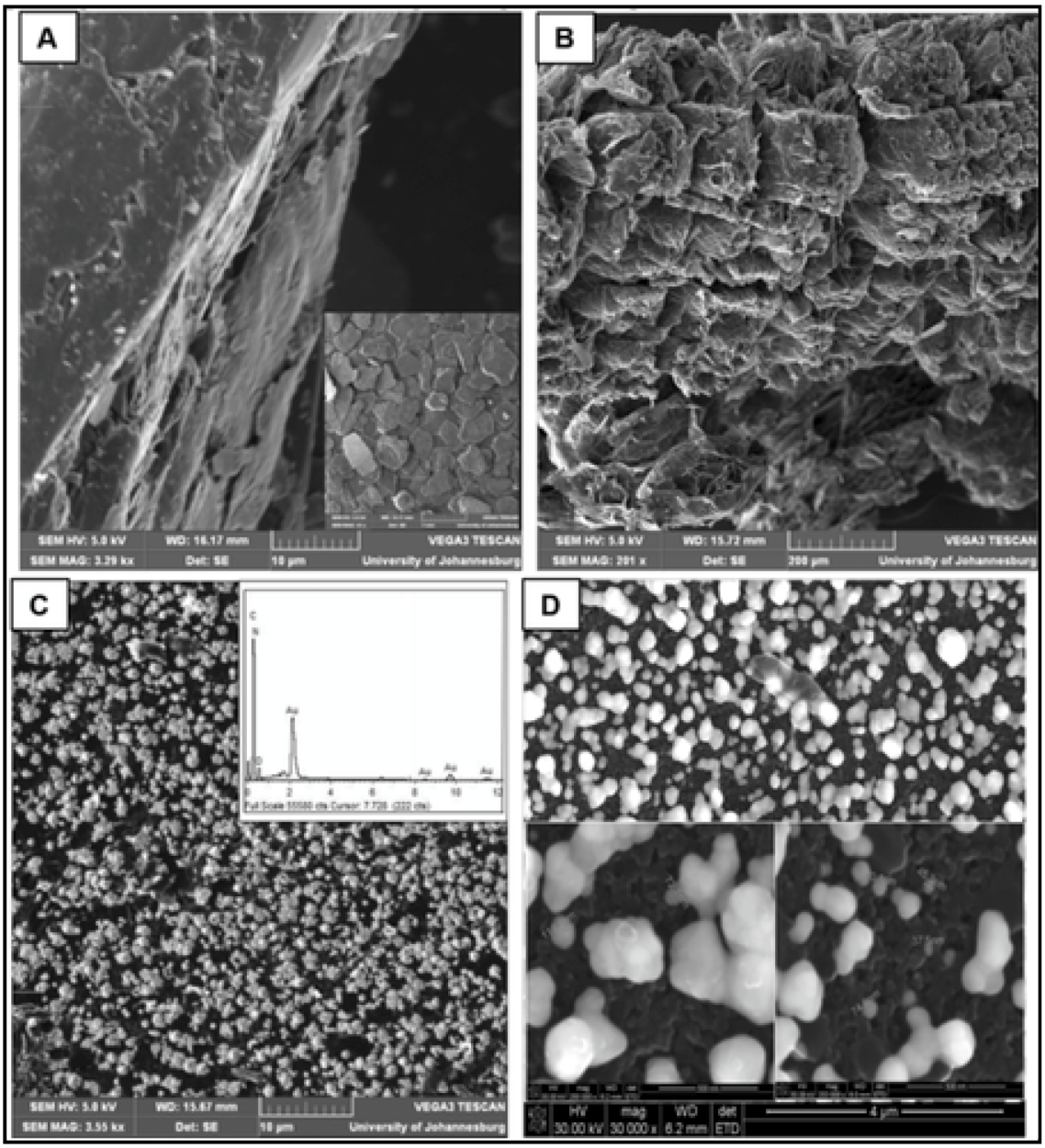

Fig. 6 Micrographs of (A) NGF; (B) EG; (C) EG-AuNPs (inset is the EDX spectrum); (D) EG-AuNPs on FE-SEM. This figure has been reproduced from ref. 141 with permission from Elsevier, copyright 2019.

optimal conditions, with a LOD of 0.092 ppb. The synergy between the two nanoparticles was able to eliminate the interference from Cd^{2+}, Cu^{2+}, and Hg^{2+} common in the detection of As^{3+}. Table 6 compares the LOD using voltametric detection of As(III) in water samples with other recent reports from other counterparts around the world.

1.6.1.2. Cadmium sensing. Fakude and co-workers[169] reported the detection of Cd^{2+} using SWV on carbon black gold nanoparticles aptamer modified screen printed carbon biosensor electrode-CB-Au NPs-Apt-/SPCE to get a LOD and LOQ of 0.14 ppb and 0.47 ppb respectively. Over the analyte concentration range of 1–50 ppb, in a 10 mM PBS, pH 7.45 supporting electrolyte, with an incubation time of 30 min, they obtained a linear regression of the Cd^{2+} concentration and current expressed as I_p (μA) = 0.2613C + 3.1216, where C is the concentration of Cd in ppb, a regression coefficient of 0.9926. The engineered aptasensor (Fig. 10) was analyzed for stability, reproducibility, and selectivity and was found to be of analytical consequence.

They sought to improve the selectivity of the aptasensor towards Cd(II) in the presence of peculiar interferences from Zn^{2+}, Cu^{2+}, and Pb^{2+}, among other likely interferences from Cr^{4+}, Mn^{2+}, Ca^{2+}, Ag^{+}, Mg^{2+}, As^{3+}, Se^{4+}, and Co^{2+}. Based on initial works, Pb^{2+}, Cu^{2+} and Zn^{2+}, can interact with aptamer in a very counterproductive way. To alleviate that, nitrilotriacetic acid (NTA) was introduced to play the role of a masking agent that

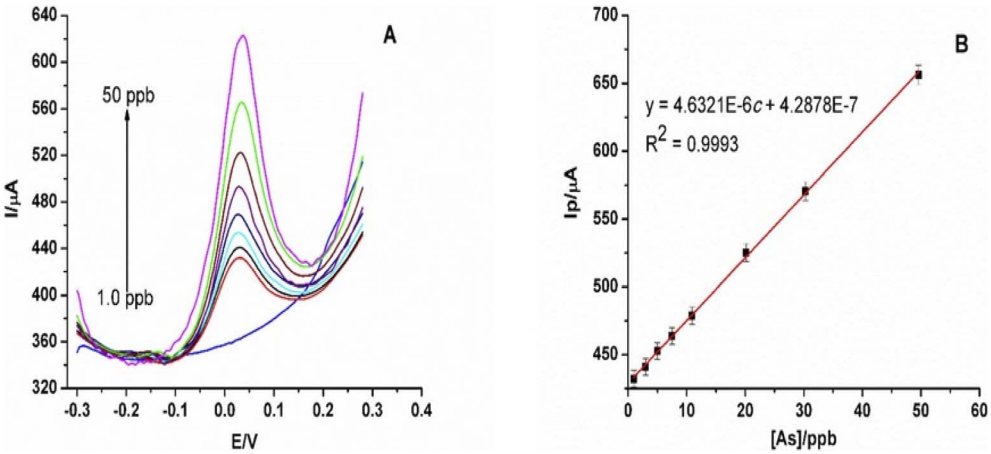

Fig. 7 (A) SWASV of different concentrations of As(III) (linear range: 1.0–50 ppb) at EG-AuNPs electrode; (B) calibration plot of peak current *vs.* As(III) concentrations. Potential *vs.* Ag/AgCl (3 M KCl). This figure has been reproduced from ref. 141 with permission from Elsevier, copyright 2019.

Table 6 Comparing the LOD using voltametric detection of As^{3+} in water samples of recent reports from various researchers[a]

WE	LOD (ppb)	Electrolyte	Detection time (s)	Technique	Continent	Ref.
Co NP-rGO/EG	0.310	HCl	90	SWASV	Africa	140
Au-CFE	0.900	0.1 M HCl	10	DPSV	South America	149
AuNPs–CeO_2–ZrO_2/GCE	0.137	0.1 M HAc–NaAc	150	SWASV	Asia	150
Porous Au/GCE	0.490	0.5 M H_2SO_4	800	ASLSV	Asia	151
$[Ru(bpy)_3]^{2+}$–GO/SPE	1.573	0.1 M citrate buffer	—	DPASV	Asia	152
PEDOT/Pd	0.52	1.0 M HCl	120	DPASV	Asia	153
Pt NPs/GCE	—	0.5 M H_2SO_4	90	SWASV	Asia	154
TTCA/rGO/AuE	0.054	—	—	SWASV	Asia	155
Bi-NPs/EG	5.0	0.1 M KNO_3	180	SWASV	Africa	142
UMEA/AuE	0.05	2.0 M HCl	80	SWASV	USA	156
CB-AuNPs/SPE	0.4	0.1 M HCl	300	ASV	Europe	157
AuNPs/GCE	0.0096	1.0 M HCl	180	LSV	Europe	158
AuNPs/GCE	1.8	3.0 M HCl	30	ASV	Asia	159
AuNPs/EG	0.58	1.0 M HNO_3	180	SWASV	Africa	160
AuNPs/SPE	0.4	1.0 M HCl	160	LSV	Europe	161
MnOx–AuNPs/GCE	0.057	0.1 M CB	200	LS-ASV	Asia	162
Au-CRV/GCE	15.0	PBS	—	DPV	Asia	163
AgNPs/GCE	1.2	1.0 M HNO_3	120	DPSV	Asia	164
GCE AuNP	0.28	0.1 M H_2SO_4	60	SWASV	Africa	165
SWCN GCE	0.008	0.1 M ABS	600	LSV	Asia	166
GENC	0.047	0.1 M EDTA and 0.1 M PB	120	SWV	Asia	167
Ibu-AuPNFs-SPCE	0.018	1 M HCl	180	CV	Asia	168
Apt/CNPs/AuNPs–GCE	0.092	10 mM PBS	—	ASV	Africa	148

[a] EG: exfoliated graphene; CFE: carbon fiber electrode; AuE: gold electrode; SPE: screen printed electrode; GCE: glassy carbon electrode; CB = carbon black; UMEA = ultramicroelectrode array; Au-CRV = gold-crystal violet; PEDOT = poly(3,4-ethylenedioxythiophene); SWCN—single-walled carbon nanotubes, GENC—gold-embedded Nafion composite, Ibu-AuPNFs-SPCE—ibuprofen-gold nanostructured screen-printed carbon electrode.

could undermine possible interferences and subsequently achieved the desired result. Using industrial effluent water and tap water as real-life samples, they obtained Cd^{2+} concentration in the former and latter to be 1.421 ppb and 0.000 ppb respectively. Using ICP-OES analysis as a basis for validation of the aptasensor, close values were realized with both techniques.

Amongst the electrochemical biosensors, electrodes modified by enzymes have gained more relevance and consequently have been deployed either directly or indirectly making use of the effects of inhibitors on trace metal ions on the enzyme.[120,170] Mambo *et al.*,[120] used a more 'indigenous and ingenious' horseradish peroxidase (HRP) biosensor. The bio-based sensor was prepared from carbonized natural organic material of maize tassel. MWNTs treated electrode for the quantification of divalent HMIs and Cd^{2+} used as a reference divalent metal.

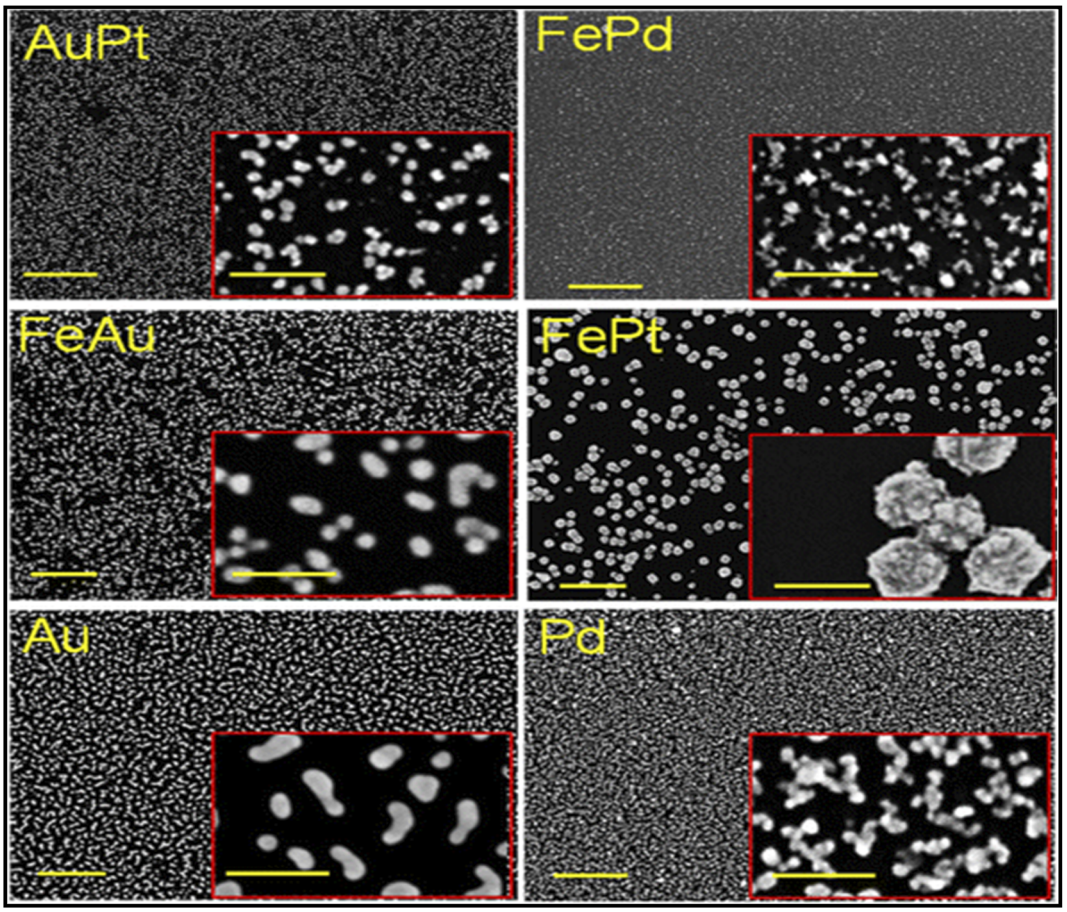

Fig. 8 SEM images of $Au_{45}Pt_{55}$, $Fe_{70}Pd_{30}$, $Fe_{40}Pt_{60}$, and $Fe_{10}Au_{90}$ bimetallic NPs and pristine Au and Pd NPs and their higher magnification images in the insets, with scale bars of 500 and 100 nm, respectively. This figure has been reproduced from ref. 144 with permission from American Chemical Society (ACS), copyright 2015.

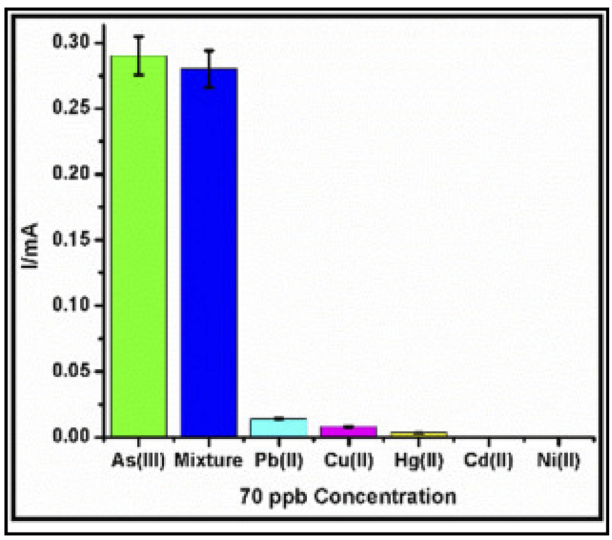

Fig. 9 Aptasensor selectivity test. This figure has been reproduced from ref. 148 with permission from Elsevier, copyright 2019.

In 0.1 M phosphate buffer solution (PBS), pH 7.0, with 20 min DT, using LSV, they realized a linear response over a 2–30 ppb Cd^{2+} concentration range, and LOD of 0.51 ppb. They concluded that the biosensor could be used for environmental applications but failed to establish the reproducibility, stability, and application from real samples analysis (Table 7).

1.6.1.3. Copper sensing. Ndlovu and co-workers[175] used SWASV on CoO NPs/eGE to investigate the quantity of Cu^{2+} present in water samples from a dam and bottled water. Under the procedural conditions of using 0.1 M HNO_3 supporting electrolyte, DP of −0.5 V and DT of 300 s, over a linear range between 100 and 2000 ppb, the peak current and the copper concentration had a response with a linear regression equation of I_p (A) $= 1.086 \times 10^{-4}C - 2.374 \times 10^{-7}$, ($C$ = concentration of Cu^{2+}), the regression coefficient of 0.998 and LOD of 94 μg L^{-1}. They argued that the low LOD obtained was first the result of the efficient sensitivity of the SWASV technique used, and secondly the contribution of the CoO in enhancing the signal of Cu^{2+} through increasing the electroactive surface area and conductivity of EG electrode and eventually causing amplification of the signal during electroanalysis. The electrode was analyzed for stability, reproducibility, and selectivity and was found to be of analytical importance in environmental monitoring. The real sample result from the analysis of the bottled water and dam using the CoO-EG electrode and the present technique was comparable with that of the standard technique-FAAS. On the

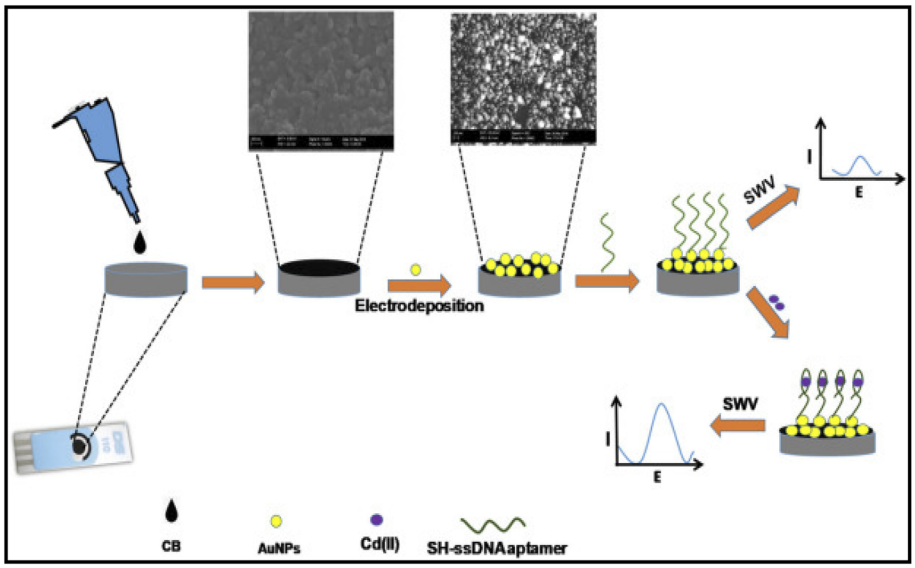

Fig. 10 Graphical demonstration of the procedure of fabrication and principle of detection of the Cd^{2+} using the aptasensor. This figure has been reproduced from ref. 169 with permission from Elsevier, copyright 2019.

Table 7 Comparing the LOD using voltametric detection of Cd^{2+} in water samples for a pool of data from different sources[a]

Working biosensor	LOD (ppb)	Electrolyte	Linear range (ppb)	Technique	Continent	Ref.
Au/aptamer	92	10 mM ABS/$NaClO_4$ (pH = 4.5)	250–1000	ACV	USA	171
ssDNA/Au	0.3	50 mM PBS (pH = 7.0)	1–20	CV	Asia	172
dsDNA-CPE	0.0003	0.50 M ABS (pH = 4.8)	0.01–1	DPV	Asia	173
BiNPs-SPE	3	0.1 M KCl (pH = 6)	0.1–150	LSV	Asia	174
SPCE-CB-AuNPs-Apt	0.14	10 mM PBS (pH = 7.45)	1–50	SWV	Africa	169
HRP-MT-MWCNT	0.51	0.1 M PBS (pH = 7.0)	2–30	LSV	Africa	120

[a] ssDNA/Au: single-stranded DNA modified Au electrode, dsDNA-CPE: double-stranded DNA-carbon printed electrode. BiNPs-SPE: bismuth NPs-screen printed electrodes. MWCNT: multi-walled carbon nanotubes.

crucial issue of the safety of our drinking water, the functionalized electrode was able to detect far below the standard for drinking water by WHO (Table 3). Additionally, the quantity of Cu^{2+} ions found in both water samples was within the limit of acceptance for safe drinking water (Table 8).

1.6.1.4. Mercury sensing. Mercury remains one of the most toxic elements in ecosystems due to its high reactivity, life-threatening volatility, and relative solubility in water and biological tissues.[182] Notwithstanding several research efforts lately, mercury contamination of soils, groundwater, sediments, and industrial effluents is a cause for concern. Additionally, the vast aqueous media mobility and extreme toxicity demand effective strategies for its detection and appropriate technologies for their quantification and monitoring in the

Table 8 Comparing the LOD using voltametric detection of Cu^{2+} in water samples of recent reports from various researchers[a]

Working electrode	LOD (ppb)	Electrolyte	Linear range (ppb)	Technique	Continent	Ref.
Ni/NiO/ZnO-6/CS	0.13	PBS (pH = 7.0)	0–958	DPV	Europe	176
GA-UiO-66-NH_2/GCE	7	0.2 M ABS (pH = 5.0)	100–3500	DPSV	Asia	177
ZIF-67-EG	2.23	0.1 M ABS (pH = 5.0)	500–3000	SWASV	Asia	178
AuNPs/CNFs/GCE	100	0.1 M PBS, (pH = 6.8)	100–1000	SWASV	Asia	179
Cu^{2+}-IIP film	2.7	50 mM ABS (pH = 5)	0.95–15.2	DPV	Europe	180
APS-CPE	0.003	0.1 M HNO_3 (pH = 1)	0.05–0.2	SWASV	Europe	181
CoO-EG	94	0.1 M HNO_3	100–20000	SWASV	Africa	175

[a] CCSC: Constant Current Stripping Chronopotentiometry; APS: aminopropyl-grafted silica gel. DPV: differential pulse voltammetry. NiC: Ni/NiO/ZnO/CS wire (CS: chitosan). IIP: ion-imprinted polymeric film. ZIF-67: Co-based zeolitic imidazolate framework-expanded graphite.

environment.[121] Matlou and co-workers[125] conducted a study on Hg^{2+} ion detection in water using self-assembled SWCNT-poly(m-amino benzene sulfonic acid (PABS)) on an AuE (Fig. 11) and SWASV technique. Reproducible results were generated. After optimization, a linear calibration in the range of 20–50 ppb Hg^{2+} concentration, with a LOD of 0.06 μM was obtained. This novel Au-DMAET-(SWCNT-PABS) sensor and the technique used were applied to mercury analysis on influent water from a wastewater treatment plant in South Africa and found to give results comparable to that obtained from using ICP-OES.

Tonle and coworkers[170] reported an interesting study using naturally existing materials to confront the vastness of the heavy metal pollution challenging Africa. With natural smectite-type clays collected from Baba hills in West Cameroon, Central Africa functionalized with organic chelating of either amino-propyl or mercaptopropyl groups they modified carbon paste electrodes to obtain two electrodes named organo-clay-modified carbon paste electrodes (OCMCPE) differentiated across chelating agents. The electrode was modified with the natural clay known as "Ba", functionalized precisely with γ-amino-propyltriethoxysilane (APTES) and 3-mercaptopropyltrimethoxysilane (MPTMS) to obtain Ba-NH_2-CPE and Ba-SH-CPE, respectively. Using DPV, they realized an optimal conditions as LOD of 87 nM and 68 nM (S/N = 3), respectively, for the Ba-NH_2-CPE and Ba-SH-CPE, over a linear response from 0.1 to 0.7

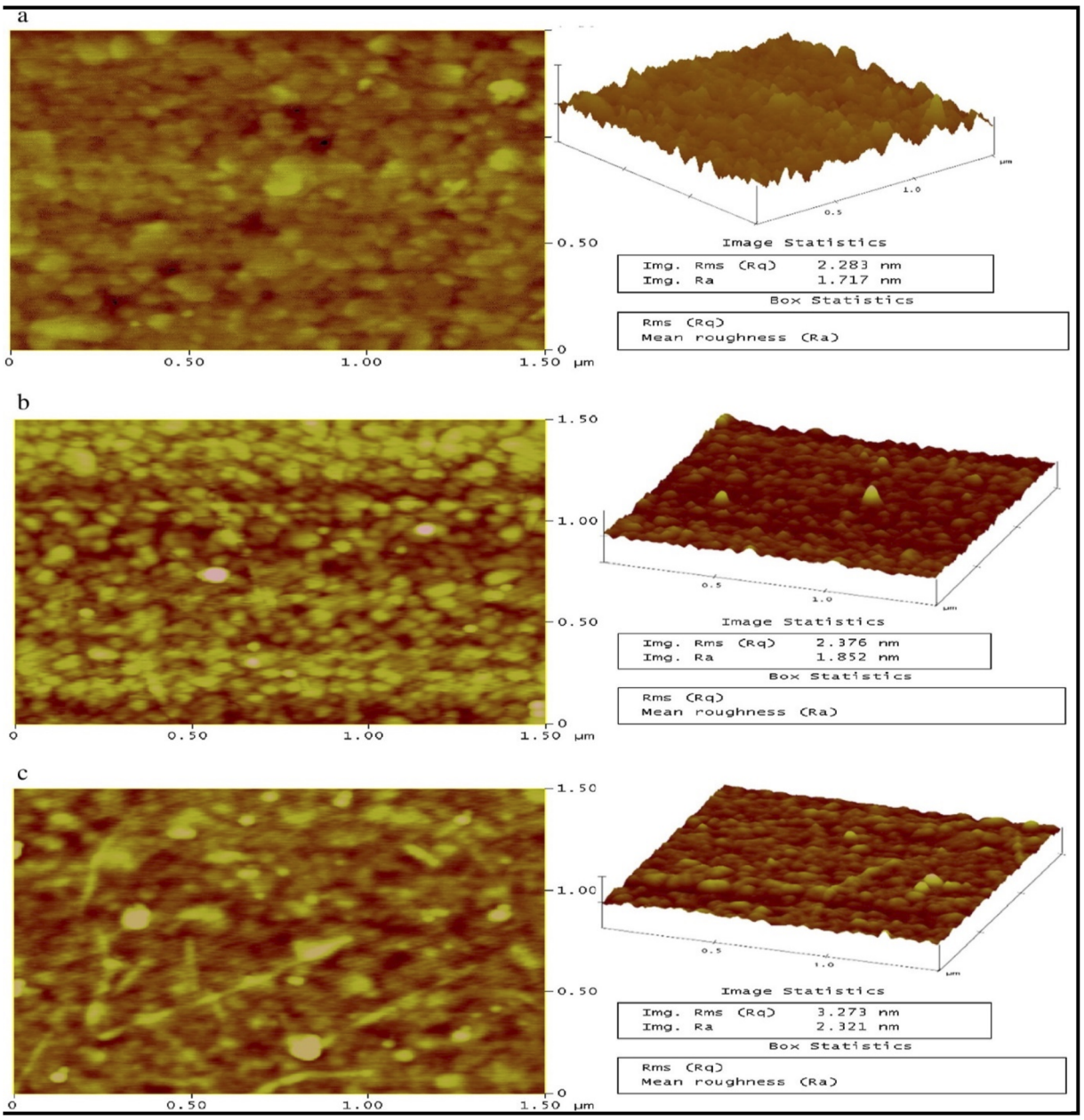

Fig. 11 2D and the resultant 3D topographical surface images of the SAM modified Au disks at a scan size of 1.5 μm. (a) Bare Au surface. (b) Au-DMAET surface. (c) Au-DMAET-(SWCNT-PABS). This figure has been reproduced from ref. 125 with permission from Elsevier, copyright 2016.

μM Hg^{2+} concentration range. Another inspiring study was presented by Tonlé and co workers on the use of organoclay (amino-functionalized attapulgite)-film modified GCE for the ultra-detection of Hg(II) in water, using laboratory tap water for real sample analysis.[183]

The modified electrode was characterized by SEM, XRD TGA/DTG analysis to ascertain their modification before deployment for electrochemical characterization. Using DPASV technique, giving carefully selected optimum conditions (Fig. 12), they realized LOD of 0.043 pM ($N = 3$), over a linear Hg^{2+} concentration range from 1 to 4 pM and regression coefficient $R^2 = 0.997$. The electrode was also very selective towards Hg^{2+} even in the presence of pestilent interfering metals like Cd^{2+} and Pb^{2+}. After some shrewd manipulation of experimental parameters, they realized a LOD of 0.091 nM (S/N = 3) over a linear response in the Hg^{2+} concentration range of 0.25–1.5 nM ($R^2 = 0.996$), in the presence of interferences from Pb^{2+} and Cd^{2+}, at DP of −0.6 V *vs.* Ag/AgCl and DT of 30 s. The proposed strategy posited functionality in the analysis of the laboratory tap water.

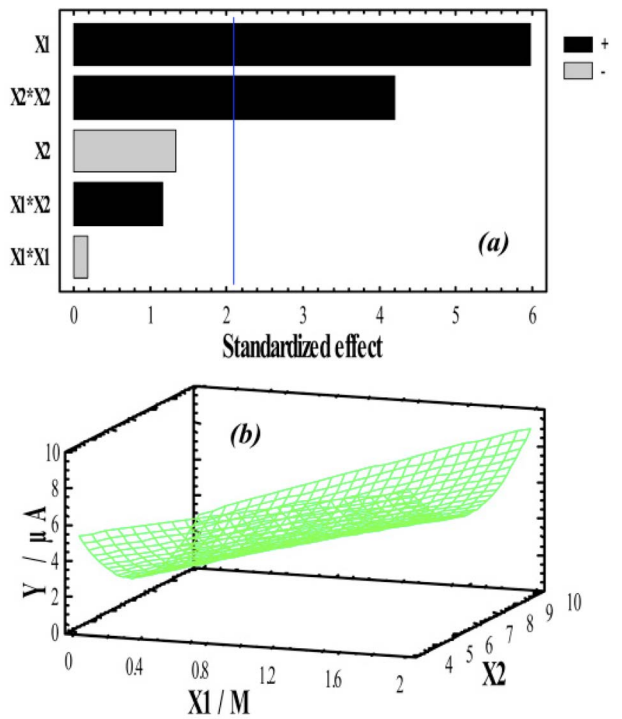

Fig. 12 Pareto chart (a) for peak currents of Hg^{2+} ions Y and response surface of a 3D plot (b) indicating the effect of concentration of detection medium and accumulation medium pH on Hg^{2+} peak current. This figure has been reproduced from ref. 183 with permission from Elsevier, copyright 2019.

Using DPASV on palladium NPs modified carbon paste electrode (Pd NPs-CPE), Aroui and coworkers[184] examined the applicability of the WE in environmental monitoring of Hg^{2+} in both wastewater and tap water. The uniqueness of their work like that of Tonle and coworkers[170] lies in their description of a very insightful method of impregnating natural phosphate with palladium NPs, and engineering of the modified CPE. The modified electrode surface was categorized, with SEM (Fig. 13), FTIR, XRD analysis (Fig. 14), and electrochemical analysis, all of which pointed to the efficient modification of the CPE surface by the NPs. They realized, given optimum conditions, a large linear concentration range of 0.5–70 μM ($R^2 = 0.98$), a LOD and LOQ for tap water to be 57.4 nM and 191.3 nM (RSD = 3.40%) respectively, while the LOD and LOQ for wastewater were 289 nM and 482 nM (RSD = 4.11%) respectively. The recoveries of mercury in tap water and wastewater at the functional concentration were above 94.9 and 64.5% respectively. They claimed that organic matter in wastewater, resulting in the decreased absorption process of mercury, accounted for the lower recovery. However, the WE (Pd-NP-CPE) using the proposed technique was found to be sensitive and selective, and thus showed good applicability in environmental monitoring of Hg^{2+} in water media.

Somerset and co-workers[185] prepared monomer solutions of aniline (ANI) and 2,2′-dithiodianiline (DTDA), an aniline derivative containing –S–S– links, and employed it in the electrochemical copolymerization of ANI and DTDA by cyclic voltammetry on SPCE in 1 M HCl (Fig. 15). The generated WEs were labelled SPCE-PANI and SPCE/PANI-PDTDA and were used in electroanalysis of Hg^{2+} in a water medium using DPASV. After

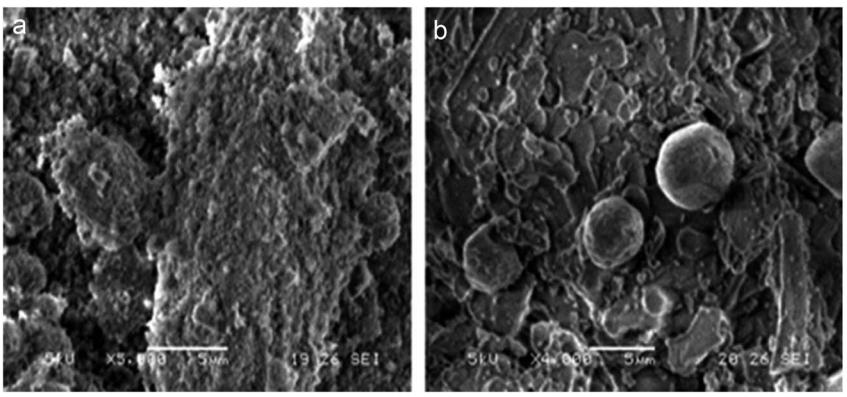

Fig. 13 SEM images of the NP (a) and Pd-NP (b) powders. This figure has been reproduced from ref. 184 with permission from WILEY-VCH, copyright 2014.

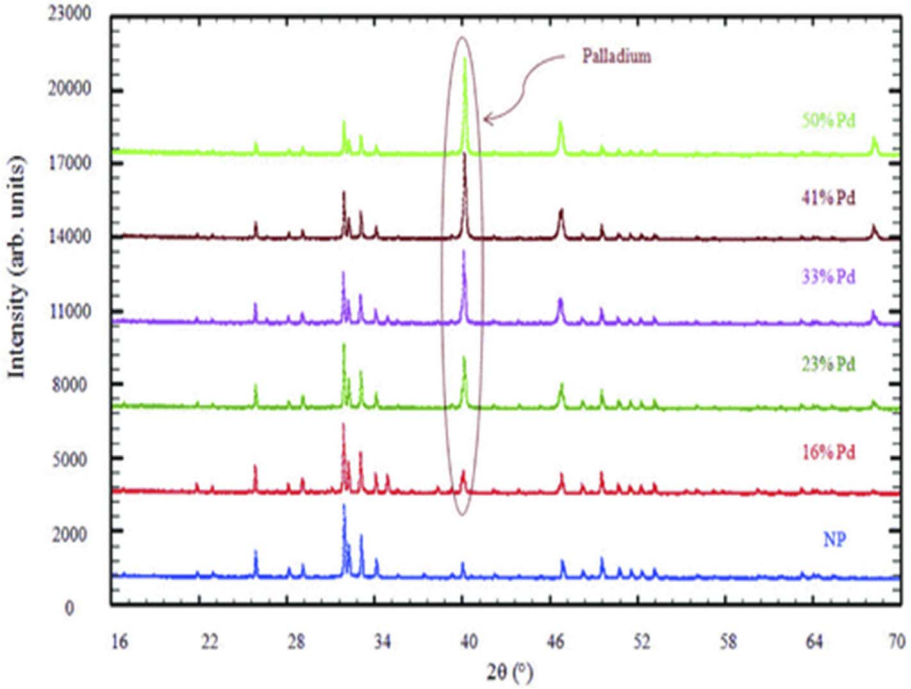

Fig. 14 X-ray diffraction of synthesized Pd-NP. This figure has been reproduced from ref. 184 with permission from WILEY-VCH, copyright 2014.

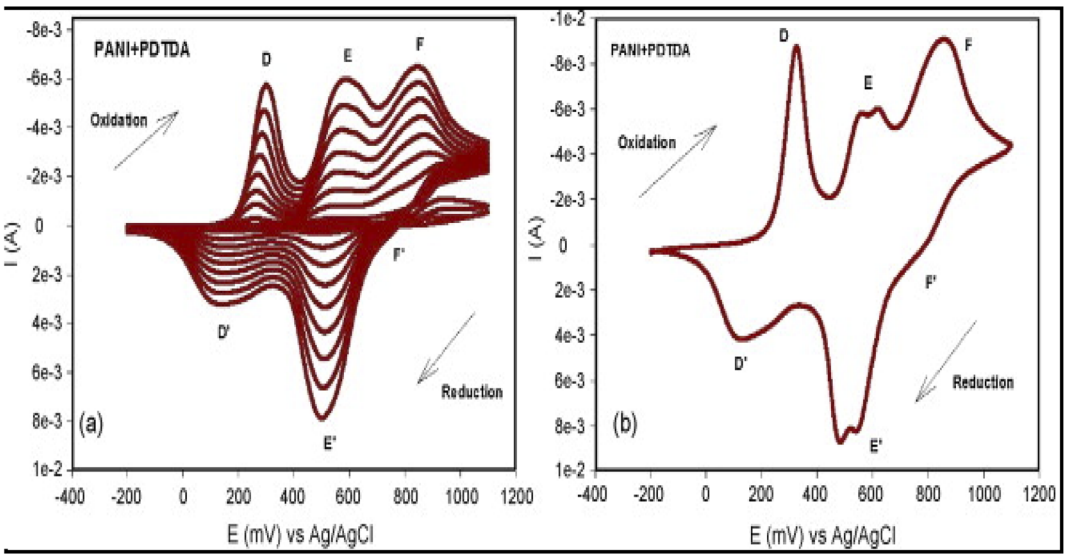

Fig. 15 A cyclic voltammogram (CV) displaying the electropolymerization of the co-polymer of PANI-PDTDA on an SPCE surface is shown in (a). The last cycle obtained for the PANI-PDTDA electropolymerization is shown in (b). The potential was cycled between −200 and +1100 mV at a scan rate of 50 mV s^{-1} for 10 cycles. This figure has been reproduced from ref. 185 with permission from Elsevier, copyright 2009.

a meticulously selected optimal condition, namely, 0.1 M H_2SO_4 containing 0.5 M HCl supporting electrolyte medium, pH of 1–2, DT and DP of 120 s and −0.3 V respectively, over a potential window of −0.3 V to 1.5 V, they realized a LOD of 56.37 ± 3.71 ppb over Hg^{2+} concentration linear range of 1–5 μM (r^2 = 0.9892). Comparatively, the LOD was in the high range as seen in Table 9. On a polyaniline-methylene blue (PANI-MB) polymer layer modified SPCE, the same group realized a slightly lower Hg^{2+} LOD of 54.27 ± 3.28 ppb, over the same linear range of 1–5 μM (r^2 = 0.9846) and similar procedural optimal conditions.[186] In a later study, using the same SPCE-PANI and SPCE/PANI-PDTDA (poly-DTDA), following successful electrodeposition of the co-polymers in an acid medium on the surface of the SPCE they realized a lower LOD of 0. 22 pM (n = 10), and 84 pM (n = 10) at the SPCE/PANI-PDTDA and SPCE/PANI sensor, respectively at a lower concentration range of 0.001–0.1 μM.[187]

Table 9 Comparing the LOD using voltametric detection of Hg^{2+} in water samples of recent reports from various researchers

Working electrode	LOD (nM)	Electrolyte	Linear range (μM)	Technique	Continent	Ref.
Ba-NH_2-CPE	87	0.1 M HNO_3 pH 1	0.1–0.7	DPASV	Africa	188
Ba-SH-CPE	68					
GCE/ATTA-NH_2	0.000043	2 M HCl pH 2	0.001–0.004 nM	DPASV	Africa	183
GCE/ATTA-NH_2[a]	0.091		0.00025–0.0015			
Au-DMAET-(SWCNT-PABS)	60	0.1 M HCl pH = 3	20–250 ppb	SWASV	Africa	189
SWCNT-PhSH/Au	3.0	0.1 M HCl pH = 1	0.005–0.09	SWASV	Asia	190
AuNPs/CFME[b]	100	0.1 M HCl	0.2–50	DPASV	Asia	191
AuNPs-GC	0.42	0.01 M HCl	0.00064–0.004	SWASV	Europe	192
Cys-AuNPs-CILE	2.3	0.1 M PBS pH 7.0	0.01–20	SWASV	Asia	193
SPGE	1.1	0.10 M HCl	0.005–0.03	SWASV	Europe	194
np-AuNPs/ITO	30	0.1 M HCl	0.1–10	DPASV	Asia	195
Silica-SH[c]/GCE	4300	1.0 M KCl	0.01–0.1	ASV	Europe	196
SAMMS-SH[d]/CPE[e]	15	0.2 M HNO_3	0.1–8	ASV	Asia	197
Metallothionein/Au	80	0.025 M Tris–HCl	0.15–0.3	CSDPV	Asia/Europe	198
Graphene–cysteamine/Au	3	0.10 M HCl	0.005–0.04	SWASV	Asia	199
MPS[f]/Au	100	—	0.1–1	DPV	Australia	200
Chit-SH[g]/multi-walled carbon nanotubes/GCE	3	—	0.01–0.14	ASV	Asia	201
CMC@AgNPs/GCE	0.19	0.1 M KCl pH 7.0	5–75	DPASV	Asia	202
PVP@AgNPs/GCE	73					
Pd-NP-CPE	49.9	0.1 M HCl pH = 1.36	0.5–70	DPASV	Africa	203
SPCE/PANI-DTDA	56	0.5 M HCl, pH = 1–2	1–5	DPASV	Africa	185
SPCE/PANI-MB	53	0.5 M HCl, pH = 1–2	1–5	DPASV	Africa	186
SPCE/PANI-PDTDA	0.00022	0.5 M HCl, pH = 1–2	0.001–1	DPASV	Africa	187

[a] Detection of Hg^{2+} ions was performed in presence of Cd^{2+} and Pb^{2+} ions. [b] Carbon fibre mat electrode. [c] Thiol-functionalized silica film. [d] Thiol terminated self-assembled monolayer on mesoporous silica. [e] Carbon paste electrode. [f] Mercaptopropyl functionalized silica. [g] Thiol functionalized chitosan.

1.6.1.5. Lead sensing. Arotiba and co-workers[123] exploited the use of carbon paste electrode modified with raw clay in the SWASV strategy for sensing Pb^{2+} ion in water samples over a linear concentration range of 1–100 ppb to get a limit of 2.48 ppb at optimal conditions. The linear regression equation for Pb(II) is represented by the relation:

$$I\,(\mathrm{A}) = 1.56746 \times 10^{-6}[\mathrm{Pb(II)}] - 7.2273 \times 10^{-5}\ (R^2 = 0.9718).$$

The overt novelty of the work rested on the chemical purification of this raw kaolin clay, its intercalation with sodium dodecyl sulphate (SDS), and subsequent modification of a graphite powder assembled carbon paste electrode. The electrode was sensitive, stable but showed no special selectivity towards Pb in the presence of interferences like Cu^{2+}, Hg^{2+}, and Cd^{2+}. The tap water sample analysis of this electrode underscored its applicability of it in real environmental monitoring, having results reconcilable with that of the ICP-OES counterpart analysis.

The same group used poly(propylene imine) (PPI) modified re-compressed eGE in SW-ASV detection of Pb^{2+} in water samples over a linear range, (2.5–40 ppb of Pb^{2+} concentration) to get a LOD of 1 ppb at optimum conditions.[204] In addition, they developed PPI dendrimer-Au nanocomposite modified GCE (GEC/PPI-Au) for Pb^{2+} ion detection in tap water using a similar technique[205] to realize a LOD of 0.96 ppb, over a broader linear range of 1–100 ppb. Sample analyses were also validated with standard techniques.

Tonle and group[206] also described a single step co-intercalation of varying concentrations of cetyltrimethylammonium ions (CTA+) and thiourea within the interlayer region of smectite and their applicability as WEs in the evaluation of Pb^{2+} in water. The organoclay modification was characterized by XRD, FTIR (Fig. 16), and N_2 adsorption–desorption and was shown to be successful.

Given optimal conditions at the organoclay thin film modified GCE, they realized a very impressive LOD (S/N = 3) of 0.029 nM from a calibration curve, over a broad range of Pb^{2+} concentrations (10–100 nM). The applicability of the electrode and the voltametric technique were examined with tap water analysis of Pb^{2+} and proved to be of environmental monitoring significance.

The same group used ASSWV at thiol-functionalized kaolinite modified CPE for quantification of Pb^{2+} (Fig. 17 and 18).[207]

Under optimal conditions (0.2 M $HClO_4$ electrolyte, potential time and deposition of 60 s and −0.9 V respectively), they obtained Pb^{2+} concentration linear response from 0.3–10 μM, with a regression correlation equation expressed as:

$$I\,(\mathrm{A}) = 2.02[\mathrm{Pb}^{2+}] + 3 \times 10^{-7}\ (R^2 = 0.9973)$$

and a LOD of 0.06 μM (S/N = 3). The proposed electrode was found to be of analytical relevance even in real-life samples using tap water. However, the authors reported likely interferences from Ag(I), Co(II), and Zn(II) and definite interferences from Cd^{2+} and Hg^{2+} which they reported could be due to the

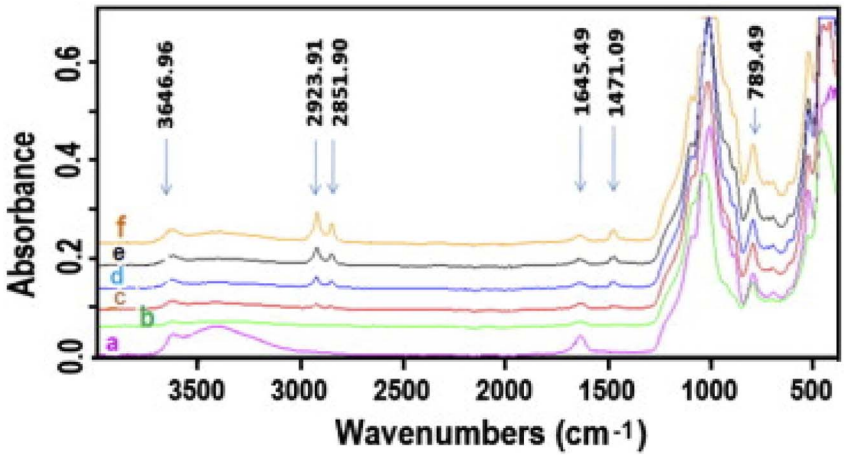

Fig. 16 FTIR spectra (4000–400 cm^{-1}) of (a) Sa(Na); (b) Sa(Na,T); (c) Sa($CTA_{0.25}$,T); (d) Sa($CTA_{0.5}$,T); (e) Sa($CTA_{0.75}$,T) and (f) Sa($CTA_{1.0}$,T). This figure has been reproduced from ref. 206 with permission from Elsevier, copyright 2014.

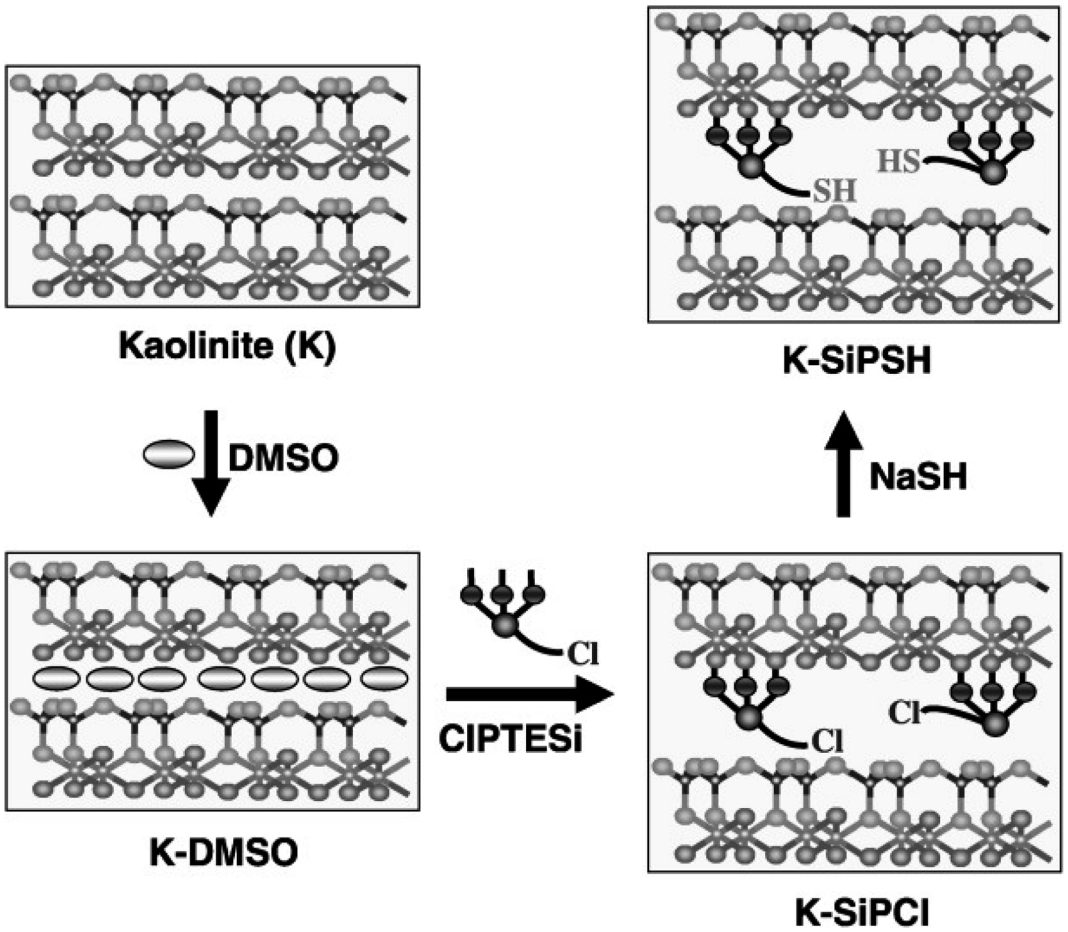

Fig. 17 Illustration of the sequential treatment of the kaolinite interlayer space resulting in the thiol-functionalized material (K–DMSO: dimethylsulfoxide-kaolinite intercalate; CIPTESi 3-chloropropyltriethoxysilane; K-SiPCL: chlorosilane; K-SiPSH: thiol-functionalized kaolinite). This figure has been reproduced from ref. 207 with permission from WILEY-VCH, copyright 2011.

high competition of the Pb^{2+}, Hg^{2+}, and Cd^{2+} for the functional chelating sites of the electrode material used.

Another interesting work by Tonlé and co-workers [Fig. 19], described the quantification of Pb^{2+} using ASDPV on another organoclay, namely functionalized amine attapulgite, and modified GCE.[208] The functionalization with amine was possible because of the covalent impregnation of [3-(2-aminoethylamino)propyl] trimethoxysilane (AEPTMS). The successful

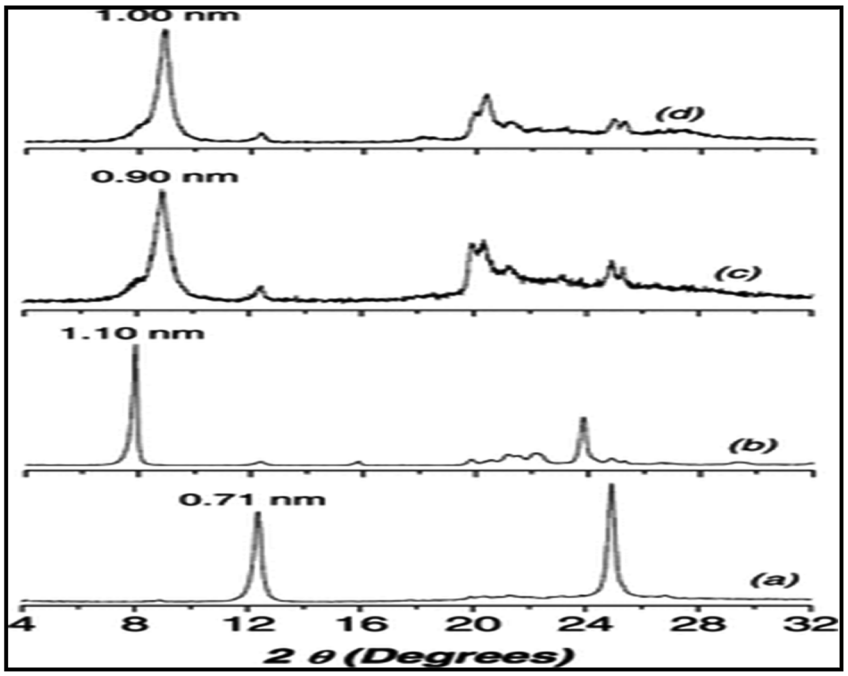

Fig. 18 XRD patterns of (a): K, (b): K–DMSO, (c): K-SiPCl and (d): K-SiPSH. This figure has been reproduced from ref. 207 with permission from WILEY-VCH, copyright 2011.

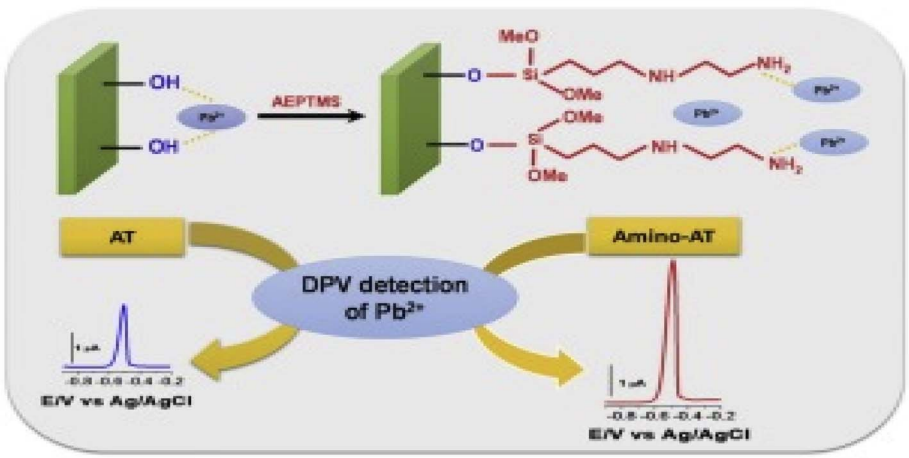

Fig. 19 Graphical summary illustrating the electrochemical detection of Pb^{2+} using the functionalized AEPTMS/GCE on DPV technique. This figure has been reproduced from ref. 208 with permission from Elsevier, copyright 2012.

grafting of the organoclay with the amine group was confirmed by physiochemical analysis of the composite using FTIR, XRD, and elemental analysis of constituent carbon–hydrogen–nitrogen. At carefully studied and selected optimal conditions (HCl electrolyte, pH = 1, accumulation time = 5 min, DP and time of −1.0 V and 40 s respectively), they obtained a linear response ($R^2 = 0.998$) in the 4 to 40 pM concentration range for Pb^{2+} and an overwhelmingly low LOD of 0.88 pM (S/N = 3). This sensitive and stable electrode and the present technique under optimal conditions were used in analysing successfully the possible contamination of Pb^{2+} in the tap water sample. The selectivity towards Pb^{2+} in the presence of Cu^{2+}, Hg^{2+}, Ti^{2+}, and In^{3+}, however, could also be improved upon.

Smith and co-workers[209] described a very novel use of low-cost paper-based ECS (Fig. 20 and 21) for water quality monitoring.

They obtained a LOD of 0.3 ppm, over a linear concentration range of Pb^{2+} between 0 and 10 ppm using SWASV on bismuth-OLC (onion-like carbon) nanoparticle ink sensor modified carbon electrode in acetate buffer solution, DT and DP of 300 s, and −1.4 V respectively, the amplitude of 0.025 V, 15 Hz

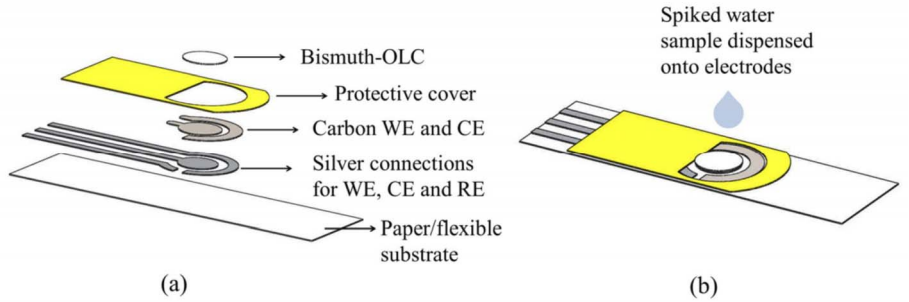

Fig. 20 Conceptual design of multi-layer paper based ECS that shows (a) a variety of materials components and layers (b) complete sensor design. This figure has been reproduced from ref. 209 with permission from Society of Photo-Optical Instrumentation Engineers (SPIE), copyright 2017.

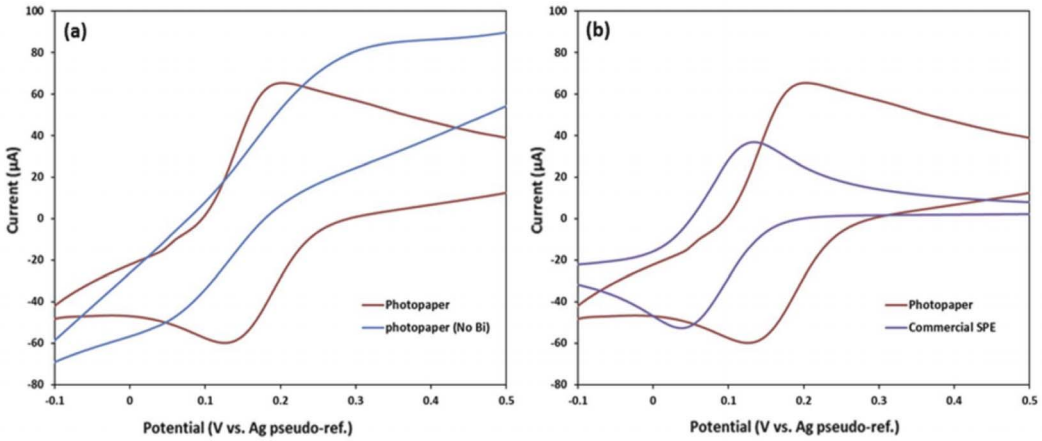

Fig. 21 Comparison of CV: (a) photo paper sensors with and without Bi-OLC coating on the WE; (b) photo paper sensor coated with Bi-OLC compared to a commercial screen-printed ceramic electrode coated with BI-OLC, CV performed in 0.1 M KCL containing 5 mM $[Fe(CN_6)]^{3-/4-}$ at 20 mV s^{-1}. This figure has been reproduced from ref. 209 with permission from Society of Photo-Optical Instrumentation Engineers (SPIE), copyright 2017.

frequency, and potential increment of 0.004 V. The linear response regression equation are presented as:

$$I_p\ (\mu A) = 24.474[Pb^{2+}]\ (ppm) - 10^{-7}\ (R^2 = 0.9956)$$

The sensor platform presented a detection limit of 0.3 ppm, which was greater than the WHO standard of lead concentration (5 ppb) for safe drinking water, and hence should be subjected to further optimization and improvement before environmental sensing applications. The significance of these sensors in environmental monitoring of lead contamination in water was huge, and comparable with that of other researchers from other continents as seen in Table 10.

1.6.1.6. Selenium sensing. Selenium may not be as common as other HMs, yet its importance in human health is no less.[219] The deficiency of it as one of the major constituents of the protein in the human body results in health complications such as liver, cardiovascular, and other heart diseases, hair losses, immunity deficiency, constant fatigue, the decline in mental health, and abnormality in reproduction.[220] However, like most HMs that are vital for human wellbeing, the boundaries between their importance and toxicity are still a narrow window.[221,222] At concentrations beyond 10 ppb in potable water, WHO considers the water unsafe as over dozed exposure could result in a nervous breakdown, gastrointestinal disturbance, nausea, vomiting, and skin sores.[223] Hence, Arotiba and co-workers[224] have described a simple and novel voltametric approach (SWASV) in monitoring selenium concentration in water using rGO modified GCE. Given optimum conditions (DP of −0.5 V, pH = 1, DT of 240 s, and 0.1 M HNO_3 supporting electrolyte), they realized a linear response with the regression equation of:

$$I\ (\mu A) = 0.8432[Se^{4+}] + 9.2359\ (R^2 = 0.9856),$$

over a linear concentration range of selenium between 0.01 and 50 ppm and LOD of 0.85 μg L^{-1}. The authors did not find the electrode having selectivity towards Se(IV) in the presence of Cu^{2+} and Cd^{2+}. However, the real water sample analysis comparable with the ICP-OES analysis validates the environmental practicability of the set used. On nitrogen-doped

Table 10 Comparing the LOD using voltametric detection of Pb^{2+} in water samples of recent reports from various researchers[a]

WE	LOD (ppb)	Electrolyte	Linear range (ppb)	Technique	Dynamic time (s)	Continent	Ref.
CPE/DMSO/SiPCl/SiPSH	2.130	0.4 M $HClO_4$	10.6–355	SWV	60	Africa	207
CPE/TPP	2.982	0.10 M ABS (pH 7)	10.65–710	DPV	300	America	210
CPE/SDS	2.481	0.1 M HNO_3	1–100	SWV	30	Africa	211
EG/PPI	1	0.1 M KCl	2.5–40	SWASV	180	Africa	204
TMFE-HF	0.0036	3 M KCl	0–4	SWASV	300	Europe	212
SPAuE	0.5	0.1 M HCl	0–50	SWASV	120	Europe	213
BiE	8	ABS/0.1 M KCl pH 4.65	25–400	SWASV	60	America	214
BiF-CPE	0.8	0.1 M ABS pH 4.50	20–200	SWASV	90–120	Europe	215
SPE-BiF	2.3	0.1 M ABS pH 4.5	20–100	SWASV	300	Asia	216
PolyChip-AgE	0.55	0.01 M HNO_3/0.01 M KCl	1–1000	SWASV	300	America	217
PPI-AuNPs/GCE	0.96	0.1 M of HNO_3	1–100	SWASV	150	Africa	205
CTA^+/GCE	29 pM	0.1 M HCl	0.01–0.1 μM	SWV	600	Africa	218
AEPTMS/GCE	0.88 pM	HCl, pH 1	4–40 pM	DPASV	300	Africa	208
Bismuth-OLC	0.3 ppm	ABS	0–10 ppm	SWASV	300	Africa	209

[a] SPAuE: Screen Print Gold Electrode TPP: tripolyphosphate-kaolinite, TMFE-HF: a thin mercury-film electrode (TMFE) plated onto an HF-resistant epoxy-impregnated graphite rotating-disc. PolyChip-AgE: polymer lab chip-silver electrode.

graphene-modified GCE (NG-GCE), at optimal conditions (0.1 M $HClO_4$ supporting electrolyte, −0.8 V DP and 50 s DT), the same group realized a linear response (R^2 = 0.9943) in the Se(IV) concentration range of 1–120 ppb and a LOD and LOQ of 0.092 ppb and 3.07 ppb respectively.[225] The problem of interference of Cu^{2+} and Cd^{2+} persisted, which they eliminated by the introduction of 0.1 M EDTA. They opined that the Cu^{2+} and Cd^{2+} from bulky complexes with EDTA, which could not be detected by the NG (film)-GCE. This current study, in so many ways, thus became an improvement on the earlier study, *vis-à-vis* the LOD, broader linear concentration range, regression coefficient, and selectivity.

1.6.1.7. Zinc sensing. Moyo[226] employed a composite of maize tassel (MT)-MWCNT as a matrix for physical adsorption of horseradish peroxidase (HRP) GCE surface through electrostatic interactions as a biosensor in the assessment of Zn^{2+} in aqueous media. The functionalized electrode was electrochemically characterized using a cyclic voltammogram in 0.1 M PBS, pH = 7.0, containing 0.1 M KCl. The biosensor operating on inhibition of the enzymes concerning the concentration of Zn^{2+} could be used to determine the presence of Zn^{2+} in the concentration range of 0.35–12 mg L^{-1} with a LOD of 0.0075 mg L^{-1}. The biosensor was found to be stable, reproducible, and highly selective and could be used in the determination of other HRP inhibiting trace metals.

Similar work was done by Iwuoha and coworkers[227] using an HRP inhibitor biosensor in the quantification of some selected metals. In this case, Cd^{2+}, Cu^{2+}, and Pb^{2+} were detected using the amperometric technique. The WE, Pt-PANI-HRP electrode was characterized with CV and DPV in the absence and presence of H_2O_2 in 0.1 M PBS, pH = 7.02. The amperometric analysis delivered a LOD (in ppb) of, 0.03, 0.10, and 0.09 for, Pb^{2+}, Cu^{2+}, and Cd^{2+} respectively. The biosensor was found to be stable, reproducible, and sensitive and promised good applicability in a real environmental application.

1.6.1.8. Nickel sensing. In 2005, Whitesides and coworkers introduced the use of microfluidic paper-based electrochemical devices (μPEDs).[228] In the report, the unique properties of paper substrates and exceptionally sensitive electrochemical sensing strategy were exploited in order to engineer cheap, disposable, and quantitative analytical methods. Pokpas and coworkers[229] reported the first use of the SWAdCSV in the detection of Ni^{2+} ion using these cheap, disposable, and pre-stored microfluidic paper-based electrochemical cells (PECs) depending on a straightforward paper disk strategy. At optimal reagents conditions, using dimethylglyoxime (DMG) as a chelating agent, mercury for adsorption of the Ni^{2+} analyte in 0.1 M NH_3/NH_4Cl buffer (pH 9.4) drop cast on the PECs, and then overlaying commercial SPCE, they realized a linear response in the concentration range of 15–120 ppb for $Ni(dmgH)_2$ on both the mercury impregnated (DMG-Hg-μPPEC) and mercury-free (DMG-Hg-free-μPPEC) paper-based sensor arrangement. They realized a LOD and sensitivity of 6.27 ppb and 7.08 μA L^{-1} μg^{-1} with a correlation coefficient of 0.997 on DMG-Hg-μPPEC and a LOD and sensitivity of 13.1 ppb and 1.89 μA L^{-1} μg^{-1} with a correlation coefficient of 0.996 on DMG-Hg-free-μPPEC for the $Ni(dmgH)_2$. The detection limit was also comparable to that of others reported in the literature for Ni^{2+} (Table 11). Over a narrower linear concentration range, the electrodes promised a higher sensitivity. The sensor and the applied technique were found to be stable, and selective towards $Ni(dmgH)_2$ in the presence of other metal interferences at a concentration up to 100 ppb, underscoring the satisfactory analytical performance of the electrode. The electrode also demonstrated applicability in real-life samples of tap water and test solutions having possible metallic interferences but performed poorly in contaminated dirt samples.

The same group used a similar electrochemical technique and electrolyte on a single-step electrode pre-concentration treatment of pencil graphite electrode (PGE) modified with electrochemically reduced graphene oxide (ERGO)/mercury film (HgF) and DMG as a chelating agent, for quantification of Ni^{2+} in tap water and natural river water samples. At optimum conditions and over a narrower Ni^{2+} dynamic linear

Table 11 Comparing the LOD using voltametric detection of Ni^{2+} in water samples of recent reports from various researchers[a]

Electrode	Modifier	Technique	DT (s)	DLR (μg L^{-1})	LOD (μg L^{-1})	Continent	Ref.
SPCE	mpBiF	AdCSV	180	1–10	0.027	Europe	232
RBiABE	—	DP-AdSV	30	0.6–41	0.18	Europe	233
SPE	PbF-	SWV	60	0.6–2.9	0.2	Europe	234
SBVE	—	SW-AdCSV	30	0–10	0.6	Europe	235
CPE	DMG-	DP-AdSV	120	80–600	27	Europe	236
SPE	DMG-N	DP-AdSV	120	60–500	30	Europe	237
PGE	ERGO-MF	SW-AdCSV	210	2–16	0.12	Africa	230
GCE	NGr-DMG	SW-AdCSV	120	2–20	1.5	Africa	231
μPPEC	DMG-Hg	SW-AdCSV	90	15–90	6.27	Africa	229
	DMG-Hg-free				13.1	Africa	

[a] RBiABE: renewable bismuth bulk (annular band) electrode; SBVE: solid bismuth vibrating electrode; DT: Deposition Time; DLR: Dynamic Linear Range; PbF: lead film.

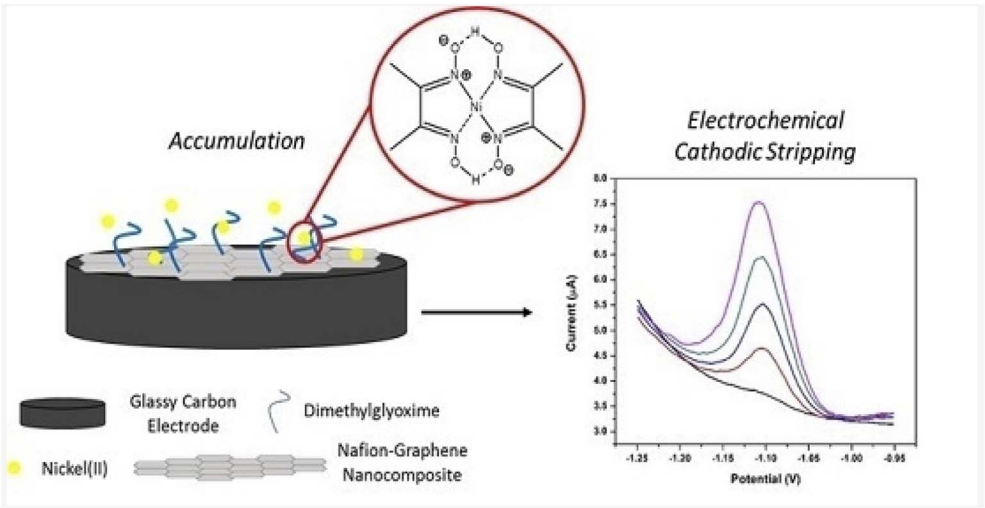

Fig. 22 Graphical abstract of the modification of NGr-DMG-GCE and application of SWCAdSV. This figure has been reproduced from ref. 231 with permission from MDPI, copyright 2017.

concentration range of 2–16 ppb, they realized a LOD and LOQ of 0.120 ± 0.002 ppb and 0.401 ± 0.007 ppb respectively.[230] The fabricated ERGO-PG-HgFE was selective even with Co^{2+} interference and could detect Ni^{2+} in water samples far below the standard set by WHO for safe water, and higher sensitivity than the DMG-Hg-μPPEC.

Another literature report by the same group detailed the use of Nafion-graphene dimethylglyoxime modified GCE (NGr-DMG-GCE) (Fig. 22) to detect Ni^{2+} in the presence of Co^{2+} and Zn^{2+} using the same technique over a slightly broader Ni^{2+} linear concentration range of 2–20 ppb and obtained a LOD of 1.5 ppb.[231] Under controlled spiking in a real water sample, the NGr-DMG-GCE promised good applicability in environmental monitoring of Ni^{2+} even in the presence of Zn^{2+} and Co^{2+}.

1.7 Cadmium and lead

Zheng and co-workers[238] presented a very ingenious use of disposable sensors. They produced WEs based on Bi NPs and composited the nanoparticles with g-C_3N_4, and their sensitivities were compared. After 5 min of electrodeposition at −1.0 V on SPCEs, the deposition was performed by stripping analysis using SWASV over a potential range of −1.4–0.2 V, 15 Hz frequency, and 25 mV amplitude. Using Cd^{2+} and Pb^{2+} as reference metal cations for the study, over a linear range of concentrations from 30 to 120 ppb and 30 to 110 ppb, for Cd^{2+} and Pb^{2+} respectively in buffer solution, a linear response with regression relationship was realized and expressed as:

$$\left.\begin{array}{l} I/\mu A = 0.0656 + 1.5108[Cd]\ \left(R^2 = 0.9661\right) \\ I/\mu A = 0.1303 + 2.4313[Pb]\ \left(R^2 = 0.9804\right) \end{array}\right\} \text{Bi-g-}C_3N_4(50\ :\ 50\ \text{wt\%})\text{-sensor}$$

$$\left.\begin{array}{l} I/\mu A = 0.0443 + 1.441[Cd]\ (R^2 = 0.987) \\ I/\mu A = 0.0169 + 0.1572[Pb]\ (R^2 = 0.9474) \\ [C]:\ \text{Concentration in ppb} \end{array}\right\} \text{Bi-NPs-sensor}$$

The LODs realized for the pairs ([Cd]; [Pb]) are (17.5 μg L^{-1}; 8.1 μg L^{-1}) and (21.8 μg L^{-1}; 10.4 μg L^{-1}) for the Bi-g-C_3N_4 (50 : 50 wt%) coated sensor and Bi-NPs coated sensor respectively. It is pellucid that the Bi-g-C_3N_4 (50 : 50 wt%) coated sensor rendered better sensitivity than the Bi-NPs coated sensor. Their tap water analysis for the functionalized sensors delivered very promising results.

Zheng and co-workers also used another innovative crafted printed paper-based ECS for low-cost point-of-need applications, a highly needed sensor platform for heavy metal monitoring in Africa. The results realized were comparable to that of commercial screen printed electrodes on SWASV using Pd^{2+} and Cd^{2+} as reference metals.[209]

1.7.1. Simultaneous detection

1.7.1.1. Arsenic and selenium. Arotiba and co-workers[239] described the use of the ASV strategy for simultaneous detection of As^{3+} and Se^{4+} in the water on an Au NPs modified GCE(Au NPs-GCE). The Au NPs also used as a substrate was electrodeposited on the surface of the GCE by cycling from −0.4 to 1.1 V. No details were presented on the physiochemical characterization of the modified electrode; however, the electrochemical characterization underscored a functional modification of the GCE with Au NPs *via* electrodeposition. After optimization of sensing parameters' conditions, namely, DP, pH, and choice of electrolytes, reproducible results were obtained, with a LOD of 0.15 and 0.22 ppb for As(III) and Se(IV) over a linear range from 0.01–0.12 ppm. The result of this simultaneous stripping of both was very comparable with other literature from researchers across the globe, based on even single detection. They reported minimal interferences from Cd^{2+} and Cu^{2+}, making the electrode moderately selective. The real-life sample was comparable with that of standard ICP-OES, guaranteeing the electrode and the engaged strategy very promising in the simultaneous environmental monitoring of As^{3+} and Se^{4+}.

1.7.1.2. Selenium and thallium. Siyamthanda and co-workers fabricated a fast, straightforward and electrochemically sensitive sensor using tin oxide nanoparticles @ multi-walled carbon nanotubes modified GCE for quantification of trace Hg(II) and Tl(I) using the SWASV technique. Under optimal conditions, the LOD and LOQ ranged from 0.9–1.2 ng L^{-1} and 3.3–4.0 ng L^{-1}, over broad linear ranges of 0.004–400 ppb and 0.003–450 ppb, for Hg(II) and Tl(I) respectively. The GCE/SnO_2/MWCNTs were used in the quantification of the target HMI thirteen surface water samples. The exactness of the results of the analysis generated using the engineered ECS compared well to those gotten using the ICP-MS.[240]

1.7.1.3. Cadmium, lead, and mercury sensing. Tonle and co-workers[221] described the use of Na_2CO_3 activated *Hordeum vulgare* L. dust (HVW) to modify CPE to get HVW-Na_2CO_3/CPE for the sensitive detection of Hg^{2+}, Pb^{2+}, and Cd^{2+} ions. The modifying materials were characterized by SEM. Given prudently selected optimum conditions, 10 mg of HVW-Na_2CO_3 on CPE, 0.5 M HCl choice of stripping medium, electrolysis and pre-concentration time of the 60 s and 300 s respectively, DP of −1.0 V, pH accumulation medium of 6.5 using ASDPV. A linear response was realized for Cd^{2+}, Pb^{2+}, and Hg^{2+} over a concentration range of 0.200–1.200 μM, 0.0025–0.0206 μM, and 0.070–0.101 μM respectively, represented by the following regression relationship:

$$I_p\ (\mu A) = 4.607[Cd^{2+}]\ (pM) - 0.28162\ (R^2 = 0.998)$$

$$I_p\ (\mu A) = 174.625[Pb^{2+}]\ (pM) + 0.59361\ (R^2 = 0.998)$$

$$I_p\ (\mu A) = 97.049[Hg^{2+}]\ (pM) - 6.27716\ (R^2 = 0.998)$$

The LOD realized for Cd^{2+}, Pb^{2+} and Hg^{2+} were 28.3 nM, 0.43 nM, and 3.3 nM which varied slightly from the results of individual detection of the metals. The sensitivity of this particular sensor as can be seen from the LODs is highest for Pb^{2+}, then Hg^{2+}, and finally Cd^{2+}. The HVW-Na_2CO_3/CPE was found to be stable and selective at optimal concentrations of some interfering anions. The river and tap water analysis results validated any proposal of the applicability of the electrode in real environmental analysis.

1.7.1.4. Zinc, cadmium, lead, and copper sensing. Iwuoha and co-workers[241] described the use of metallo-graphene nanocomposite (Fig. 23) and mercury film electrode for a very highly sensitive electrochemical detection of zinc, cadmium, lead, and copper in 0.1 M ABS (pH 4.6) using SWASV. Interestingly, they reported both the individual analysis of Zn^{2+}, Cd^{2+}, Pb^{2+}, and Cu^{2+} and simultaneous detection of Zn^{2+}, Cd^{2+}, and Pb^{2+}. Given optimal conditions, reproducible results were generated over a linear concentration range of 1–7 ppb for Zn^{2+}, Cd^{2+}, Pb^{2+}, and 20–180 ppb for Cu^{2+} on individual analysis. The LODs and correlation coefficients realized on the Nafion-G HgFE were 0.07 ppb (R^2 = 0.997), 0.08 ppb (R^2 = 0.999), 0.07 ppb (R^2 = 0.992) and 0.13 ppb (R^2 = 0.985) for Zn^{2+}, Cd^{2+}, Pb^{2+} and Cu^{2+} respectively. The simultaneous detection of the same technique on the same electrode gave a LOD of 0.14 ppb, 0.13 ppb, and 0.07 ppb for Zn^{2+}, Cd^{2+}, and Pb^{2+}. The comparison of the sensitivities of the metals in the individual and simultaneous analysis shows that the sensitivity was higher for the individual analysis for Cd^{2+} and Zn^{2+} but relatively the same for Pb^{2+}.

The applicability of the electrode was evaluated using recovery studies for both the individual and simultaneous studies and compared with the standard ICP-MS method. The recovery results were comparable with the standard technique for all the other metals except for Zn^{2+}. Real sample analysis was also done, and the authors believed the presence of organic compounds in the Edith Stephens Wetlands Park water sample could have affected the sensitivity of the Nafion-G HgFE. Nonetheless, Nafion-G HgFE was able to detect Zn^{2+}, Cd^{2+}, and Pb^{2+}. The same group used SWASV to thoroughly investigate the individual and co-quantification of Zn^{2+}, Cd^{2+}, and Pb^{2+} in the water on Nafion-graphene nanocomposite *in situ* plated

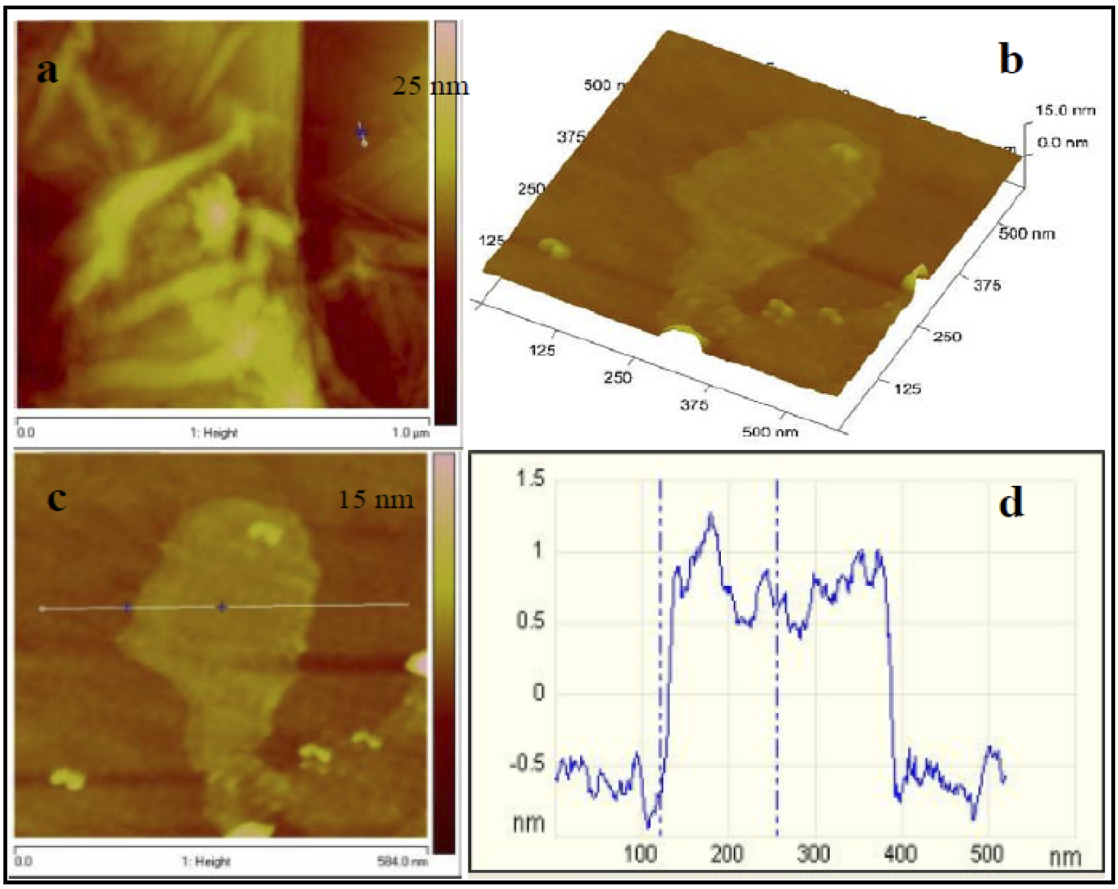

Fig. 23 (a) and (c) AFM topography image of graphene, (b) 3D representation of the selected area in (a) and (c), (d) line scan of the selected individual graphene. This figure has been reproduced from ref. 241 with permission from MDPI, copyright 2011.

bismuth-film electrodes on pencil graphite substrate (NG-PG-BiE).[242] After a careful optimization of the instrumental parameters as 0.1 M acetate buffer (pH 4.6) electrolyte choice, DT and potential of 120 s and −1.4 V, rotation speed, frequency, amplitude, and sweep rate of 1000 rpm, 50 Hz, 0.04 V, and 0.2975 V s^{-1} respectively, reproducible and stable results were obtained. Much like the previous work, the LOD for individual and simultaneous detection was compared over two concentration ranges of 2–20 ppb and 10–100 ppb (Fig. 24). The results of the comparisons also share similar sympathy. The limit of detection in sampled water was lower than the USEPA standard for drinking water using the functionalized electrode and the SWASV. The electrode and the employed technique can be confidently considered analytical significance in the environmental monitoring of trace HMs. However, since they used the same water samples, consequently their work did not show improvement in mitigating the impact of organic matters by using a voltametric approach in the quantification of HMs in water samples even though Nafion-G HgFE gave a lower limit of detection than NG-PG-BiE. Table 12, shows the comparison of their works with other literature reports.

1.7.1.5. Arsenic, cadmium, mercury, and lead sensing. Perhaps the first in African literature to report a simultaneous detection of four metals was done by Nombona and co-workers.[250] They described a simultaneous determination of arsenic, cadmium, mercury, and lead using DPASV on metallophthalocyanine and silica-coated iron oxide composites modified GCE (MPc/Si-NP). They employed two metallophthalocyanine of either cobalt or iron resulting in a design of two WE, namely cobalt-phthalocyanines and silica-coated iron oxide composites modified GCE (CoPc/Si-NPs-GCE) and iron-phthalocyanines and silica-coated iron oxide composites modified GCE (FePc/Si-NPs-GCE). Meanwhile, the synthesized Si NPs were characterized by TEM, XRD, XPS, and VSM. The following procedural conditions were followed, DP and time of −1.0 V and 180 s respectively, over a stripping potential window of −1.0 and 1.0 V, frequency, 25 Hz; amplitude, 20 mV; increment potential 5 mV and pH of 4.5 in acetate buffer or phosphate buffer solution. At optimum conditions, the LODs in ppb evaluated for individual detection of As^{3+}, Cd^{2+}, Hg^{2+} and Pb^{2+} on the two electrodes in this pair (CoPc/Si-NPs-GCE; FePc/Si-NPs-GCE) over a linear concentration range between 10 and 100 ppb were (4.39; 3.66 1), (14.62; 11.56), (4.890, 2.280) and (6.060; 4.540) respectively. FePc/Si-NPs-GCE has higher sensitivity towards all the metals. They also demonstrated the capability of the electrodes for simultaneous detection of the four toxic metals and compared their performance with other electrodes in the quantification of As^{3+}, Cd^{2+}, Hg^{2+}, and Pb^{2+} (Table

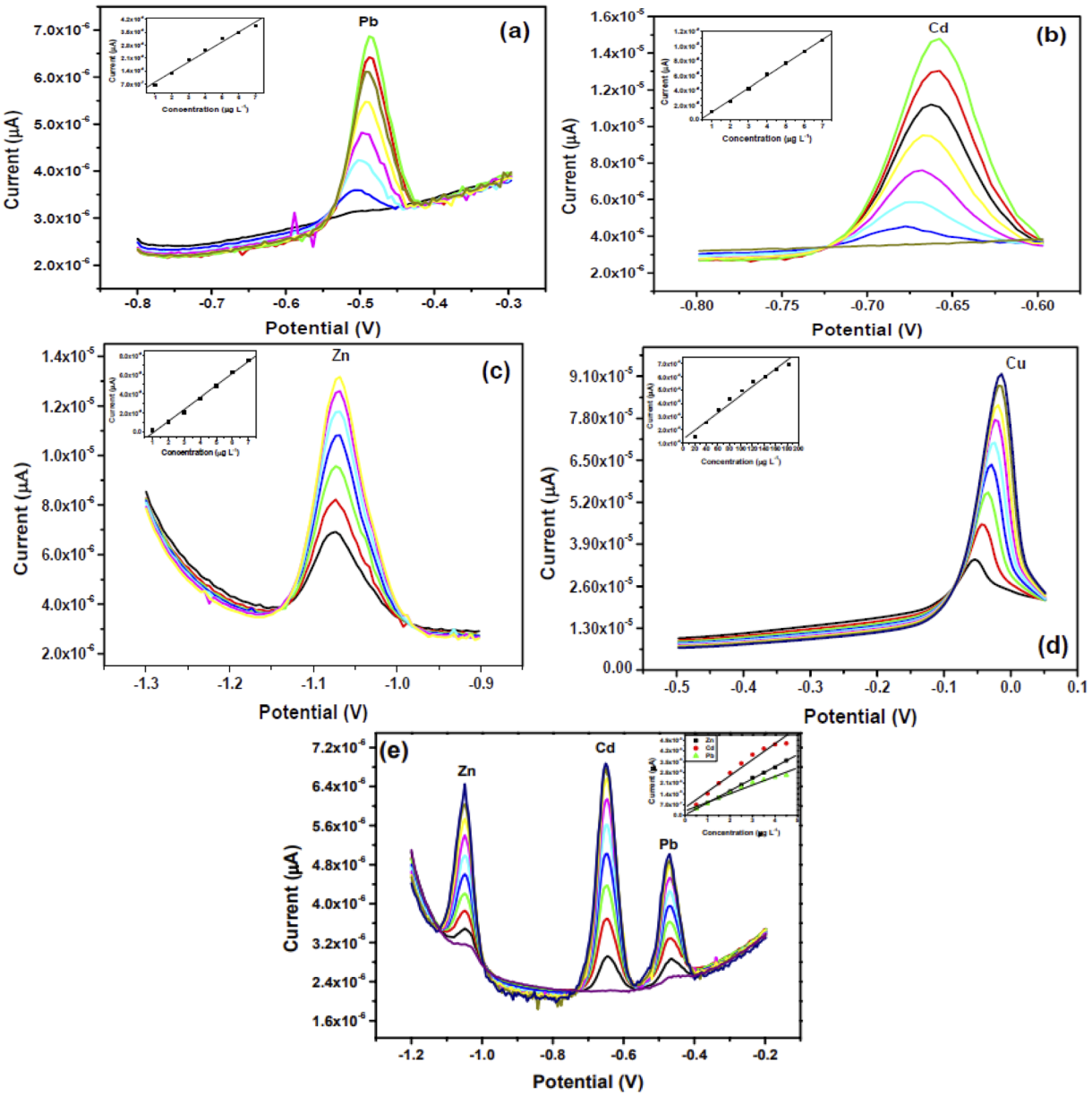

Fig. 24 SWASVs of (a) Pb^{2+}, (b) Cd^{2+}, (c) Zn^{2+}, (d) Cu^{2+} and simultaneous detection of Pb^{2+}, Cd^{2+} and Zn^{2+} in (e) 0.1 M acetate buffer (pH 4.6). This figure has been reproduced from ref. 242 with permission from ESG, copyright 2014.

13). The electrode could hence be employed in the environmental assessment of toxic HMs.

1.7.1.6. Platinum group metals (PGMs) sensing. The increase in the use of platinum group metals commonly called PGMs in catalysis coupled with rising mining activities of these metals has predisposed the surrounding aquatic environment to contamination. Examples of these metals include ruthenium, platinum, iridium, palladium, osmium, and rhodium. Consequently, Somerset and co-workers[259] described the use of mercury-free sensor electrodes for the determination of PGMs in environmental samples. They employed bismuth film modified GCE (BiF-GCE) for the quantification of platinum, palladium, and rhodium on the AdCSV technique using dimethylglyoxime (DMG) as a complexing agent. Optimum experimental conditions including supporting electrolyte composition, the concentration of the complexing agent, DP, DT, and instrumental voltammetry parameters were carefully selected.

Under this condition, the LOD for Pt^{2+}, Pd^{2+}, and Rh^{2+} was 0.12 ppb, 0.04 ppb, and 0.23 ppb, respectively, over a linear concentration range between 0 and 3.5 ppb. The electrode was found reproducible and applicable further underscored by the analysis of environmental water and sediment samples. Somerset and co-workers[260] also described an investigation of the use of Bismuth film modified SPCE for AdDPSV analysis of PGMs in environmental samples too. The procedural conditions were carefully optimized, and palladium (Pd), platinum (Pt), and rhodium (Rh) were quantified. The linear responses

Table 12 Comparing the LOD using voltametric detection of Cd^{2+}, Pb^{2+} and Zn^{2+} in water samples of recent reports from various researchers

WE	Metal	Technique	DT (s)	LOD (μg L^{-1})	Ref.
Nafion-G BiFE	Pb^{2+}, Cd^{2+}	DPASV	300	Pb^{2+} = 0.02 Cd^{2+} = 0.02	243
BiF-PGE	Pb^{2+}, Cd^{2+}, Zn^{2+}	SWASV	120	Pb^{2+} = 0.40 Cd^{2+} = 0.30 Zn^{2+} = 0.40	244
ERGO-PG-BiE	Pb^{2+}, Cd^{2+}, Zn^{2+}	SWASV	120	Pb^{2+} = 0.12 Cd^{2+} = 0.09 Zn^{2+} = 0.19	242
NC(Bpy)BiFE	Pb^{2+}, Cd^{2+}, Zn^{2+}	SWASV	120	Pb^{2+} = 0.08 Cd^{2+} = 0.12	245
Bi film C-paste	Pb^{2+}, Cd^{2+}	SWASV	120	Pb^{2+} = 0.80 Cd^{2+} = 1.00	246
Bi/GNFsNafion/GCE	Pb^{2+}, Cd^{2+}	DPASV	300	Pb^{2+} = 0.02 Cd^{2+} = 0.09	247
Bi-CNT/GCE	Pb^{2+}, Cd^{2+}, Zn^{2+}	SWASV	300	Pb^{2+} = 1.30 Cd^{2+} = 0.70 Zn^{2+} = 12.0	248
Bi nanopowder on carbon	Pb^{2+}, Cd^{2+}	SWASV	180	Pb^{2+} = 0.15 Cd^{2+} = 0.07	249
NG-PG-BiE (simultaneous analysis)	Pb^{2+}, Cd^{2+}, Zn^{2+}	SWASV	120	Pb^{2+} = 0.22 Cd^{2+} = 0.09 Zn^{2+} = 0.20	242
NG-PG-BiE (individual analysis)	Pb^{2+}, Cd^{2+}, Zn^{2+}	SWASV	120	Pb^{2+} = 0.17 Cd^{2+} = 0.09 Zn^{2+} = 0.13	242

Table 13 Comparing the LOD using voltametric detection of As^{3+}, Cd^{2+}, Hg^{2+}, and Pb^{2+} in water samples of recent reports from various researchers[a]

WE	Technique	Metal ion	LOD (ppb)	Sensitivity μA μg L^{-1}	Ref.
CoPc/Si-NP-GCE	DPASV	As^{3+}	4.39	0.18	251
FePc/Si-NP-GCE	DPASV	As^{3+}	3.66	0.20	251
Nano Au-CRV film-GCE	DPV	As^{3+}	15.58	0.8075 μA μM^{-1} cm^2	163
NPG-AuE	ASV	As^{3+}	1.499	13.0 nA μM^{-1}	252
CoPc/Si-NP-GCE	DPASV	Cd^{2+}	14.62	0.10	251
FePc/Si-NP-GCE	DPASV	Cd^{2+}	11.56	0.15	251
Cr-CPE	SWASV	Cd^{2+}	3.000	—	253
SnO_2 QDs-AuE	CV	Cd^{2+}	500.0	77.5×10^2 nA ppm^{-1} cm^{-2}	254
CoPc/Si-NP-GCE	DPASV	Hg^{2+}	4.890	0.17	251
FePc/Si-NP-GCE	DPASV	Hg^{2+}	2.280	0.37	251
Hg^{2+} IIP-CILE	DPASV	Hg^{2+}	20.06	—	255
MnPc-GCE	SWASV	Hg^{2+}	401.2	1.45 A cm^{-2} M^{-1}	256
CoPc/Si-NP-GCE	DPASV	Pb^{2+}	6.060		251
FePc/Si-NP-GCE	DPASV	Pb^{2+}	4.540		251
BRMCPE-CPE	SWASV	Pb^{2+}	15.00		257
MWCNT-CPE	PSA	Pb^{2+}	7.015		258

[a] CRV crystal violet, DPV differential pulse voltammetry, NPG nanoporous gold, Cr chromium(III) oxide, QDs quantum dots, IIP ion-imprinted polymer, BRMCPE black rice, CPE carbon paste electrode, MWCNT multiwalled carbon nanotube, PSA potentiometric stripping analysis.

obtained for Pd(II), Pt(II) and Rh(III) were in the concentration ranges of 0–0.1 ppb, 0.02–0.1 ppb, and 0–0.08 ppb respectively.

The LOD of the modified SPCE/BiF sensor and the employed technique, for Pd(II), Pt(II), and Rh(III) realized were 0.008 g L^{-1}, 0.006 g L^{-1}, and 0.005 g L^{-1}. They also presented the simultaneous detection of the metals in pairs of Pd and Rh and Pt and Rh with the SPCE/BiF sensor in a 0.01 M ammonia buffer (pH = 9.2) solution over a concentration range of 0.01–0.1 g L^{-1}. In each pair, the Rh counterpart had a less pronounced sensitivity towards the employed electrode. Worthy of note is their realization of a lower detection limit with SPCE/BiF sensor than previously used GCE/BiF sensor and identification of ammonia buffer (pH = 9.2) solution as a better electrolyte for the SPCE/BiF sensor than acetate buffer (pH = 4.8) solution. Ultimately, the performance of the SPCE/BiF sensor presents a better

promising analytical performance, in environmental monitoring of the investigated PGMs.

Progressively and interestingly, the same group investigated the use of reduced graphene oxide-antimony nanofilm (GCE/rGO-SbNPs) sensors for simultaneous determination of PGMs.[261] The determination was done in pairs of Pt^{2+} and Rh^{2+} and Pd^{2+} and Rh^{2+} using AdDPCSV strategy in supporting electrolyte of 0.2 M NaOAc buffer (pH = 5.2) solution. The one pair of Pd^{2+} and Rh^{2+} resulted in a linear response over a concentration range of 0.24–0.36 ng L^{-1} for the two cations, with regression coefficient values of 0.981 and 0.991, respectively. And the other pair of Pt^{2+} and Rh^{2+} resulted in a linear response over a concentration range of 0–0.40 ng L^{-1} and 0–0.56 ng L^{-1} with regression coefficient values of 0.987 and 0.988, respectively. A detection limit of 0.46 ng L^{-1} and 0.55 ng L^{-1} was calculated for the pair of Pd^{2+} and Rh^{2+} while LOD of approximately 0.52 ng L^{-1} and 0.48 ng L^{-1} was estimated for the other pair of Pt^{2+} and Rh^{2+}.

The same group also employed rGO impregnated antimony nanoparticle modified GCE sensor for electrochemical evaluation of the PGMs[262] and achieved sharp stripping peaks and a comparatively constant peak potential with a good linear response in the range of concentration examined from 0.040–0.400 ng L^{-1} for all metal ions studied. The LOD realized were 0.49, 0.49, and 0.45 pg L^{-1} (S/N = 3) for Pt(II), Rh(III), and Pd(II), respectively. The fabricated ECS demonstrated also good stability with an RSD of 2.67%, 4.2%, and 2.55% for 5 consecutive measurements for Rh(III), Pd(II), and Pt(II), respectively. The fabricated nanostructure exhibited efficiency in ECS application as underscored by its sensitivity and stability.

Other, works by the same group[263] described the use of AdDPSV on Bi-Ag NPs modified GCE for detection of Pt in a 10 mL of 0.2 M ABS (pH = 4.7) containing 1×10^{-5} M dimethylglyoxime, over a DP and potential window of −900 mV and 300 mV to 100 mV (*versus* Ag/AgCl) respectively, and accumulation time of 90 s for Pt^{2+}, and the solution stirred at 100 rev/min. They realized a linear response over a Pt^{2+} concentration range of 0.2–1 ng L^{-1} represented by the expression $I\,(\mu A) = 5.907[Pt^{2+}] + 1.048$ ($R^2 = 0.970$) and LOD of 0.2 ng L^{-1}. The developed sensor was, hence, highly sensitive and selective, simple and low cost, very appropriate for environmental applications in Africa. It also showed improved electrocatalytic performance when compared with the performance of their individual counterparts of either Bi-GCE or Bi-SPCE.

Using the same AdDPCSV on GCE-rGO-Sb NPs, and DMG as chelating agent over a broader concentration range of 40–400 pg L^{-1}, in 0.2 M NaOAc buffer solution (pH = 5.2), the same group got a lower detection limit of 0.45 pg L^{-1}, 0.49 pg L^{-1} and 0.49 pg L^{-1} Pd^{2+}, Pt^{2+} and Rh^{3+} respectively. The fabricated electrode was stable, though found to be prone to interferences from some metal ions despite the technique employed. The stripping analysis of Pd^{2+} was affected by the presence of Co^{2+}, Fe^{2+}, and Na^{+}, that of Pt^{2+} by Cu^{2+}, Na^{+} and SO_4^{2-} and Rh^{3+} by Fe^{3+}. However, the recovery after the spiking of the PGMs in real water sample analysis underscored the applicability of the sensor and the employed technique in the field of environmental monitoring.

1.7.2. Other works. One of the most comprehensive and earliest works on the voltametric analysis of trace HMs in water samples was done by Woldemichael and co-workers.[264] They described a solar UV-treatment of water samples to eliminate organic matters that may undermine the sensitivity of the stripping-voltametric technique of trace heavy metal assessment in Awash River, Ethiopia.

The UV-pre-treatment was optimized to undertake total degradation of dissolved organic matter that could affect the voltametric approach through the formation of complexing metal ions and surfactant properties interferences. Subsequently, on hanging drop mercury electrode(HMDE), using generally DPSV, and specifically DPASV for Zn(II), Cd(II), Pb(II), Cu(II), and DPAdSV for Ni(II), Co(II) and U(VI) from five different collection site, they successfully obtained the level of contamination of each heavy metal ion in the Awash River water samples.

Mbui and coworkers[265] reported also the use of bare and Kenyan bentonite modified polished graphite carbon electrodes for possible detection of copper, zinc, cobalt, iron, and nickel in the water sample. They leveraged the capacity of the bentonite to absorb the heavy metal, which is equivalent to preconcentration. Using 0.1 M H_2SO_4 as a supporting electrolyte, they established a calibration curve from 10 to 50 mg L^{-1} of each of the metal solutions to be considered, for both the bare and modified electrode and realized a pronounced modification of the graphite carbon electrode.

Somerset and co-workers[266] also described the amperometric quantification individually, of mercury, lead, and cadmium, metal ions using a novel polymer immobilized horseradish peroxidase (HRP) biosensor platform. They assembled this unique enzyme polymeric biosensor electrode made up of poly (aniline-*co*-2,2′-dithiodianiline) [PANI-*co*-PDTDA] and horseradish peroxidase (HRP) on a platinum disc WE. The resultant biosensor designated Pt/PANI-*co*-PDTDA/HRP working on the principle of inhibition in relation to the concentration of the toxic metals was evaluated for its sensitivity, selectivity, reproducibility, and inhibition kinetics in buffer solution and real-life sample in optimum conditions. Using DPCSV, over a linear concentration range of 0–1 $\times 10^{-2}$ μg L^{-1}, 0–1 μg L^{-1}, 0–1 μg L^{-1} for Cd^{2+}, Pb^{2+}, Hg^{2+}, Pt/PANI-*co*-PDTDA/HRP they obtained a LOD (in ppm) and LOQ (in ppm) of 8.01×10^{-4} and 2.67×10^{-3} ($R^2 = 0.993$), 9.38×10^{-4} and 3.13×10^{-3} (0.949) and 7.89×10^{-4} and 2.63×10^{-3} (0.982) for Cd^{2+}, Pb^{2+}, Hg^{2+} respectively.

The LOD and LOQ derived to indicate the good sensitivity of the biosensor. The inhibition performance was also extensively compared with a parallel conventional Pt/PANI/HPR biosensor

Table 14 The detection limit at the different CPEs using DPASV

LOD (μM)	Hg^{2+}	Pb^{2+}	Ni^{2+}	Cd^{2+}
CPE/PANI-PDTDA	0.13	0.17	0.32	0.29
CPE/PANI	15.0	1.3	0.97	0.86
CPE/MBT	38	63	1.0	1.4

Table 15 Electrochemical detection of HMIs in water using diverse techniques as employed by various indigenous electrochemists

Electrode	Modifier	Metal detected	Technique	Linear range (ppb)	Electrolyte	DT (s)	Detection method	LOD (ppb)	Ref.
SPCE	CB-AuNPs-Apt	Cd^{2+}	SWV	1–50	10 mM PBS, pH = 7.45	—	Individual	0.14	169
BiE	NG-PG	Zn^{2+}	SWASV	2–20	0.1 M ABS pH = 4.6	120	Individual	0.167	242
		Cd^{2+}						0.151	
		Pb^{2+}						0.125	
BiE	NG-PG	Zn^{2+}	SWASV	2–20		120	Simultaneous	0.257	242
		Cd^{2+}						0.098	
		Pb^{2+}						0.204	
BiE	NG-PG	Zn^{2+}	SWASV	10–100		120	Individual	0.168	242
		Cd^{2+}						0.098	
		Pb^{2+}						0.141	
BiE	NG-PG	Zn^{2+}	SWASV	10–100		120	Simultaneous	0.224	242
		Cd^{2+}						0.099	
		Pb^{2+}						0.177	
HgFE	Nafion-G	Pb^{2+}	SWASV	1–7		120	Individual	0.07	267
		Cd^{2+}						0.08	
		Zn^{2+}						0.07	
		Cu^{2+}		20–180				0.13	
		Pb^{2+}		0.5–5.0			Simultaneous	0.07	
		Cd^{2+}						0.13	
		Zn^{2+}						0.14	
GCE	Bi-Ag F	Pt^{2+}	DPAdSV	0.2–1 ng L^{-1}	0.2 ABS pH = 4.7	90	Individual	0.2	268
SPCE	DMG-Hg-μPPEC	Ni^{2+}	SWAdCSV	15–90	0.1 M NH_3/NH_4Cl buffer pH = 9.4	90	Individual	6.27	222
	DMG-Hg-free-μPPEC							13.1	
PGE	ERGO-HgFE	Ni^{2+}	SWAdCSV	2–16	0.1 M NH_3/NH_4Cl buffer pH = 9.4	90	Individual	0.120	230
GCE	NGr-DMG	Ni^{2+}	SWAdCSV	2–20	0.1 M NH_3/NH_4Cl buffer pH = 9.3		Individual	1.5	231
GCE	BiF	Pt^{2+}	DPAdSV	0–3.5	0.2 ABS pH = 4.7	90	Individual	0.2	269
SPCE	Bi F	Pt^{2+}	DPAdSV	0.02–0.1 ng L^{-1}	0.2 ABS pH = 4.7	90	Individual	0.006	260
EGE	Bi	Pb^{2+}	SWASV	5.0–250	0.1 M ABS pH = 5	120	Individual	0.83	121
		Hg^{2+}		5.0–200				0.46	
		Pb^{2+}		1.0–250			Simultaneous	0.053	
		As^{3+}						0.014	
		Hg^{2+}						0.081	
AuE	DMAET-(SWCNT-PABS)	Hg^{2+}	SWASV	20–250	0.1 M HCl pH = 3	30	Individual	0.06 μM	125
GCE	CNPs/AuNPs-Apt	As^{3+}	SWASV	0.5–100	0.1 mM $[Ru(NH_3)_6]^{3+}$ in 10 mM PBS pH = 7.2	—	Individual	0.092	139
GCE	rGO	Se^{4+}	SWASV	0.01–50 mg L^{-1}	0.1 M HNO_3 pH = 1	240	Individual	0.85	270
EGE	Co NPs-rGO	As^{3+}	SWASV	1–50	HCl pH = 1	90	Individual	0.31	126
GCE	NG	Se^{4+}	SWASV	1–120	0.1 M $HClO_4$	50	Individual	0.092	225
EGE	Bi	As^{3+}	SWASV	20–100	0.1 M HNO_3 pH = 6	180	Individual	5	127
CPE	SDS-PKC	Pb^{2+}	SWASV	1–100	0.1 M HNO_3	30	Individual	2.48	123
	FePc/Si-NP	As^{3+}		10–100	pH = 4.0			3.66	
		Cd^{2+}		20–100	pH = 4.0			11.56	
		Hg^{2+}		10–100	pH = 4.5			2.280	
GCE	CoPc/Si-NP	Pb^{2+}	DPASV	10–100	pH = 5.5	180	Individual	4.540	250
		As^{3+}		10–100	pH = 4.0			4.39	
		Cd^{2+}		20–100	pH = 4.0			14.62	
		Hg^{2+}		10–100	pH = 4.5			4.890	
		Pb^{2+}		10–100	pH = 5.0			6.060	

Table 15 (*Contd.*)

Electrode	Modifier	Metal detected	Technique	Linear range (ppb)	Electrolyte	DT (s)	Detection method	LOD (ppb)	Ref.
EGE	CoO NPs	Cu^{2+}	SWASV	0.1–20 mg L^{-1}	0.1 M HNO_3	300	Individual	94	124
GCE	Au NPs	As^{3+}	SWASV	0.01–50 ppm	0.1 M H_2SO_4 pH = 1	60	Individual	0.28	143
EGE	Au NPs	As^{3+}	SWASV	1–50	1.0 M HNO_3 pH = 1	180	Individual	0.58	271
EGE	PPI	Pb^{2+}	SWASV	2.5–40	0.1 M KCl	180	Individual	1	272
GCE	Au NPs	Se^{4+}	SWASV	0.001–50 mg L^{-1}	0.1 M H_2SO_4 pH = 1	60	Individual	0.64	224
GCE	Au NPs	As^{3+}	SWASV	0.01–12 ppm	0.1 M H_2SO_4 pH = 1	30	Simultaneous	0.15	239
		Se^{4+}						0.22	
CPE	HVW-Na_2CO_3	Cd^{2+}	ASDPV	10–85 nM	0.5 M HCl pH = 6.5	60	Individual	1.82 nM	273
		Pb^{2+}		0.2–14 nM				0.0696 nM	
		Hg^{2+}		1–11.5 nM				0.237 nM	
		Cd^{2+}		200–1200 nM			Simultaneous	28.3 n M	
		Pb^{2+}		2.5–20.6 nM				0.43 nM	
		Hg^{2+}		70–101 nM				3.3 nM	
CPE	Ba-SH	Hg^{2+}	ASDPV	0.1 to 0.7 μM	0.1 M HNO_3 pH = 2	60	Individual	87 nM	170
	Ba-NH_2							67 nM	
GCE	Sa($CTA_{0.25}$,T)	Pb^{2+}	SWV	10–100 nM	0.1 M HCl pH = 3.5	60	Individual	0.029 nM	206
GCE	Amino-AT	Pb^{2+}	ASDPV	4–40 pM	HCl pH = 1	40	Individual	0.88 pM	274
HMDE	—	Zn^{2+}	DPASV	—	0.05 M ABS + 0.1 M KCl pH 4.6	120	Individual	441	264
CPCE		Pb^{2+}		10–110				20.4	
		Cd^{2+}		10–110				52.8	
CPE	K-SiPSH	Pb^{2+}	ASSWV	0.3–10 μM	0.4 M $HClO_4$	240	Individual	60 nM	275
GCE	HRP/MT-MWCNT	Zn^{2+}	—	0.35–12 mg L^{-1}	0.1 M PBS pH = 7.0	—	Individual	7.5	226
GCE	SnO_2-MWC	Hg^{2+}	SWASV	0.004–400	0.10 M ABS pH = 4.5	180		0.0012	240
	NTs	Ni^{2+}	DPAdSV		Ammonia buffer + DMG pH = 9.5	120	Simultaneous	20.44	
		Co^{2+}	DPAdSV			120		0.57	
		U^{4+}	DPAdSV		Chloranilic acid pH = 2	30		1.41	
SPCE	BiF	Pd^{2+}	AdDPSV	0–0.1	0.01 M	150	Individual	0.008	268
		Pt^{2+}		0.02–0.1	Ammonium buffer (pH = 9.2)			0.006	
		Rh^{2+}		0–0.08				0.005	
GCE	GO-SbNPs	Pd^{2+}	AdDPCSV	40–400 pg L^{-1}	0.2 M NaOAc pH = 5.2	120	Individual	0.45	276
		Pt^{2+}		0–260 pg L^{-1}				0.49	
		Rh^{2+}		40–400 pg L^{-1}				0.49	
PtE	PANI-HRP	Cd^{2+}	DPSV/amperometry	4.76–55.3	0.1 M PBS pH = 7.02	—	Individual	0.091	227
		Pb^{2+}		4.76–40.5				0.033	
		Cu^{2+}		2.38–52.8				0.100	
PCGE	Bentonite clay	Cu^{2+}	CV	10–50 mg L^{-1}	0.1 M H_2SO_4	—	Individual	—	265
		Zn^{2+}						—	
		Ni^{2+}						—	
		Fe^{3+}						—	
		Co^{2+}						—	
CPE	Pd-NP	Hg^{2+}	DPASV	0.5–50 μM	0.1 M HCl pH = 1.36	30	Individual	49.9 nM L^{-1}	184
PPCE	Bi-OLC NPs ink	Pb^{2+}	SWASV	0–10 ppm	ABS pH = 5	300	Individual	0.3 ppm	209
GCE	HRP/MTMWCNT	Cd^{2+}	LSV/amperometry	2–30	0.1 M PBS pH = 7.0	—	Individual	0.51	120
SPCE	Bi/g-C_3N_4	Pb^{2+}	SWASV	30–110	0.1 M ABS pH = 5	300	Individual	8.1	238
		Cd^{2+}		30–120			Individual	17.5	
DSSPCE		Pb^{2+}	SWASV	30–90 ppb	Buffer solution	300	Individual	20	277

to possibly underscore the exceptional performance of the Pt/PANI-*co*-PDTDA/HRP. Reproducible and better inhibition was obtained with the Pt/PANI-*co*-PDTDA/HRP biosensor than with the conventional Pt/PANI/HPR biosensor. They concluded with a real sample analysis of tap and river water and realized very satisfactory recoveries in the range of 96–132%. The detection limit realized for all the metals was amply less than the standard for safe water by WHO. Hence, the developed biosensor in their study could be applied to monitor the presence of any of these metals in environmental water samples.[188]

Somerset and co-workers[187] optimized CPEs as "mercury-free" ECSs in the quantification of Hg^{2+}, Pb^{2+}, Ni^{2+}, and Cd^{2+} in aqueous solutions. To amplify the selectivity of the CPEs towards the target metals, they impregnated them with electroactive compounds which have preferential reactivity towards metal ions. Procedural conditions were optimized at the CPEs with −0.4 V and 120 s deposited potential and time respectively found adequate for the quantification using the employed technique (DPASV) and WEs. Over a concentration range between 1×10^{-9} M and 1×10^{-6} M, they realized a simultaneous detection limit on the various CPEs as summarized in Table 14. The electrode demonstrated sensitivity to the simultaneous detection of the target metals but with quite high LODs while Table 15 shows the electrochemical detection of HMIs in water using diverse techniques as employed by various indigenous electrochemists.

2. Conclusions and implications

• This work examined the various advances made by African indigenous electrochemists in the use of diverse electrochemical techniques in the environmental monitoring of HMs contamination in African waters.

• Various electrochemical techniques such as SWV, LSV, DPV, and amperometry over a broad range of electrodes and modifiers were used to construct very sensitive chemical sensors and biosensors over 15 years (2005–2020) (Table 15).

• From the earliest work by Tonlé and co-workers in 2005 to the most recent, diverse WEs/sensors (including point of care paper electrodes) and techniques have been successfully used to detect target heavy metal analytes in both buffer solutions and real samples with detection limits often far less than the standards set by WHO, and other environmental protection agencies for safe drinking, domestic, and river waters.

• In most cases, the techniques were simple, the electrodes were inexpensive and often featured point-of-care analysis aspects. The working electrodes were often modified with natural clays or enzymes extracted from native plants.

• Profound has been the results generated from these elaborate works; however, it must be noted that like our conventional sensing techniques, most of these works still live within the laboratory walls.

• Additionally, the presence of interferences from other metal ions and organic materials in some samples, such as wastewater and river water still affected the applicability of the sensors in real water analysis.

• The choice of electrodes, chelating, adhesive, and modifying materials may mean an additional bias in the ecosystem, as some of them are toxic too. If we have to pollute the environment to eliminate a pollutant, we still have more work to be done.

• The introduction of nanomaterials to electrochemical techniques also resulted in quick response time, high sensitivity, reproducibility, simultaneous detection with a very low limit of detection, and quantification, in online assessment due to the large surface area to volume ratio, high catalytic activity, and strong adsorption capacity of nanomaterials.

• The route to the synthesis of the nanoparticles is often not green. Not a single report of green synthesis of the nanoparticles used in the modification of the electrodes, from either plant extract or microbes.

• Bringing out the sensors from the laboratory walls to real commercial-scale applications in environmental monitoring of these HMs, with environmentally benign and low-cost chelating, electrode surface adhesive, and modifying materials, remain areas of great research interests.

Conflicts of interest

There are no conflicts to declare.

References

1 A. L. Srivastav and M. Ranjan, Inorganic water pollutants, *Inorganic Pollutants in Water*, Elsevier, 2020, pp. 1–15.
2 CPCB, *Guidelines for water quality monitoring*, Central Pollution Control Board, 2008.
3 M. Sajid, M. K. Nazal, N. Baig and A. M. Osman, Removal of heavy metals and organic pollutants from water using dendritic polymers based adsorbents: a critical review, *Sep. Purif. Technol.*, 2018, **191**, 400–423.
4 B. Ruj, Water quality and corrosivity of groundwater of northwestern part of Bankura District, West Bengal, *J. Environ. Pollut.*, 2001, **8**(4), 329–332.
5 P. Punia, M. K. Bharti, S. Chalia, R. Dhar, B. Ravelo, P. Thakur and A. Thakur, Recent advances in synthesis, characterization, and applications of nanoparticles for contaminated water treatment-A review, *Ceram. Int.*, 2020, 1526–1550.
6 M. A. Iqbal and S. Gupta, Studies on heavy metal ion pollution of ground water sources as an effect of municipal solid waste dumping, *Afr. J. Basic Appl. Sci.*, 2009, **1**(5–6), 117–122.
7 A. Boretti and L. Rosa, Reassessing the projections of the world water development report, *npj Clean Water*, 2019, **2**(1), 1–6.
8 F. Fernandez-Luqueno, F. López-Valdez, P. Gamero-Melo, S. Luna-Suárez, E. N. Aguilera-González, A. I. Martínez, M. García-Guillermo, G. Hernández-Martínez, R. Herrera-Mendoza and M. A. Álvarez-Garza, Heavy metal pollution in drinking water-a global risk for human health: A review, *Afr. J. Environ. Sci. Technol.*, 2013, **7**(7), 567–584.

9 P. H. Gleick, *Water in crisis, Pacific Institute for Studies in Dev., Environment & Security*. Stockholm Env. Institute, Oxford Univ. Press, 1993, vol. 100.
10 E. Yeboah-Assiamah, Involvement of private actors in the provision of urban sanitation services; potential challenges and precautions, *Manag. Environ. Qual. Int. J.*, 2015, **26**, 270–287.
11 S. Dos Santos, E. Adams, G. Neville, Y. Wada, A. De Sherbinin, E. M. Bernhardt and S. Adamo, Urban growth and water access in sub-Saharan Africa: Progress, challenges, and emerging research directions, *Sci. Total Environ.*, 2017, **607**, 497–508.
12 Organization, W. H., *Health in 2015: from MDGs, millennium development goals to SDGs, sustainable development goals*, 2015.
13 M. R. Hopewell and J. P. Graham, Trends in access to water supply and sanitation in 31 major sub-Saharan African cities: an analysis of DHS data from 2000 to 2012, *BMC Publ. Health*, 2014, **14**(1), 208.
14 M. R. Hopewell and J. P. Graham, Trends in access to water supply and sanitation in 31 major sub-Saharan African cities: an analysis of DHS data from 2000 to 2012, *BMC Publ. Health*, 2014, **14**(1), 1–12.
15 S. Hickling, Status of sanitation and hygiene in Africa, *Sanitation and Hygiene in Africa: Where do We Stand?*, 2013, vol. 36, p. 11.
16 H. Ritchie and M. Roser, *Water use and stress*, Our World in Data, 2017.
17 A.-S. Savadogo, Monitoring sanitation in Africa Ongoing initiatives and lessons from the field, *Sanitation and Hygiene in Africa: Where do We Stand?*, 2013, vol. 165.
18 E. Mintz, J. Bartram, P. Lochery and M. Wegelin, Not just a drop in the bucket: expanding access to point-of-use water treatment systems, *Am. J. Publ. Health*, 2001, **91**(10), 1565–1570.
19 K. M. Zeinu, H. Hou, B. Liu, X. Yuan, L. Huang, X. Zhu, J. Hu, J. Yang, S. Liang and X. Wu, A novel hollow sphere bismuth oxide doped mesoporous carbon nanocomposite material derived from sustainable biomass for picomolar electrochemical detection of lead and cadmium, *J. Mater. Chem. A*, 2016, **4**(36), 13967–13979.
20 S. Mishra, R. N. Bharagava, N. More, A. Yadav, S. Zainith, S. Mani and P. Chowdhary, Heavy metal contamination: an alarming threat to environment and human health, *Environmental biotechnology: For sustainable future*, Springer, 2019, pp. 103–125.
21 A. Valavanidis and T. Vlachogianni, *Metal pollution in ecosystems. Ecotoxicology studies and risk assessment in the marine environment*, Dept. of Chemistry, University of Athens University Campus Zografou, 2010, p. 15784.
22 P. F. T. Schunk, I. C. Kalil, E. F. Pimentel-Schmitt, D. Lenz, T. U. de Andrade, J. S. Ribeiro and D. C. Endringer, ICP-OES and micronucleus test to evaluate heavy metal contamination in commercially available Brazilian herbal teas, *Biol. Trace Elem. Res.*, 2016, **172**(1), 258–265.
23 H. Hou, K. M. Zeinu, S. Gao, B. Liu, J. Yang and J. Hu, Recent advances and perspective on design and synthesis of electrode materials for electrochemical sensing of heavy metals, *Energy Environ. Mater.*, 2018, **1**(3), 113–131.
24 L.-D. Wang, F.-Y. Zhou, X.-M. Li, L.-D. Sun, X. Song, Y. Jin, J.-M. Li, G.-Q. Kong, H. Qi and J. Cui, Genome-wide association study of esophageal squamous cell carcinoma in Chinese subjects identifies a susceptibility locus at PLCE1, *Nat. Genet.*, 2010, **42**(9), 759–763.
25 M. S. Luce, N. Ziadi, B. Gagnon and A. Karam, Visible near infrared reflectance spectroscopy prediction of soil heavy metal concentrations in paper mill biosolid-and liming by-product-amended agricultural soils, *Geoderma*, 2017, **288**, 23–36.
26 A. Mehder, Y. Habibullah, M. Gondal and U. Baig, Qualitative and quantitative spectro-chemical analysis of dates using UV-pulsed laser induced breakdown spectroscopy and inductively coupled plasma mass spectrometry, *Talanta*, 2016, **155**, 124–132.
27 J. Yu, S. Yang, D. Sun, Q. Lu, J. Zheng, X. Zhang and X. Wang, Simultaneously determination of multi metal elements in water samples by liquid cathode glow discharge-atomic emission spectrometry, *Microchem. J.*, 2016, **128**, 325–330.
28 A. Thongsaw, W. C. Chaiyasith, R. Sananmuang, G. M. Ross and R. J. Ampiah-Bonney, Determination of cadmium in herbs by SFODME with ETAAS detection, *Food Chem.*, 2017, **219**, 453–458.
29 H. Gitet, M. Hilawie, M. Muuz, Y. Weldegebriel, D. Gebremichael and D. Gebremedhin, Bioaccumulation of heavy metals in crop plants grown near Almeda Textile Factory, Adwa, Ethiopia, *Environ. Monit. Assess.*, 2016, **188**(9), 500.
30 A. dos Santos Augusto, É. F. Batista and E. R. Pereira-Filho, Direct chemical inspection of eye shadow and lipstick solid samples using laser-induced breakdown spectroscopy (LIBS) and chemometrics: proposition of classification models, *Anal. Methods*, 2016, **8**(29), 5851–5860.
31 M. A. Gondal, M. A. Shemis, A. A. Khalil, M. M. Nasr and B. Gondal, Retracted article: laser produced plasma diagnosis of carcinogenic heavy metals in gallstones, *J. Anal. At. Spectrom.*, 2016, **31**(2), 506–514.
32 A. M. AC, Electroanalytical Sensor Technology, *Electrochemistry*, InTech, 2013.
33 M. O. Oyagi, *Development of Polyacrylic Acid Based Electrochemical Sensor for Detection of Selected Heavy Metals in Water*, University of Nairobi, 2017.
34 S. P. Kounaves, *Voltametric techniques*, Prentice Hall, Upper Saddle River, NJ, USA, 1997, pp. 709–726.
35 N. Srivastava and C. Majumder, Novel biofiltration methods for the treatment of heavy metals from industrial wastewater, *J. Hazard Mater.*, 2008, **151**(1), 1–8.
36 L. Pujol, D. Evrard, K. Groenen-Serrano, M. Freyssinier, A. Ruffien-Cizsak and P. Gros, Electrochemical sensors and devices for heavy metals assay in water: the French groups' contribution, *Front. Chem.*, 2014, **2**, 19.
37 S. Roy, Overview of heavy metals and aquatic environment with notes on their recovery, *Ecoscan*, 2010, **4**(2–3), 235–240.

38 E. Callender, Treatise on Geochemistry, *Environmental Geochemistry*, Elsevier Pergamon, 2004, vol. 9.
39 J. Musarrat, A. Zaidi, M. S. Khan, M. A. Siddiqui and A. A. Al-Khedhairy, Genotoxicity assessment of heavy metal–contaminated soils, *Biomanagement of metal-contaminated soils*, Springer, 2011, pp. 323–342.
40 S. Prabhakar, A. Singh and D. Pooni, Effect of environmental pollution on animal and human health: a review, *Indian J. Anim. Sci.*, 2012, **82**(3), 244–255.
41 P. Tchounwou, C. Yedjou, A. Patlolla and D. Sutton, Heavy metal toxicity and the environment, *Molecular, Clinical and Environmental Toxicology: Volume 3: Environmental Toxicology*, ed. A. Luch, Springer Basel, 2012.
42 V. Masindi, K. J. S. Muedi and R. F. Aglan, Environmental contamination by heavy metals, *Heavy Metals*, ed. H. El-Din M. Saleh, 2018, vol. 10.
43 M. Jaishankar, T. Tseten, N. Anbalagan, B. B. Mathew and K. N. Beeregowda, Toxicity, mechanism and health effects of some heavy metals, *Interdiscip. Toxicol.*, 2014, **7**(2), 60–72.
44 V. Masindi and K. L. Muedi, Environmental contamination by heavy metals, *Heavy Metals*, 2018, vol. 10, pp. 115–132.
45 F. Fernandez-Luqueno, F. López-Valdez, P. Gamero-Melo, S. Luna-Suárez, E. N. Aguilera-González, A. I. Martínez, M. García-Guillermo, G. Hernández-Martínez, R. Herrera-Mendoza and M. A. Álvarez-Garza, Heavy metal pollution in drinking water-a global risk for human health: A review, *Afr. J. Environ. Sci. Technol.*, 2013, **7**(7), 567–584.
46 World Health Organization, *The cost of a polluted environment: 1.7 million child deaths a year says WHO*, News release, 2017, vol. 6.
47 N. T. Joutey, W. Bahafid, H. Sayel and N. El Ghachtouli, Biodegradation: involved microorganisms and genetically engineered microorganisms, *Biodegradation—Life of Science*, 2013, pp. 289–320.
48 N. Srivastava and C. Majumder, Novel biofiltration methods for the treatment of heavy metals from industrial wastewater, *J. Hazard. Mater.*, 2008, **151**(1), 1–8.
49 A. S. A. J. A. Oyekunle and O. Suliat, Speciation Study of the Heavy Metals in Commercially, *Environ. Monit. Assess.*, 2011, **169**, 597–606.
50 S. S. Devi, M. Sethu and P. G. Priya, Effect of Artemia franciscana on the Removal of Nickel by Bioaccumulation, *Biocontrol Sci.*, 2014, **19**(2), 79–84.
51 F. Tortora, V. Innocenzi, M. Prisciandaro, F. Vegliò and G. M. Di Celso, Heavy metal removal from liquid wastes by using micellar-enhanced ultrafiltration, *Water, Air, Soil Pollut.*, 2016, **227**(7), 240.
52 C. Borba, R. Guirardello, E. Silva, M. Veit and C. Tavares, Removal of nickel (II) ions from aqueous solution by biosorption in a fixed bed column: experimental and theoretical breakthrough curves, *Biochem. Eng. J.*, 2006, **30**(2), 184–191.
53 J. Ihedioha and C. Okoye, Levels of some trace metals (Zn, Cr, and Ni) in the muscle and internal organs of cattle in Nigeria, *Hum. Ecol. Risk Assess.*, 2013, **19**(4), 989–998.
54 N. Oyaro, J. Ogendi, E. N. Murago and E. Gitonga, *The contents of Pb, Cu, Zn and Cd in meat in Nairobi, Kenya*, 2007.
55 S. S. Al Moharbi, M. G. Devi, B. Sangeetha and S. Jahan, Studies on the removal of copper ions from industrial effluent by Azadirachta indica powder, *Appl. Water Sci.*, 2020, **10**(1), 23.
56 R. Naseem and S. Tahir, Removal of Pb (II) from aqueous/acidic solutions by using bentonite as an adsorbent, *Water Res.*, 2001, **35**(16), 3982–3986.
57 B. Fernandes Azevedo, L. Barros Furieri, F. M. Peçanha, G. A. Wiggers, P. Frizera Vassallo, M. Ronacher Simões, J. Fiorim, P. Rossi de Batista, M. Fioresi and L. Rossoni, Toxic effects of mercury on the cardiovascular and central nervous systems, *J. Biomed. Biotechnol.*, 2012, **2012**, 1–11.
58 C. Namasivayam and K. Kadirvelu, Uptake of mercury (II) from wastewater by activated carbon from an unwanted agricultural solid by-product: coirpith, *Carbon*, 1999, **37**(1), 79–84.
59 C. Namasivayam and K. Kadirvelu, Uptake of mercury (II) from wastewater by activated carbon from an unwanted agricultural solid by-product: coirpith, *Carbon*, 1999, **37**(1), 79–84.
60 F. Fu and Q. Wang, Removal of heavy metal ions from wastewaters: a review, *J. Environ. Manag.*, 2011, **92**(3), 407–418.
61 A. Banjo, O. Lawal, B. Fasunwon and G. Alimi, Alkali and heavy metal contaminants of some selected edible arthropods in south western Nigeria, *Am.-Eurasian J. Toxicol. Sci.*, 2010, **2**, 25–29.
62 P. J. Chedrese, M. Piasek and M. C. Henson, Cadmium as an endocrine disruptor in the reproductive system, *Immunol., Endocr. Metab. Agents Med. Chem.*, 2006, **6**(1), 27–35.
63 C. de Angelis, M. Galdiero, C. Pivonello, C. Salzano, D. Gianfrilli, P. Piscitelli, A. Lenzi, A. Colao and R. Pivonello, The environment and male reproduction: The effect of cadmium exposure on reproductive function and its implication in fertility, *Reprod. Toxicol.*, 2017, **73**, 105–127.
64 B. Sharma, S. Singh and N. J. Siddiqi, Biomedical implications of heavy metals induced imbalances in redox systems, *BioMed Res. Int.*, 2014, **2014**, 640754.
65 X. Gao and D. G. Schulze, Chemical and mineralogical characterization of arsenic, lead, chromium, and cadmium in a metal-contaminated Histosol, *Geoderma*, 2010, **156**(3–4), 278–286.
66 M. D. Royer and L. A. Smith, *Contaminants and remedial options at selected metals contaminated sites-a technical resource document*, Citeseer, 1995.
67 D. L. Sparks, *Environmental soil chemistry*, Elsevier, 2003.
68 M. Wołowiec, M. Komorowska-Kaufman, A. Pruss, G. Rzepa and T. Bajda, Removal of heavy metals and metalloids from water using drinking water treatment residuals as adsorbents: A review, *Minerals*, 2019, **9**(8), 487.
69 E. Elkhatib, A. Mahdy, F. Sherif and H. Hamadeen, Evaluation of a novel water treatment residual nanoparticles as a sorbent for arsenic removal, *J. Nanomater.*, 2015, **2015**, 1–10.

70 A. G. Caporale, P. Punamiya, M. Pigna, A. Violante and D. Sarkar, Effect of particle size of drinking-water treatment residuals on the sorption of arsenic in the presence of competing ions, *J. Hazard. Mater.*, 2013, **260**, 644–651.
71 M. Valko, H. Morris and M. Cronin, Metals, toxicity and oxidative stress, *Curr. Med. Chem.*, 2005, **12**(10), 1161–1208.
72 Y.-Y. Chen, S.-H. Yu, H.-F. Jiang, Q.-Z. Yao, S.-Q. Fu and G.-T. Zhou, Performance and mechanism of simultaneous removal of Cd (II) and Congo red from aqueous solution by hierarchical vaterite spherulites, *Appl. Surf. Sci.*, 2018, **444**, 224–234.
73 N. Ercal, H. Gurer-Orhan and N. Aykin-Burns, Toxic metals and oxidative stress part I: mechanisms involved in metal-induced oxidative damage, *Curr. Top. Med. Chem.*, 2001, **1**(6), 529–539.
74 W. Cao, Z. Wang, H. Ao and B. Yuan, Removal of Cr (VI) by corn stalk based anion exchanger: the extent and rate of Cr (VI) reduction as side reaction, *Colloids Surf., A*, 2018, **539**, 424–432.
75 M. Dinari and A. Haghighi, Ultrasound-assisted synthesis of nanocomposites based on aromatic polyamide and modified ZnO nanoparticle for removal of toxic Cr (VI) from water, *Ultrason. Sonochem.*, 2018, **41**, 75–84.
76 A. Dayan and A. Paine, Mechanisms of chromium toxicity, carcinogenicity and allergenicity: review of the literature from 1985 to 2000, *Hum. Exp. Toxicol.*, 2001, **20**(9), 439–451.
77 S. Kumar Dey and S. Roy, Effect of chromium on certain aspects of cellular toxicity, *Iran. J. Toxicol.*, 2009, **2**(4), 260–267.
78 L. P. Lingamdinne, J. R. Koduru, H. Roh, Y.-L. Choi, Y.-Y. Chang and J.-K. Yang, Adsorption removal of Co (II) from waste-water using graphene oxide, *Hydrometallurgy*, 2016, **165**, 90–96.
79 H. Hu, X. Li, P. Huang, Q. Zhang and W. Yuan, Efficient removal of copper from wastewater by using mechanically activated calcium carbonate, *J. Environ. Manag.*, 2017, **203**, 1–7.
80 N. Khatri, S. Tyagi and D. Rawtani, Recent strategies for the removal of iron from water: A review, *J. Water Proc. Eng.*, 2017, **19**, 291–304.
81 J. Liu, T. Mwamulima, Y. Wang, Y. Fang, S. Song and C. Peng, Removal of Pb (II) and Cr (VI) from aqueous solutions using the fly ash-based adsorbent material-supported zero-valent iron, *J. Mol. Liq.*, 2017, **243**, 205–211.
82 L. Patrick, Lead toxicity part II: the role of free radical damage and the use of antioxidants in the pathology and treatment of lead toxicity, *Alternative Med. Rev.*, 2006, **11**(2), 114–127.
83 A. S. Ettinger and A. M. Wengrovitz, *Guidelines for the identification and management of lead exposure in pregnant and lactating women*, 2010.
84 C. Liu, R. Bai and Q. San Ly, Selective removal of copper and lead ions by diethylenetriamine-functionalized adsorbent: behaviors and mechanisms, *Water Res.*, 2008, **42**(6–7), 1511–1522.
85 R. Dubey, J. Bajpai and A. Bajpai, Chitosan-alginate nanoparticles (CANPs) as potential nanosorbent for removal of Hg (II) ions, *Environ. Nanotechnol., Monit. Manage.*, 2016, **6**, 32–44.
86 I. Ali, The quest for active carbon adsorbent substitutes: inexpensive adsorbents for toxic metal ions removal from wastewater, *Sep. Purif. Rev.*, 2010, **39**(3–4), 95–171.
87 X. Zhang and X. Wang, Adsorption and desorption of nickel (II) ions from aqueous solution by a lignocellulose/montmorillonite nanocomposite, *PLoS One*, 2015, **10**(2), e0117077.
88 F. S. Hoseinian, B. Rezai, E. Kowsari and M. Safari, Kinetic study of Ni (II) removal using ion flotation: Effect of chemical interactions, *Miner. Eng.*, 2018, **119**, 212–221.
89 M. Omraei, H. Esfandian, R. Katal and M. Ghorbani, Study of the removal of Zn (II) from aqueous solution using polypyrrole nanocomposite, *Desalination*, 2011, **271**(1–3), 248–256.
90 J. Nriagu, *Zinc toxicity in humans*, 2019.
91 A. Smalinskienė, R. Gailevičiūtė, V. Lesauskaitė, I. Sadauskienė, O. Abdrakhmanov and L. Ivanov, Effects of cadmium and zinc ions on mitotic activity and protein synthesis in mouse liver, *Medicina*, 2005, **41**(6), 506–511.
92 M. Hashemi, S. Ghavami, M. Eshraghi, E. P. Booy and M. Los, Cytotoxic effects of intra and extracellular zinc chelation on human breast cancer cells, *Eur. J. Pharmacol.*, 2007, **557**(1), 9–19.
93 H. Gong and X. Li, Y-type, C-rich DNA probe for electrochemical detection of silver ion and cysteine, *Analyst*, 2011, **136**(11), 2242–2246.
94 F. D'Eramo, J. J. Silber, A. H. Arévalo and L. E. Sereno, Electrochemical detection of silver ions and the study of metal–polymer interactions on a polybenzidine film electrode, *J. Electroanal. Chem.*, 2000, **494**(1), 60–68.
95 S. Selvaraj, S. Krishnaswamy, V. Devashya, S. Sethuraman and U. M. Krishnan, Investigations on membrane perturbation by chrysin and its copper complex using self-assembled lipid bilayers, *Langmuir*, 2011, **27**(21), 13374–13382.
96 E. Oluyemi, A. Adekunle, A. Adenuga and W. Makinde, Physico-chemical properties and heavy metal content of water sources in Ife North Local Government Area of Osun State, Nigeria, *Afr. J. Environ. Sci. Technol.*, 2010, **4**(10), 691–697.
97 J. Yabe, M. Ishizuka and T. Umemura, Current levels of heavy metal pollution in Africa, *J. Vet. Med. Sci.*, 2010, **72**(10), 1257–1263.
98 C. V. Mohod and J. Dhote, Review of heavy metals in drinking water and their effect on human health, *Int. J. Innov. Res. Sci. Eng. Technol.*, 2013, **2**(7), 2992–2996.
99 M. Olade, *Heavy Metal Pollution and the Need for Monitoring: Illustrated for Developing Countries in West Africa*, 1987.
100 V. A. Jackson, A. Paulse, J. P. Odendaal and W. Khan, Identification of point sources of metal pollution in the Berg River, Western Cape, South Africa, *Water, Air, Soil Pollut.*, 2013, **224**(3), 1477.

101 H. K. Okoro, O. S. Fatoki, F. A. Adekola, B. J. Ximba and R. G. Snyman, *A review of sequential extraction procedures for heavy metals speciation in soil and sediments*, 2012.
102 J. N. Edokpayi, J. O. Odiyo and S. O. Olasoji, Assessment of heavy metal contamination of Dzindi river, in Limpopo Province, South Africa, *Int. J. Nat. Sci. Res.*, 2014, **2**(10), 185–194.
103 J. Lalah, E. Ochieng and S. Wandiga, Toxicology, Sources of heavy metal input into Winam Gulf, Kenya, *Bull. Environ. Contam. Toxicol.*, 2008, **81**(3), 277–284.
104 L. N. Nthunya, M. L. Masheane, S. P. Malinga, E. N. Nxumalo, B. B. Mamba and S. D. Mhlanga, Determination of toxic metals in drinking water sources in the Chief Albert Luthuli Local Municipality in Mpumalanga, South Africa, *Phys. Chem. Earth, Parts A/B/C*, 2017, **100**, 94–100.
105 R. Reza and G. Singh, Heavy metal contamination and its indexing approach for river water, *Int. J. Environ. Sci. Technol.*, 2010, **7**(4), 785–792.
106 B. Caruso, T. Cox, R. L. Runkel, M. Velleux, K. E. Bencala, D. K. Nordstrom, P. Julien, B. Butler, C. N. Alpers and A. Marion, *Metals fate and transport modelling in streams and watersheds: state of the science and USEPA workshop review*, 2008.
107 J. Mohanty, S. Misra and B. Nayak, Sequential leaching of trace elements in coal: A case study from Talcher coalfield, Orissa, *J. Geol. Soc. India*, 2001, **58**(5), 441–448.
108 C. A. Cravotta III, Dissolved metals and associated constituents in abandoned coal-mine discharges, Pennsylvania, USA. Part 1: Constituent quantities and correlations, *Appl. Geochem.*, 2008, **23**(2), 166–202.
109 S. Shahtaheri, M. Abdollahi, F. Golbabaei, F. A. Rahimi and F. Ghamari, *Monitoring of mandelic acid as a biomarker of environmental and occupational exposures to styrene*, 2008.
110 A. Rim-Rukeh, O. G. Ikhifa and A. Okokoyo, Effects of agricultural activities on the water quality of Orogodo River, Agbor Nigeria, *J. Appl. Sci. Res.*, 2006, **2**(5), 256–259.
111 G. Khadse, P. Patni, P. Kelkar and S. Devotta, Qualitative evaluation of Kanhan river and its tributaries flowing over central Indian plateau, *Environ. Monit. Assess.*, 2008, **147**(1–3), 83–92.
112 D. Juang, C. Lee and S. Hsueh, Chlorinated volatile organic compounds found near the water surface of heavily polluted rivers, *Int. J. Environ. Sci. Technol.*, 2009, **6**(4), 545–556.
113 T. Venugopal, L. Giridharan and M. Jayaprakash, *Characterization and risk assessment studies of bed sediments of River Adyar-an application of speciation study*, 2009.
114 K. Sekabira, H. O. Origa, T. Basamba, G. Mutumba and E. Kakudidi, Assessment of heavy metal pollution in the urban stream sediments and its tributaries, *Int. J. Environ. Sci. Technol.*, 2010, **7**(3), 435–446.
115 O. Fatoki and S. Mathabatha, An assessment of heavy metal pollution in the East London and Port Elizabeth harbours, *Water SA*, 2001, **27**(2), 233–240.
116 M. Orosun, P. Tchokossa, L. Nwankwo, T. Lawal, S. Bello and S. Ige, Assessment of heavy metal pollution in drinking water due to mining and smelting activities in Ajaokuta, Nigeria, *Niger. J. Technol. Dev.*, 2016, **13**(1), 31–39.
117 N. S. Che, S. Bett, E. C. Okpara, P. O. Olagbaju, O. E. Fayemi and M. Mathuthu, *An Assessment of Land Use and Land Cover Changes and Its Impact on the Surface Water Quality of the Crocodile River Catchment, South Africa*, 2021.
118 D. O. Ogoyi, C. Mwita, E. K. Nguu and P. M. Shiundu, *Determination of heavy metal content in water, sediment and microalgae from Lake Victoria, East Africa*, 2011.
119 S. Cobbina, M. Myilla and K. Michael, Small scale gold mining and heavy metal pollution: Assessment of drinking water sources in Datuku in the Talensi-Nabdam District, *Int. J. Sci. Technol. Res.*, 2013, **2**(1), 96–100.
120 M. Mambo, O. O. Jonathan and A. M. Nana, *HRP biosensor based on carbonized maize tassel-MWNTs modified electrode for the detection of divalent trace metal ions*, SENSORS, 2013 IEEE, 2013, pp. 1–4.
121 P. J. Mafa, A. O. Idris, N. Mabuba and O. A. Arotiba, Electrochemical co-detection of As (III), Hg (II) and Pb (II) on a bismuth modified exfoliated graphite electrode, *Talanta*, 2016, **153**, 99–106.
122 H. Hou, K. M. Zeinu, S. Gao, B. Liu, J. Yang and J. Hu, Recent advances and perspective on design and synthesis of electrode materials for electrochemical sensing of heavy metals, *Energy Environ. Mater.*, 2018, **1**(3), 113–131.
123 S. P. Akanji, O. A. Arotiba and D. Nkosi, Voltametric Determination of Pb (II) Ions at a Modified Kaolinite-Carbon Paste Electrode, *Electrocatalysis*, 2019, **10**(6), 643–652.
124 T. Ndlovu, O. Arotiba, S. Sampath, R. Krause and B. Mamba, Electroanalysis of copper as a heavy metal pollutant in water using cobalt oxide modified exfoliated graphite electrode, *Phys. Chem. Earth, Parts A/B/C*, 2012, **50**, 127–131.
125 G. G. Matlou, D. Nkosi, K. Pillay and O. Arotiba, Electrochemical detection of Hg (II) in water using self-assembled single walled carbon nanotube-poly (m-amino benzene sulfonic acid) on gold electrode, *Sens. Bio-Sens. Res.*, 2016, **10**, 27–33.
126 A. Jimana, M. Peleyeju, L. Tshwenya, K. Pillay and O. Arotiba, Voltametric analysis of as (III) at a cobalt nanoparticles/reduced graphene oxide modified exfoliated graphite electrode, *Int. J. Electrochem. Sci.*, 2018, **13**, 10127–10140.
127 T. Ndlovu, B. B. Mamba, S. Sampath, R. W. Krause and O. A. Arotiba, Voltametric detection of arsenic on a bismuth modified exfoliated graphite electrode, *Electrochim. Acta*, 2014, **128**, 48–53.
128 G. March, T. D. Nguyen and B. Piro, Modified electrodes used for electrochemical detection of metal ions in environmental analysis, *Biosensors*, 2015, **5**(2), 241–275.
129 M. Li, H. Gou, I. Al-Ogaidi and N. Wu, Nanostructured sensors for detection of heavy metals: a review, *ACS Sustainable Chem. Eng.*, 2013, **1**(7), 713–723.

130 J. Barek, Possibilities and limitations of mercury and mercury-based electrodes in practical electroanalysis of biologically active organic compounds, *Port. Electrochim. Acta*, 2013, **31**(6), 291–295.

131 K. M. Zeinu, H. Hou, B. Liu, X. Yuan, L. Huang, X. Zhu, J. Hu, J. Yang, S. Liang and X. Wu, A novel hollow sphere bismuth oxide doped mesoporous carbon nanocomposite material derived from sustainable biomass for picomolar electrochemical detection of lead and cadmium, *J. Mater. Chem. A*, 2016, **4**(36), 13967–13979.

132 L. Pujol, D. Evrard, K. Groenen-Serrano, M. Freyssinier, A. Ruffien-Cizsak and P. Gros, Electrochemical sensors and devices for heavy metals assay in water: the French groups contribution, *Front. Chem.*, 2014, **2**, 19.

133 X. Gao, W. Wei, L. Yang, T. Yin and Y. Wang, Simultaneous determination of lead, copper, and mercury free from macromolecule contaminants by square wave stripping voltammetry, *Anal. Lett.*, 2005, **38**(14), 2327–2343.

134 N. Ullah, M. Mansha, I. Khan and A. Qurashi, Nanomaterial-based optical chemical sensors for the detection of heavy metals in water: Recent advances and challenges, *TrAC, Trends Anal. Chem.*, 2018, **100**, 155–166.

135 M. Oyama, Recent nanoarchitectures in metal nanoparticle-modified electrodes for electroanalysis, *Anal. Sci.*, 2010, **26**(1), 1–12.

136 A. Waheed, M. Mansha and N. Ullah, Nanomaterials-based electrochemical detection of heavy metals in water: current status, challenges and future direction, *TrAC, Trends Anal. Chem.*, 2018, **105**, 37–51.

137 M. Li, D.-W. Li, G. Xiu and Y.-T. Long, Applications of screen-printed electrodes in current environmental analysis, *Curr. Opin. Electrochem.*, 2017, **3**(1), 137–143.

138 Y. Lu, X. Liang, C. Niyungeko, J. Zhou, J. Xu and G. Tian, A review of the identification and detection of heavy metal ions in the environment by voltammetry, *Talanta*, 2018, **178**, 324–338.

139 T. Mushiana, N. Mabuba, A. O. Idris, G. M. Peleyeju, B. O. Orimolade, D. Nkosi, R. F. Ajayi and O. A. Arotiba, An aptasensor for arsenic on a carbon-gold bi-nanoparticle platform, *Sens. Bio-Sens. Res.*, 2019, **24**, 100280.

140 A. Jimana, M. Peleyeju, L. Tshwenya, K. Pillay and O. Arotiba, Voltametric analysis of as (III) at a cobalt nanoparticles/reduced graphene oxide modified exfoliated graphite electrode, *Int. J. Electrochem. Sci.*, 2018, **13**, 10127–10140.

141 J. Mafa, N. Mabuba and O. Arotiba, An exfoliated graphite based electrochemical sensor for As (III) in water, *Electroanalysis*, 2016, **28**(7), 1462–1469.

142 T. Ndlovu, B. B. Mamba, S. Sampath, R. W. Krause and O. A. Arotiba, Voltametric detection of arsenic on a bismuth modified exfoliated graphite electrode, *Electrochim. Acta*, 2014, **128**, 48–53.

143 A. Idris, J. Mafa, N. Mabuba and O. Arotiba, Nanogold modified glassy carbon electrode for the electrochemical detection of arsenic in water, *Russ. J. Electrochem.*, 2017, **53**(2), 170–177.

144 N. Moghimi, M. Mohapatra and K. T. Leung, Bimetallic nanoparticles for arsenic detection, *Anal. Chem.*, 2015, **87**(11), 5546–5552.

145 H. H. Nguyen, S. H. Lee, U. J. Lee, C. D. Fermin and M. Kim, Immobilized enzymes in biosensor applications, *Materials*, 2019, **12**(1), 121.

146 G. L. Turdean, Design and development of biosensors for the detection of heavy metal toxicity, *Int. J. Electrochem.*, 2011, **2011**, 1–15.

147 A. Waheed, M. Mansha and N. Ullah, Nanomaterials-based electrochemical detection of heavy metals in water: current status, challenges and future direction, *TrAC, Trends Anal. Chem.*, 2018, **105**, 37–51.

148 T. Mushiana, N. Mabuba, A. O. Idris, G. M. Peleyeju, B. O. Orimolade, D. Nkosi, R. F. Ajayi and O. A. Arotiba, An aptasensor for arsenic on a carbon-gold bi-nanoparticle platform, *Sens. Bio-Sens. Res.*, 2019, **24**, 100280.

149 P. Carrera, P. J. Espinoza-Montero, L. Fernández, H. Romero and J. Alvarado, Electrochemical determination of arsenic in natural waters using carbon fiber ultra-microelectrodes modified with gold nanoparticles, *Talanta*, 2017, **166**, 198–206.

150 M. Yang, P.-H. Li, W.-H. Xu, Y. Wei, L.-N. Li, Y.-Y. Huang, Y.-F. Sun, X. Chen, J.-H. Liu and X.-J. Huang, Reliable electrochemical sensing arsenic (III) in nearly groundwater pH based on efficient adsorption and excellent electrocatalytic ability of AuNPs/CeO_2-ZrO_2 nanocomposite, *Sens. Actuators, B*, 2018, **255**, 226–234.

151 L. Chao, X. Xiong, J. Liu, A. Xu, T. Huang, F. He and Q. Xie, Preparation of a porous Au electrode with a sacrificed Prussian blue analogue template for anodic stripping voltametric analysis of trace arsenic (III), *Sens. Actuators, B*, 2017, **253**, 603–611.

152 M. B. Gumpu, M. Veerapandian, U. M. Krishnan and J. B. B. Rayappan, Electrochemical sensing platform for the determination of arsenite and arsenate using electroactive nanocomposite electrode, *Chem. Eng. J.*, 2018, **351**, 319–327.

153 S. Dash and N. Munichandraiah, Electroanalysis of As (III) at nanodendritic Pd on PEDOT, *Analyst*, 2014, **139**(7), 1789–1795.

154 D.-D. Han, Z.-G. Liu, J.-H. Liu and X.-J. Huang, The size effect of Pt nanoparticles: a new route to improve sensitivity in electrochemical detection of As (III), *RSC Adv.*, 2015, **5**(48), 38290–38297.

155 Y.-H. Yuan, X.-H. Zhu, S.-H. Wen, R.-P. Liang, L. Zhang and J.-D. Qiu, Electrochemical assay for As (III) by combination of highly thiol-rich trithiocyanuric acid and conductive reduced graphene oxide nanocomposites, *J. Electroanal. Chem.*, 2018, **814**, 97–103.

156 R. Feeney and S. P. Kounaves, On-site analysis of arsenic in groundwater using a microfabricated gold ultramicroelectrode array, *Anal. Chem.*, 2000, **72**(10), 2222–2228.

157 S. Cinti, S. Politi, D. Moscone, G. Palleschi and F. Arduini, Stripping analysis of As (III) by means of screen-printed

electrodes modified with gold nanoparticles and carbon black nanocomposite, *Electroanalysis*, 2014, **26**(5), 931–939.

158 X. Dai, O. Nekrassova, M. E. Hyde and R. G. Compton, Anodic stripping voltammetry of arsenic (III) using gold nanoparticle-modified electrodes, *Anal. Chem.*, 2004, **76**(19), 5924–5929.

159 M. M. Hossain, M. M. Islam, S. Ferdousi, T. Okajima and T. Ohsaka, Anodic stripping voltametric detection of arsenic (III) at gold nanoparticle-modified glassy carbon electrodes prepared by electrodeposition in the presence of various additives, *Electroanalysis*, 2008, **20**(22), 2435–2441.

160 J. P. Mafa, N. Mabuba and O. A. Arotiba, An Exfoliated Graphite Based Electrochemical Sensor for As(III) in Water, *Electroanalysis*, 2016, **28**(7), 1462–1469.

161 M. Khairy, D. K. Kampouris, R. O. Kadara and C. E. Banks, Gold nanoparticle modified screen printed electrodes for the trace sensing of arsenic (III) in the presence of copper (II), *Electroanalysis*, 2010, **22**(21), 2496–2501.

162 S. Wu, Q. Zhao, L. Zhou and Z. Zhang, Stripping analysis of trace arsenic based on the MnOx/AuNPs composite film modified electrode in alkaline media, *Electroanalysis*, 2014, **26**(8), 1840–1849.

163 M. Rajkumar, S. Thiagarajan and S.-M. Chen, Electrochemical detection of arsenic in various water samples, *Int. J. Electrochem. Sci.*, 2011, **6**(8), 3164–3177.

164 S. Prakash, T. Chakrabarty, A. K. Singh and V. K. Shahi, Silver nanoparticles built-in chitosan modified glassy carbon electrode for anodic stripping analysis of As (III) and its removal from water, *Electrochim. Acta*, 2012, **72**, 157–164.

165 A. Idris, J. Mafa, N. Mabuba and O. Arotiba, Nanogold modified glassy carbon electrode for the electrochemical detection of arsenic in water, *Russ. J. Electrochem.*, 2017, **53**(2), 170–177.

166 Y. Liu and W. Wei, Jointly modified single-walled carbon nanotubes on low resistance monolayer modified electrode for arsenic (III) detection, *J. Electroanal. Chem.*, 2008, **624**(1–2), 299–304.

167 J.-F. Huang and H.-H. Chen, Gold-nanoparticle-embedded nafion composite modified on glassy carbon electrode for highly selective detection of arsenic (III), *Talanta*, 2013, **116**, 852–859.

168 S. S. Hassan, A. R. Solangi, T. G. Kazi, M. S. Kalhoro, Y. Junejo, Z. A. Tagar and N. H. Kalwar, Nafion stabilized ibuprofen–gold nanostructures modified screen printed electrode as arsenic (III) sensor, *J. Electroanal. Chem.*, 2012, **682**, 77–82.

169 C. T. Fakude, O. A. Arotiba and N. Mabuba, Electrochemical aptasensing of cadmium (II) on a carbon black-gold nano-platform, *J. Electroanal. Chem.*, 2020, **858**, 113796.

170 I. K. Tonle, E. Ngameni and A. Walcarius, Preconcentration and voltametric analysis of mercury (II) at a carbon paste electrode modified with natural smectite-type clays grafted with organic chelating groups, *Sens. Actuators, B*, 2005, **110**(2), 195–203.

171 H. R. L. Z. Zhad, Y. M. R. Torres and R. Y. Lai, A reagentless and reusable electrochemical aptamer-based sensor for rapid detection of Cd (II), *J. Electroanal. Chem.*, 2017, **803**, 89–94.

172 J. Qu, L. Wu, H. Liu, J. Li, H. Lv, X. Fu and Y. Song, A novel electrochemical biosensor based on DNA for rapid and selective detection of cadmium, *Int. J. Electrochem. Sci.*, 2015, **10**, 4020–4028.

173 M. Ebrahimi, J. B. Raoof and R. Ojani, Design of an electrochemical DNA-based biosensor for selective determination of cadmium ions using a DNA hybridization indicator, *Int. J. Biol. Macromol.*, 2018, **108**, 1237–1241.

174 G. Fan, D. Zhai and D. Zou, Highly sensitive electrochemical determination of cadmium (II) in environmental water based on the electrodeposited bismuth nanoparticles, *Int. J. Electrochem. Sci.*, 2016, **11**, 4362–4370.

175 T. Ndlovu, O. Arotiba, S. Sampath, R. Krause and B. Mamba, Electroanalysis of copper as a heavy metal pollutant in water using cobalt oxide modified exfoliated graphite electrode, *Phys. Chem. Earth, Parts A/B/C*, 2012, **50**, 127–131.

176 J. Yu, X. Zhang, M. Zhao, Y. Ding, Z. Li, Y. Ma, H. Li and H. Cui, Fabrication of the Ni-based composite wires for electrochemical detection of copper (II) ions, *Anal. Chim. Acta*, 2021, **1143**, 45–52.

177 M. Lu, Y. Deng, Y. Luo, J. Lv, T. Li, J. Xu, S.-W. Chen and J. Wang, Graphene aerogel–metal–organic framework-based electrochemical method for simultaneous detection of multiple heavy-metal ions, *Anal. Chem.*, 2018, **91**(1), 888–895.

178 L. Ma, X. Zhang, M. Ikram, M. Ullah, H. Wu and K. Shi, Controllable synthesis of an intercalated ZIF-67/EG structure for the detection of ultratrace Cd^{2+}, Cu^{2+}, Hg^{2+} and Pb^{2+} ions, *Chem. Eng. J.*, 2020, **395**, 125216.

179 B. Zhang, J. Chen, H. Zhu, T. Yang, M. Zou, M. Zhang and M. Du, Facile and green fabrication of size-controlled AuNPs/CNFs hybrids for the highly sensitive simultaneous detection of heavy metal ions, *Electrochim. Acta*, 2016, **196**, 422–430.

180 S. Di Masi, A. Pennetta, A. Guerreiro, F. Canfarotta, G. E. De Benedetto and C. Malitesta, Sensor based on electrosynthesised imprinted polymeric film for rapid and trace detection of copper (II) ions, *Sens. Actuators, B*, 2020, **307**, 127648.

181 M. Etienne, J. Bessiere and A. Walcarius, Voltametric detection of copper (II) at a carbon paste electrode containing an organically modified silica, *Sens. Actuators, B*, 2001, **76**(1–3), 531–538.

182 L. Rai, J. Gaur and H. Kumar, Phycology and heavy-metal pollution, *Biol. Rev.*, 1981, **56**(2), 99–151.

183 S. L. Jiokeng, L. M. Dongmo, E. Ymélé, D. B. Nde and I. K. Tonlé, Organoclay-film modified electrode for the detection of ultra-traces of Hg^{2+} ions: Approach of one factor at a time by an experimental design, *Electrochim. Acta*, 2019, **316**, 152–161.

184 F. El Aroui, S. Lahrich, A. Farahi, M. Achak, L. El Gaini, M. Bakasse, A. Bouzidi and M. El Mhammedi, Palladium Particles-Impregnated Natural Phosphate Electrodes for Electrochemical Determination of Mercury in Ambient Water Samples, *Electroanalysis*, 2014, **26**(8), 1751–1760.

185 V. Somerset, J. Leaner, R. Mason, E. Iwuoha and A. Morrin, Development and application of a poly (2, 2′-dithiodianiline)(PDTDA)-coated screen-printed carbon electrode in inorganic mercury determination, *Electrochim. Acta*, 2010, **55**(14), 4240–4246.

186 V. Somerset, J. Leaner, R. Mason, E. Iwuoha and A. Morrin, Determination of inorganic mercury using a polyaniline and polyaniline-methylene blue coated screen-printed carbon electrode, *Int. J. Environ. Anal. Chem.*, 2010, **90**(9), 671–685.

187 V. S. Somerset, L. H. Hernandez and E. I. Iwuoha, Stripping voltametric measurement of trace metal ions using screen-printed carbon and modified carbon paste electrodes on river water from the Eerste-Kuils River System, *J. Environ. Sci. Health, Part A: Toxic/Hazard. Subst. Environ. Eng.*, 2011, **46**(1), 17–32.

188 I. K. Tonle, E. Ngameni and A. Walcarius, Preconcentration and voltametric analysis of mercury (II) at a carbon paste electrode modified with natural smectite-type clays grafted with organic chelating groups, *Sens. Actuators, B*, 2005, **110**(2), 195–203.

189 G. G. Matlou, D. Nkosi, K. Pillay and O. Arotiba, Electrochemical detection of Hg (II) in water using self-assembled single walled carbon nanotube-poly (m-amino benzene sulfonic acid) on gold electrode, *Sens. Bio-Sens. Res.*, 2016, **10**, 27–33.

190 J. Wei, D. Yang, H. Chen, Y. Gao and H. Li, Stripping voltametric determination of mercury (II) based on SWCNT-PhSH modified gold electrode, *Sens. Actuators, B*, 2014, **190**, 968–974.

191 D. Li, J. Li, X. Jia and E. Wang, Gold nanoparticles decorated carbon fiber mat as a novel sensing platform for sensitive detection of Hg (II), *Electrochem. Commun.*, 2014, **42**, 30–33.

192 T. Hezard, K. Fajerwerg, D. Evrard, V. Collière, P. Behra and P. Gros, Gold nanoparticles electrodeposited on glassy carbon using cyclic voltammetry: Application to Hg (II) trace analysis, *J. Electroanal. Chem.*, 2012, **664**, 46–52.

193 A. Safavi and E. Farjami, Construction of a carbon nanocomposite electrode based on amino acids functionalized gold nanoparticles for trace electrochemical detection of mercury, *Anal. Chim. Acta*, 2011, **688**(1), 43–48.

194 E. Bernalte, C. M. Sánchez and E. P. Gil, Determination of mercury in ambient water samples by anodic stripping voltammetry on screen-printed gold electrodes, *Anal. Chim. Acta*, 2011, **689**(1), 60–64.

195 Y. Lin, Y. Peng and J. Di, Electrochemical detection of Hg (II) ions based on nanoporous gold nanoparticles modified indium tin oxide electrode, *Sens. Actuators, B*, 2015, **220**, 1086–1090.

196 I. Cesarino and É. T. G. Cavalheiro, Thiol-functionalized silica thin film modified electrode in determination of mercury ions in natural water, *Electroanalysis*, 2008, **20**(21), 2301–2309.

197 W. Yantasee, Y. Lin, T. S. Zemanian and G. E. Fryxell, Voltametric detection of lead (II) and mercury (II) using a carbon paste electrode modified with thiol self-assembled monolayer on mesoporous silica (SAMMS), *Analyst*, 2003, **128**(5), 467–472.

198 H. Ju and D. Leech, Electrochemical study of a metallothionein modified gold disk electrode and its action on Hg^{2+} cations, *J. Electroanal. Chem.*, 2000, **484**(2), 150–156.

199 H. Zhou, X. Wang, P. Yu, X. Chen and L. Mao, Sensitive and selective voltametric measurement of Hg^{2+} by rational covalent functionalization of graphene oxide with cysteamine, *Analyst*, 2012, **137**(2), 305–308.

200 A. Walcarius and C. Delacôte, Mercury (II) binding to thiol-functionalized mesoporous silicas: critical effect of pH and sorbent properties on capacity and selectivity, *Anal. Chim. Acta*, 2005, **547**(1), 3–13.

201 W. Deng, Y. Tan, Y. Li, Y. Wen, Z. Su, Z. Huang, S. Huang, Y. Meng, Q. Xie and Y. Luo, Square wave voltametric determination of Hg (II) using thiol functionalized chitosan-multiwalled carbon nanotubes nanocomposite film electrode, *Microchim. Acta*, 2010, **169**(3–4), 367–373.

202 S. Meenakshi, S. Devi, K. Pandian, K. Chitra and P. Tharmaraj, Aniline-mediated synthesis of carboxymethyl cellulose protected silver nanoparticles modified electrode for the differential pulse anodic stripping voltammetry detection of mercury at trace level, *Ionics*, 2019, **25**(7), 3431–3441.

203 F. El Aroui, S. Lahrich, A. Farahi, M. Achak, L. El Gaini, M. Bakasse, A. Bouzidi and M. El Mhammedi, Palladium Particles-Impregnated Natural Phosphate Electrodes for Electrochemical Determination of Mercury in Ambient Water Samples, *Electroanalysis*, 2014, **26**(8), 1751–1760.

204 T. Ndlovu, O. A. Arotiba, S. Sampath, R. W. Krause and B. B. Mamba, Electrochemical detection and removal of lead in water using poly (propylene imine) modified re-compressed exfoliated graphite electrodes, *J. Appl. Electrochem.*, 2011, **41**(12), 1389–1396.

205 N. Mabuba and O. Arotiba, *The development of a dendrimer-gold nanocomposite electrochemical sensor for the detection of lead (II) ion in water*, 2019.

206 G. B. Ngassa, I. K. Tonle, A. Walcarius and E. Ngameni, One-step co-intercalation of cetyltrimethylammonium and thiourea in smectite and application of the organoclay to the sensitive electrochemical detection of Pb (II), *Appl. Clay Sci.*, 2014, **99**, 297–305.

207 I. K. Tonlé, S. Letaief, E. Ngameni, A. Walcarius and C. Detellier, Square Wave Voltametric Determination of Lead (II) Ions Using a Carbon Paste Electrode Modified by a Thiol-Functionalized Kaolinite, *Electroanalysis*, 2011, **23**(1), 245–252.

208 S. L. Jiokeng, L. M. Dongmo, E. Ymélé, E. Ngameni and I. K. Tonlé, Sensitive stripping voltammetry detection of

Pb (II) at a glassy carbon electrode modified with an amino-functionalized attapulgite, *Sens. Actuators, B*, 2017, **242**, 1027–1034.

209 S. Smith, P. Bezuidenhout, M. Mbanjwa, H. Zheng, M. Conning, N. Palaniyandy, K. Ozoemena and K. Land, *Development of paper-based electrochemical sensors for water quality monitoring, Fourth Conference on Sensors, MEMS, and Electro-Optic Systems*, International Society for Optics and Photonics, 2017, p. 100360C.

210 Y. Gómez, L. Fernández, C. Borrás, J. Mostany and B. Scharifker, Characterization of a carbon paste electrode modified with tripolyphosphate-modified kaolinite clay for the detection of lead, *Talanta*, 2011, **85**(3), 1357–1363.

211 S. P. Akanji, O. A. Arotiba and D. Nkosi, Voltametric Determination of Pb (II) Ions at a Modified Kaolinite-Carbon Paste Electrode, *Electrocatalysis*, 2019, **10**(6), 643–652.

212 C. Truzzi, A. Annibaldi, S. Illuminati, E. Bassotti and G. Scarponi, Square-wave anodic-stripping voltametric determination of Cd, Pb, and Cu in a hydrofluoric acid solution of siliceous spicules of marine sponges (from the Ligurian Sea, Italy, and the Ross Sea, Antarctica), *Anal. Bioanal. Chem.*, 2008, **392**(1), 247–262.

213 S. Laschi, I. Palchetti and M. Mascini, Gold-based screen-printed sensor for detection of trace lead, *Sens. Actuators, B*, 2006, **114**(1), 460–465.

214 Z. Zou, A. Jang, E. Macknight, P.-M. Wu, J. Do, P. L. Bishop and C. H. Ahn, Environmentally friendly disposable sensors with microfabricated on-chip planar bismuth electrode for in situ heavy metal ions measurement, *Sens. Actuators, B*, 2008, **134**(1), 18–24.

215 I. Švancara, L. Baldrianová, E. Tesařová, S. B. Hočevar, S. A. A. Elsuccary, A. Economou, S. Sotiropoulos, B. Ogorevc and K. Vytřas, Recent Advances in Anodic Stripping Voltammetry with Bismuth-Modified Carbon Paste Electrodes, *Electroanalysis*, 2006, **18**(2), 177–185.

216 G.-H. Hwang, W.-K. Han, J.-S. Park and S.-G. Kang, An electrochemical sensor based on the reduction of screen-printed bismuth oxide for the determination of trace lead and cadmium, *Sens. Actuators, B*, 2008, **135**(1), 309–316.

217 W. Jung, A. Jang, P. L. Bishop and C. H. Ahn, A polymer lab chip sensor with microfabricated planar silver electrode for continuous and on-site heavy metal measurement, *Sens. Actuators, B*, 2011, **155**(1), 145–153.

218 G. B. Ngassa, I. K. Tonle, A. Walcarius and E. Ngameni, One-step co-intercalation of cetyltrimethylammonium and thiourea in smectite and application of the organoclay to the sensitive electrochemical detection of Pb (II), *Appl. Clay Sci.*, 2014, **99**, 297–305.

219 S. Khanna, A. Udas, G. K. Kumar, S. Suvarna and F. Karjodkar, Trace elements (copper, zinc, selenium and molybdenum) as markers in oral sub mucous fibrosis and oral squamous cell carcinoma, *J. Trace Elem. Med. Biol.*, 2013, **27**(4), 307–311.

220 T. Himoto, H. Yoneyama, K. Kurokohchi, M. Inukai, H. Masugata, F. Goda, R. Haba, S. Watababe, S. Kubota and S. Senda, Selenium deficiency is associated with insulin resistance in patients with hepatitis C virus–related chronic liver disease, *Nutr. Res.*, 2011, **31**(11), 829–835.

221 L. G. Djemmoe, E. Njanja, F. M. Tchieno, D. T. Ndinteh, P. G. Ndungu and I. K. Tonle, Activated Hordeum vulgare L. dust as carbon paste electrode modifier for the sensitive electrochemical detection of Cd^{2+}, Pb^{2+} and Hg^{2+} ions, *Int. J. Environ. Anal. Chem.*, 2020, **100**(13), 1429–1445.

222 K. Pokpas, N. Jahed and E. Iwuoha, Tuneable, Pre-stored Paper-Based Electrochemical Cells (μPECs): an Adsorptive Stripping, Voltametric Approach to Metal Analysis, *Electrocatalysis*, 2019, **10**(4), 352–364.

223 A. O. Idris, N. Mabuba and O. A. Arotiba, Electroanalysis of selenium in water on an electrodeposited gold-nanoparticle modified glassy carbon electrode, *J. Electroanal. Chem.*, 2015, **758**, 7–11.

224 A. Idris, N. Mabuba and O. Arotiba, Electroanalysis of selenium in water on an electrodeposited gold-nanoparticle modified glassy carbon electrode, *J. Electroanal. Chem.*, 2015, **758**, 7–11.

225 C. T. Fakude, O. A. Arotiba, R. Moutloali and N. Mabuba, Nitrogen-doped Graphene Electrochemical Sensor for Selenium (IV) in Water, *Int. J. Electrochem. Sci.*, 2019, **14**, 9391–9403.

226 M. Moyo, Horseradish peroxidase biosensor to detect zinc ions in aqueous solutions, *Open J. Appl. Biosens.*, 2014, **2014**, DOI: 10.4236/ojab.2014.31001.

227 P. N. Nomngongo, J. C. Ngila, V. O. Nyamori, E. A. Songa and E. I. Iwuoha, Determination of Selected Heavy Metals Using Amperometric Horseradish Peroxidase (HRP) Inhibition Biosensor, *Anal. Lett.*, 2011, **44**(11), 2031–2046.

228 V. Linder, S. K. Sia and G. M. Whitesides, Reagent-loaded cartridges for valveless and automated fluid delivery in microfluidic devices, *Anal. Chem.*, 2005, **77**(1), 64–71.

229 K. Pokpas, N. Jahed and E. Iwuoha, Tuneable, pre-stored paper-based electrochemical cells (μPECs): an adsorptive stripping voltametric approach to metal analysis, *Electrocatalysis*, 2019, **10**(4), 352–364.

230 R. Tekenya, K. Pokpas, N. Jahed and E. I. Iwuoha, Enhanced specificity and sensitivity for the determination of nickel (II) by square-wave adsorptive cathodic stripping voltammetry at disposable graphene-modified pencil graphite electrodes, *Anal. Lett.*, 2019, **52**(2), 373–398.

231 K. Pokpas, N. Jahed, P. G. Baker and E. I. Iwuoha, Complexation-based detection of nickel (II) at a graphene-chelate probe in the presence of cobalt and zinc by adsorptive stripping voltammetry, *Sensors*, 2017, **17**(8), 1711.

232 S. Dal Borgo, H. Sopha, S. Smarzewska, S. B. Hočevar, I. Švancara and R. Metelka, Macroporous Bismuth Film Screen-Printed Carbon Electrode for Simultaneous Determination of Ni (II) and Co (II), *Electroanalysis*, 2015, **27**(1), 209–216.

233 B. Baś, K. Węgiel and K. Jedlińska, The renewable bismuth bulk annular band working electrode: fabrication and application in the adsorptive stripping voltametric

determination of nickel (II) and cobalt (II), *Anal. Chim. Acta*, 2015, **881**, 44–53.

234 A. Bobrowski, A. Królicka, M. Maczuga and J. Zarębski, A novel screen-printed electrode modified with lead film for adsorptive stripping voltametric determination of cobalt and nickel, *Sens. Actuators, B*, 2014, **191**, 291–297.

235 G. M. Alves, J. M. Magalhães and H. M. Soares, Simultaneous determination of nickel and cobalt using a solid bismuth vibrating electrode by adsorptive cathodic stripping voltammetry, *Electroanalysis*, 2013, **25**(5), 1247–1255.

236 A. Ferancová, M. K. Hattuniemi, A. M. Sesay, J. P. Räty and V. T. Virtanen, Electrochemical monitoring of nickel (II) in mine water, *Mine Water Environ.*, 2016, **35**(4), 547–552.

237 A. Ferancová, M. K. Hattuniemi, A. M. Sesay, J. P. Räty and V. T. Virtanen, Rapid and direct electrochemical determination of Ni (II) in industrial discharge water, *J. Hazard. Mater.*, 2016, **306**, 50–57.

238 H. Zheng, L. Ntuli, M. Mbanjwa, N. Palaniyandy, S. Smith, M. Modibedi, K. Land and M. J. E. Mathe, The Effect of gC_3N_4 Materials on Pb (II) and Cd (II) Detection Using Disposable Screen-Printed Sensors, *Electrocatalysis*, 2019, **10**(2), 149–155.

239 A. Idris, N. Mabuba and O. Arotiba, Electrochemical co-detection of arsenic and selenium on a glassy carbon electrode modified with gold nanoparticles, *Int. J. Electrochem. Sci.*, 2017, **12**, 10–21.

240 S. H. Mnyipika and P. N. Nomngongo, Square wave anodic stripping voltammetry for simultaneous determination of trace Hg (II) and Tl (I) in surface water samples using SnO_2@ MWCNTs modified glassy carbon electrode, *Int. J. Electrochem. Sci.*, 2017, **12**, 4811–4827.

241 C. M. Willemse, K. Tlhomelang, N. Jahed, P. G. Baker and E. I. Iwuoha, Metallo-graphene nanocomposite electrocatalytic platform for the determination of toxic metal ions, *Sensors*, 2011, **11**(4), 3970–3987.

242 K. Pokpas, N. Jahed, O. Tovide, P. G. Baker and E. I. Iwuoha, Nafion-graphene nanocomposite in situ plated bismuth-film electrodes on pencil graphite substrates for the determination of trace heavy metals by anodic stripping voltammetry, *Int. J. Electrochem. Sci.*, 2014, **9**(9), 5092–5115.

243 J. Li, S. Guo, Y. Zhai and E. Wang, High-sensitivity determination of lead and cadmium based on the Nafion-graphene composite film, *Anal. Chim. Acta*, 2009, **649**(2), 196–201.

244 D. Demetriades, A. Economou and A. Voulgaropoulos, A study of pencil-lead bismuth-film electrodes for the determination of trace metals by anodic stripping voltammetry, *Anal. Chim. Acta*, 2004, **519**(2), 167–172.

245 F. Torma, M. Kádár, K. Tóth and E. Tatár, Nafion®/2, 2′-bipyridyl-modified bismuth film electrode for anodic stripping voltammetry, *Anal. Chim. Acta*, 2008, **619**(2), 173–182.

246 I. Švancara, L. Baldrianová, E. Tesařová, S. B. Hočevar, S. A. Elsuccary, A. Economou, S. Sotiropoulos, B. Ogorevc and K. Vytřas, Recent advances in anodic stripping voltammetry with bismuth-modified carbon paste electrodes, *Electroanalysis*, 2006, **18**(2), 177–185.

247 D. Li, J. Jia and J. Wang, Simultaneous determination of Cd (II) and Pb (II) by differential pulse anodic stripping voltammetry based on graphite nanofibers–Nafion composite modified bismuth film electrode, *Talanta*, 2010, **83**(2), 332–336.

248 G. H. Hwang, W. K. Han, J. S. Park and S. G. Kang, Determination of trace metals by anodic stripping voltammetry using a bismuth-modified carbon nanotube electrode, *Talanta*, 2008, **76**(2), 301–308.

249 G.-J. Lee, H.-M. Lee and C.-K. Rhee, Bismuth nano-powder electrode for trace analysis of heavy metals using anodic stripping voltammetry, *Electrochem. Commun.*, 2007, **9**(10), 2514–2518.

250 D. Gounden, S. Khene and N. Nombona, Electroanalytical detection of heavy metals using metallophthalocyanine and silica-coated iron oxide composites, *Chem. Pap.*, 2018, **72**(12), 3043–3056.

251 D. Gounden, S. Khene and N. Nombona, Electroanalytical detection of heavy metals using metallophthalocyanine and silica-coated iron oxide composites, *Chem. Pap.*, 2018, **72**(12), 3043–3056.

252 J. Jiang, N. Holm and K. O'Brien, Improved anodic stripping voltametric detection of arsenic (III) using nanoporous gold microelectrode, *ECS J. Solid State Sci. Technol.*, 2015, **4**(10), S3024.

253 Z. Koudelkova, T. Syrovy, P. Ambrozova, Z. Moravec, L. Kubac, D. Hynek, L. Richtera and V. Adam, Determination of zinc, cadmium, lead, copper and silver using a carbon paste electrode and a screen printed electrode modified with chromium (III) oxide, *Sensors*, 2017, **17**(8), 1832.

254 G. Bhanjana, N. Dilbaghi, R. Kumar, A. Umar and S. Kumar, SnO_2 quantum dots as novel platform for electrochemical sensing of cadmium, *Electrochim. Acta*, 2015, **169**, 97–102.

255 A. Bahrami, A. Besharati-Seidani, A. Abbaspour and M. Shamsipur, A highly selective voltametric sensor for nanomolar detection of mercury ions using a carbon ionic liquid paste electrode impregnated with novel ion imprinted polymeric nanobeads, *Mater. Sci. Eng., C*, 2015, **48**, 205–212.

256 B. Ceken, M. Kandaz and A. Koca, Electrochemical metal-ion sensors based on a novel manganese phthalocyanine complex, *Synth. Met.*, 2012, **162**(17–18), 1524–1530.

257 H. Devnani, D. S. Rajawat and S. P. Satsangee, Black rice modified carbon paste electrode for the voltametric determination of Pb (II), Cd (II), Cu (II) and Zn (II), *Proc. Natl. Acad. Sci., India, Sect. A*, 2014, **84**(3), 361–370.

258 C. R. T. Tarley, V. S. Santos, B. E. L. Baêta, A. C. Pereira and L. T. Kubota, Simultaneous determination of zinc, cadmium and lead in environmental water samples by potentiometric stripping analysis (PSA) using multiwalled carbon nanotube electrode, *J. Hazard Mater.*, 2009, **169**(1–3), 256–262.

259 B. Silwana, C. Van Der Horst, E. Iwuoha and V. Somerset, A brief review on recent developments of electrochemical

sensors in environmental application for PGMs, *J. Environ. Sci. Health, Part A: Toxic/Hazard. Subst. Environ. Eng.*, 2016, **51**(14), 1233–1247.

260 B. Silwana, C. van der Horst, E. Iwuoha and V. Somerset, Screen-printed carbon electrodes modified with a bismuth film for stripping voltametric analysis of platinum group metals in environmental samples, *Electrochim. Acta*, 2014, **128**, 119–127.

261 B. Silwana, C. van der Horst, E. I. Iwuoha and V. Somerset, A Sensitive Reduced Graphene Oxide-Antimony Nanofilm Sensor for Simultaneous Determination of PGMs, *J. Nano Res.*, 2016, 134–141.

262 B. Silwana, C. van der Horst, E. Iwuoha and V. Somerset, Reduced graphene oxide impregnated antimony nanoparticle sensor for electroanalysis of platinum group metals, *Electroanalysis*, 2016, **28**(7), 1597–1607.

263 C. Van der Horst, B. Silwana, E. Iwuoha and V. S. Somerset, Voltametric analysis of platinum group metals using a bismuth-silver bimetallic nanoparticles sensor, *Recent Prog. Organomet. Chem.*, 2017, 123–137.

264 G. Woldemichael, T. Tulu and G.-U. Flechsig, Solar UV-treatment of water samples for stripping-voltametric determination of trace heavy metals in Awash river, Ethiopia, *Heliyon*, 2016, **2**(3), e00091.

265 D. Mbui, D. O. Orata, G. Jackson and D. Kariuki, Investigation of Kenyan bentonite in adsorption of some heavy metals in aqueous systems using cyclic voltametric techniques, *Int. J. Phys. Sci.*, 2014, **9**(5), 102–108.

266 B. Silwana, C. Van Der Horst, E. Iwuoha and V. Somerset, Amperometric determination of cadmium, lead, and mercury metal ions using a novel polymer immobilised horseradish peroxidase biosensor system, *J. Environ. Sci. Health, Part A: Toxic/Hazard. Subst. Environ. Eng.*, 2014, **49**(13), 1501–1511.

267 C. M. Willemse, K. Tlhomelang, N. Jahed, P. G. Baker and E. I. Iwuoha, Metallo-graphene nanocomposite electrocatalytic platform for the determination of toxic metal ions, *Sensors*, 2011, **11**(4), 3970–3987.

268 K. Pokpas, N. Jahed, O. Tovide, P. G. Baker and E. I. Iwuoha, Nafion-graphene nanocomposite in situ plated bismuth-film electrodes on pencil graphite substrates for the determination of trace heavy metals by anodic stripping voltammetry, *Int. J. Electrochem. Sci.*, 2014, **9**(9), 5092–5115.

269 B. Silwana, C. Van Der Horst, E. Iwuoha and V. Somerset, A brief review on recent developments of electrochemical sensors in environmental application for PGMs, *J. Environ. Sci. Health, Part A: Toxic/Hazard. Subst. Environ. Eng.*, 2016, **51**(14), 1233–1247.

270 A. O. Idris, N. Mabuba, D. Nkosi, N. Maxakato and O. A. Arotiba, Electrochemical detection of selenium using glassy carbon electrode modified with reduced graphene oxide, *Int. J. Environ. Anal. Chem.*, 2017, **97**(6), 534–547.

271 J. Mafa, N. Mabuba and O. Arotiba, An exfoliated graphite based electrochemical sensor for As (III) in water, *Electroanalysis*, 2016, **28**(7), 1462–1469.

272 T. Ndlovu, O. A. Arotiba, S. Sampath, R. W. Krause and B. B. Mamba, Electrochemical detection and removal of lead in water using poly (propylene imine) modified re-compressed exfoliated graphite electrodes, *J. Appl. Electrochem.*, 2011, **41**(12), 1389–1396.

273 L. G. Djemmoe, E. Njanja, F. M. Tchieno, D. T. Ndinteh, P. G. Ndungu and I. K. Tonle, Activated Hordeum vulgare L. dust as carbon paste electrode modifier for the sensitive electrochemical detection of Cd^{2+}, Pb^{2+} and Hg^{2+} ions, *Int. J. Environ. Anal. Chem.*, 2019, 1–17.

274 S. L. Jiokeng, L. M. Dongmo, E. Ymélé, E. Ngameni and I. K. Tonlé, Sensitive stripping voltammetry detection of Pb (II) at a glassy carbon electrode modified with an amino-functionalized attapulgite, *Sens. Actuators, B*, 2017, **242**, 1027–1034.

275 I. K. Tonlé, Square wave voltametric determination of lead (II) ions using a carbon paste electrode modified by a thiol-functionalized kaolinite, *Electroanalysis*, 2011, **23**(1), 245–252.

276 B. Silwana, C. van der Horst, E. Iwuoha and V. Somerset, Reduced graphene oxide impregnated antimony nanoparticle sensor for electroanalysis of platinum group metals, *Electroanalysis*, 2016, **28**(7), 1597–1607.

277 S. Smith, P. Madzivhandila, L. Ntuli, P. Bezuidenhout, H. Zheng and K. Land, Printed paper–based electrochemical sensors for low-cost point-of-need applications, *Electrocatalysis*, 2019, **10**(4), 342–351.